NONLINEAR RESPONSE PREDICTION OF SPAR PLATFORM USING ARTIFICIAL NEURAL NETWORK

MD. ALHAZ UDDIN

FACULTY OF ENGINEERING
UNIVERSITY OF MALAYA
KUALA LUMPUR

2012

NONLINEAR RESPONSE PREDICTION OF SPAR PLATFORM USING ARTIFICIAL NEURAL NETWORK

MD. ALHAZ UDDIN

DISSERTATION SUBMITTED IN FULFILMENT OF THE REQUIREMENTS FOR THE DEGREE OF MASTER OF ENGINEERING SCIENCE

FACULTY OF ENGINEERING
UNIVERSITY OF MALAYA
KUALA LUMPUR

2012

UNIVERSITY OF MALAYA

ORIGINAL LITERARY WORK DECLARATION

Name of the Candidate: **Md. Alhaz Uddin**

Passport No:

Registration /Metric No: **KGA 100061**

Name of the degree: **Master of Engineering Science.**

Title of Project Paper/Dissertation/Thesis: **NONLINEAR RESPONSE PREDICTION OF SPAR PLATFORM USING ARTIFICIAL NEURAL NETWORK**

Field of study: **Structural Engineering and Materials**

I do solemnly and sincerely declare that:

1. I am the sole author/writer of this work;
2. This work is original;
3. Any use of any work in which copy exists was done by way of fair dealing and for permitted purposes and any excerpt or extract from, or reference to or reproduction of any copyright work has been disclosed expressly and sufficiently and the title of the work and its authorship have been acknowledged;
4. I do not have any actual knowledge nor do I ought reasonably to know that the making of this work constitutes an infringement of any copyright work;
5. I hereby assign all and every rights in the copyright to this work to the University of Malaya (UM), who henceforth shall be owner of the copyright of this work and that any reproduction or use in any form or by any means whatsoever is prohibited without the written consent of UM having been first had and obtained;
6. I am fully aware that if in the course of making this work I have infringed any copyright whether intentionally or otherwise, I may be subject to legal action or any other action as may be determined by UM.

Candidate's Signature Date

Subscribed and solemnly declared before,

Witness's Signature Date

Name:

Designation:

ABSTRACT

Due to global energy demand, offshore industries are moving towards deep and ultra-deep waters for oil and gas exploration in ocean environment. Floating offshore structures such as spar platform is considered to be the most economic and suitable offshore structure in deep water regions. During oil and gas exploration, floating offshore structures may sometimes be affected by critical environmental forces. Quick decision must be taken either to continue or to stop production, on the basis of response prediction of offshore structures under forecasted environmental conditions. Finite Element Method (FEM) is an important technique to predict the response of offshore structures considering all nonlinearities. However, FEM is a highly time-consuming process for predicting the response of platforms and usually used as a final analysis tool. On the other hand, Artificial Neural Networks (ANN) can predict response in rapid mode. ANNs are also capable of providing efficient solutions to problems such as damage detection, time series prediction and control where formal analysis is highly complex.

This study presents nonlinear response prediction of spar platform for various environmental forces using ANN. The neural network has three layers, namely the input, output, and hidden layer. A hyperbolic tangent function is considered in the present study as an activation function. Environmental forces and structural parameters are used as inputs and FEM-based time history of spar platform responses are used as targets. Feed-forward neural networks with back-propagation algorithm are used to train the network. After training the network, the response of the spar platform is obtained promptly for newly selected environmental forces.

The response obtained using ANN is validated by conventional FEM analysis. It has been observed that using completely new environmental forces as input to ANN, the time history response of spar platform can be very accurately predicted. Results show that the ANN approach is very efficient and significantly reduces the time for predicting response time histories.

ABSTRAK

Memandangkan permintaan untuk sumber tenaga dunia semakin meningkat, industri di luar rantau telah menuju kearah menyelami dasar laut pada peringkat yang lebih mendalam untuk tujuan carigali minyak dan gas dalam persekitaran laut. Struktur-struktur apungan di luar rantau yang seperti pelantar terapung (spar platform) dikatakan sebagai struktur luar rantau laut dalam yang paling ekonomik dan sesuai. Semasa mengkaji carigali minyak, pelantar apungan rantau jauh kadangkala boleh mengalami gangguan alam sekitar. Keputusan yang cepat harus dibuat samada untuk berhenti atau menyambung pengeluaran, berdasarkan tindakbalas struktur apungan tersebut di bawah keadaan persekitaran yang diramal. Kaedah Elemen Kecilan atau lebih dikenali dengan nama kacdah unsur terhingga adalah suatu teknik yang digunakan untuk meramal tindakbalas struktur rantau jauh tersebut, dengan mengambil kira semua ketidaklinearan data yang diperoleh. Walaupun begitu, FEM adalah kaedah yang mengambil masa yang lama untuk menjalankan perkiraan tersebut. Tetapi, Jaringan Saraf Buatan atau lebih dikenali dengan nama “Artificial Neural Networks” (ANN) boleh digunakan pada kadar yang lebih cepat. ANN juga boleh digunakan untuk menyelesaikan permasalahan sekitar pengesanan kerosakan, ramalan siri masa dan system kawalan dimana teknik analisa yang formal adalah terlalu rumit.

Kajian ini mempersembahkan ramalan ketidaklinearan tindakbalas terhadap medan pelantar yang disebabkan oleh alam sekitar menggunakan ANN. Rangkaian saraf buatan (ANN) akan mempunyai tiga peringkat, iaitu peringkat kemasukan (input), keluaran (output) dan peringkat yang tersirat. Fungsi tangen hiperbolaan telah dipilih untuk kajian ini sebagai fungsi pembukaan. Kesan persekitaran dan parameter struktur digunakan sebagai input dan latarbelakang masa FEM medan pelantat tersebut digunakan sebagai sasaran. Algoritma rangkaian saraf suap depan digunakan dengan

teknik penyebaran songsang digunakan untuk melatih rangkaian ini. Selepas selesainya latihan ini, rangkaian tindakbalas medan pelantar ini diperoleh untuk sebarang daya persekitaran.

Tindakbalas yang diperoleh dengan ANN ini disahkan dengan analisa FEM yang konvensional. Penggunaan daya persekitaran sebagai sebahagian daripada input pembolehubah kepada ANN tersebut telah berjaya menunjukkan bahawa tindakbalas berkalaan medan pelantar tersebut boleh diramal dengan tahap kepersisan yang tinggi. Kajian ini menunjukkan bahawa kaedah ANN ini adalah kaedah yang mempunyai tahap kecekapan yang tinggi dan mengambil masa yang lebih singkat untuk memperoleh tindakbalas masa.

ACKNOWLEDGEMENTS

I would like to thank almighty Allah (SWT) for providing me the opportunity to pursue my studies as well as instilling the patience and persistence during my research work**.**

I wish to express my sincere thanks and profound appreciation to my supervisor, Dr. Muhammed Jameel for his guidance, encouragement and valuable time spent on the fruitful discussion throughout the work, which was extremely valuable in conducting this research work.

I would also like to express my gratefulness to my supervisor Prof. Dr. Hashim Bin Abdul Razak for his treasured and relevant advice throughout the study.

I would like to acknowledge the grant (UMRG) provided from the University of Malaya to fulfill the study as well as the research works.

I would like to thanks to PhD student A.B.M. Saiful Islam who help me every stage of my research.

Finally, I would like to thank the most important people in my life, my parents, brother, and sisters who have provided their endless support and patience throughout the years.

TABLE OF CONTENTS

LIST OF FIGURES

LIST OF TABLES

LIST OF NOTATION

ANN	artificial neural network
ART	adaptive resonance theory
BPN	back-propagation network
[C]	damping Matrix
CFOC	classical-state feed-back optimal control
f(.)	transfer function
Φ	modal matrix
FFBPN	feed-forward back-propagation network
FFN	feed-forward network
FFMLP	feed-forward multilayer perceptron
FFOC	feed-forward and feedback optimal control
FEM	finite element method
FPSO	floating production system and offloading
I	produced response
ξ	structural damping ratio
[K]	stiffness matrix
LMBP	Levenberg-marquardt back-propagation
LPNN	lattice probabilistic neural network
[M]	total mass matrix
MAE	mean absolute error
MLP	multi-layer perceptron
MLFFN	multilayer feed-forward network
MLPBPN	multilayer perceptron back-propagation network
MLPNN	multilayer perceptron neural network

MSE	mean of squared errors
m_i	generalized mass
MSE	mean of squared errors
NA	not available
N	number of increments
N_x	number of delays for surge
N_y	number of delays for surge
N_z	number of delays for pitch
O	output
O_j	output for node j.
PNN	Probabilistic neural network
PMI	prescribed motion inputs
RBF	radial basis function
RMSE	root mean square error
RNN	rough neural networks
SSE	sum of squared errors
TLCD	tuned liquid column damper
TLP	tension leg platform
Δt	time step
θ	bias
θ_j	bias for node j
W	connection weight
W_{ij}	connection weight between nodes j and i
ω_i	natural frequency
X	input

X_i	input from node i, i = 0, 1, …, n
$x(t)$	surge response time histories
$\{X\}$	6 DOF structural displacements at each node
$\{\dot{X}\}$	structural velocity vector
$\{\ddot{X}\}$	structural acceleration vector
x_i	observed value at the i^{th} step
$\bar{x}$	observed mean value
y_i	simulated value at the same point
$\bar{y}$	simulated mean value
$y(t)$	heave response time histories
$z(t)$	pitch response time histories

CHAPTER 1.0 INTRODUCTION

1.1 Background

Offshore structures provide great possibilities for the development and utilization of oceanic resources and energy. These structures are usually subjected to more severe load conditions than those on the land. There are two types of offshore structures on the basis of mobility, such as: fixed offshore structure and compliant floating offshore structures. Fixed types (jacket and gravity platforms) of offshore structures are economically viable for shallow-water region. The use of fixed platforms in deep water (approximately > 300 m) is hindered by technical difficulties coupled with economic factors that grow dramatically with increased water depth. On the other hand, compliant floating structures (e. g. spar platforms, tension leg platforms, etc.) provide economic solution for deep-and ultra-deep water exploration and production facilities (Ng et al., 2010). In any case, floating offshore structures are extensively affected by the uncertainties associated with steep nonlinear waves, currents, and wind leading to springing and ringing of Tension Leg Platforms (TLPs), slow drift yaw motion of Floating Production, Storage and Offloading (FPSOs), as well as large oscillations of spar platforms as a result of vortex shedding (Kim, 2008).

Analyses of floating offshore structures, like spar platforms, considering environmental loads are complex due to various nonlinearities such as geometric, variable submergence, varying pretention, etc. Finite Element Method (FEM) is an important technique to cope with this kind of analysis. A number of studies have recently been performed in order to predict response of spar platforms with different types of conventional methods (Liu et al., 2011; Montasir et al., 2008; Prislin et al., 2001; Steen

et al., 2004). However response analyses of spar platforms by these methods are very complicated and time-consuming process.

Artificial neural networks (ANNs) are very sophisticated modeling techniques capable of providing extremely rapid and efficient solution modes where formal analyses are highly complex. ANNs are conducive to manage problems related to offshore engineering for damage detection, time series prediction, and controlling in cases where formal analysis is time consuming or unfeasible. Therefore, Simoes et al. (2002) developed a neural network for prediction of mooring forces and analysis of the dynamic behaviour of FPSO and a shuttle ship in tandem configuration. This approach was suitable for preventing collisions of the ships and maintenance of mooring line. For prediction of extreme excursion and mooring force of FPSO over an N-year life period, response-based hydrodynamic models (SAMRES) have been proposed by Mazaheri et al. (2006; 2005). They calculated responses of a floating offshore platform subjected to arbitrary wind, wave, and current loads. Hybrid ANN–FEM approach has been adopted by Guarize et al. (2007) for long time history response prediction of FPSO, for random dynamic response of mooring lines and risers. Pina et al. (2010) developed a model with application of surrogate models, on the basis of ANN, to predict response of offshore structures; replacing dynamic analyses with FEM. For the testing model, they used mooring line tension of FPSO, and results have shown that ANNs are very efficient in predicting responses accurately and in considerably less time. Moghim et al. (2007); Shafiefar et al. (2011); Shafiefar and Moghim (2005); Zhou and Luan (2009) used ANNs to predict hydrodynamic forces, generated by waves, and current forces on slender cylinders.

This study presents nonlinear response prediction of spar platform under environmental forces like wave height and wave period using ANN. It has been observed that using

completely new environmental forces as inputs to ANN, the time history response of spar platform can be very accurately predicted. Results show that the ANN approach is very efficient and significantly reduces the time for predicting response time histories.

1.2 Malaysian Offshore Structures

In the year 1957, the first offshore platform was installed in Malaysia both off Sabah and Sarawak for the purpose of oil and gas exploration, but it was not momentous. Following this, in 1960, massive explorations were started around Temana, offshore of Bintulu (Chai, 2005). Today, the total number of offshore platforms in the waters of Malaysia is 200. The Malaysian government is focused on efforts to enhance output from existing oil and gas explorations and developing new fields in deep-water areas. For this reason, oil and gas explorations by industries have been extended to the deep water regions. The first deep water floating offshore structure spar platform was installed in 1330 m of water at Kikeh field, near Sabah in 2007 (Tuhaijan et al., 2011).

Malaysian acreage of oil and gas comprises 494,183 km^2, including 337,167 km^2 in the offshore continental shelf area, and 63,968 km^2 in deep-waters. The acreage is divided into 54 blocks, among them 28 blocks (a total of 205,500 km^2) are presently operated by Petronas and other seven offshore oil companies (Razalli, 2005). Nearly all of Malaysia's oil comes from offshore fields. The sedimentary basins of Malaysia are a great resource of energy beneath the seabed (EIA, 2011). Most of the country's oil reserves are to be found in the Malay basin and tend to be of high quality.

1.3 Problem Statement

Spar platform is a modern floating offshore platform for oil and gas exploration in deep sea. It has a huge potential in future and is expected to greatly encourage operations in

deep sea explorations. During oil and gas exploration, spar platforms may sometimes be affected by critical environmental forces like extreme storm, cyclone etc. Considering safety of life, quick decisions must be taken either to continue or to stop production, based on the response predictions for the offshore structure under forecasted environmental conditions. Meteorological department usually forecasts wind forces not waves. The prediction of wave height and wave period from forecasted wind forces can be used in FEM and ANN. Response analysis of spar platform by FEM is very complicated and time-consuming process. To this end, this study presents response prediction of spar platform applying ANNs that can predict response under critical circumstances very fast. Methodical response prediction through factual analysis is required for the development of better and safer construction guidelines for spar platform. This study also emphasizes the need for extensive study on the response prediction model of spar platforms using ANN.

1.4 Research Objective

1. To create a neural network for predicting wave height and wave period using wind speed in Malaysian sea.
2. To carry out nonlinear finite element analysis of spar platform.
3. To generate a Resp-Pred approach adopting ANN for predicting the response of spar platform under wave loads.
4. To predict maximum mooring tension response of spar platform subjected to several sea states using ANN.
5. To generate hybrid FEM-ANN based time-domain nonlinear dynamic network for predicting long time history response using short time history response of spar platform.

1.5 Scope of Study

The scope of this study is focused on the response prediction of spar platform under environmental loading conditions. This study is carried out to predict the extreme condition of the ocean environments based on the met-ocean data obtained from Malaysian waters.

A finite element model is used to implement the fully coupled integrated spar platform. The analysis of spar platform, considering actual physical coupling between the rigid vertical floating hull and mooring lines is carried out using FEM. In actual field problems hydrodynamic loads due to wave height, wave period, and current are operated simultaneously on spar platform and mooring lines. This model can handle such nonlinearities, loading, and boundary conditions associated with these extreme situations. The finite element code ABAQUS/AQUA is used to obtain the response of the spar platform.

Environmental forces and structural parameters are used as inputs and FEM-based time history of spar platform responses are used as targets in ANN for training the network. This study is also carried out in the non-linear dynamic, time domain analysis by taking into account ANN in MATLAB toolbox. The network consists of a Multilayer Perceptron which takes input of past input and output values and computes the current output. The resulting network has purely feed-forward architecture, and static back-propagation can be used for training.

1.6 Outline of the Thesis

Chapter 1 provides a brief background and discusses Malaysian offshore structure, objectives of present study, scope of work, and the problem statement.

Chapter 2 presents different types of offshore structures and technical description of spar platform. Theoretical approaches related to the Artificial Neural Network (ANN) are also briefly introduced in this chapter. A detail literature review of the existing research works as well as identification of research gaps related to the current work are described in this chapter.

Chapter 3 describes the Finite Element Method related to the spar platform. This chapter is concerned with describing and developing methods of ANN approach for predicting environmental forces and response of spar platform.

Chapter 4 reports the results and discussion of the study, the response prediction of spar platform by Finite Element Method (FEM) and ANN. FEM results and ANN predicted results are also compared in this chapter.

Chapter 5 presents the conclusions and recommendations for future works.

CHAPTER 2.0 LITERATURE REVIEW

2.1 Introduction

In 1947, the first offshore platform was installed in 6m depth of water off the coast of Lousiana. Due to global energy demands, offshore industries are moving towards deep and ultra-deep waters. Several types of offshore structures have been installed for oil and gas extraction in ocean environment. Currently, approximately 7000 offshore structures are established across the world in water depths of up to 2000m (King, 2012). The selection of offshore structure depends on the purpose (drilling, production, utility etc.), the lateral and vertica1 loads which are influenced by the environmental forces (wind, wave, current, earthquake etc.), the water depth, and the lateral and vertical resistance of the fluid-structure-soil system (restoring forces, soil resistance) (DNV, 1996).

An extensive background and literature review has been presented to justify the research gaps found for the research work in this thesis. The significance of this research as well as the literature review on the response of ANN found in existing researches is analyzed briefly in this chapter.

2.2 Typical Offshore Structures

Offshore structures can be broadly divided into two groups; e.g. fixed and floating structures. Oil and gas extraction offshore structures have been divided into following categories on the basis of mobility.

2.2.1 Fixed Offshore Structures

Fixed offshore structures are the most popular offshore structures for drilling and production of oil and gas in ocean environment. It is suitable in shallow water as it is extended to the seabed. It is economical for a water depth up to 400 m (King, 2012), and generally have good performance in harsh oceanic environment. Usually fixed offshore structure poses high stiffness and experiences relatively small displacement.

2.2.1.1 Steel Jacket Platform

The jacket or template structures are the most common type of fixed offshore structures used in offshore industry today (Figure 2.1). Around the world, about 95% offshore structures have installed jacket support (Twomey, 2010). Fixed jacket platform is a space truss consisting of tubular steel members with a deck and fastened to the seabed with piles driven through the legs. The number of legs vary from 4 to 16 and are stiffened by bracings that carry the horizontal forces (Chai, 2005). Topsides and environmental loads are transferred to the foundation through the legs. Some platforms may contain enlarged legs to provide self-buoyancy during installation.

Figure 2.1: Fixed offshore platform (MOG, 2010)

2.2.1.2 Concrete Gravity Structure

Gravity platform is usually constructed where pile driving is difficult due to hard soil conditions. It is kept in position by its own weight against the large lateral loads from wind, waves, and currents; it is usually made of reinforced concrete. Usually gravity platforms contain a large base which has the capacity for significant oil storage and which supports a few columns to house the deck as shown in Figure 2.2. Concrete gravity platforms have been constructed in water depths as much as 350m (Nallayarasu, 2009).

Figure 2.2: Concrete gravity structure (MOG, 2010)

2.2.1.3 Compliant Tower

Compliant towers are relatively slender, flexible framed structures and are supported by piled foundations. They have conventional deck for drilling and production operations. Unlike the fixed platform, the compliant tower (Figure 2.3) survives large lateral forces

by tolerating significant lateral defections, and is usually used in water depths up to approximately 914 m (Weggel, 1997). It involves high financial risk and cannot be relocated due to its heavy and expensive structure.

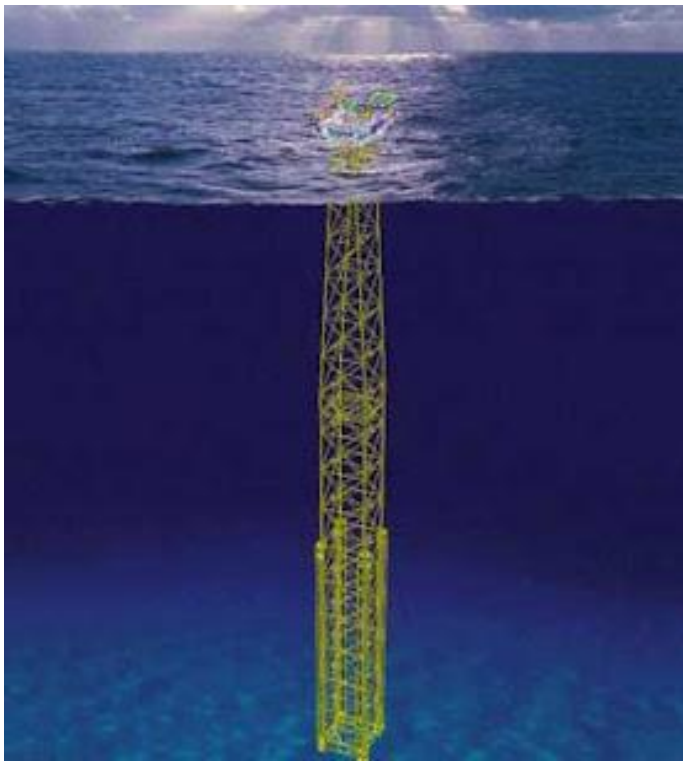

Figure 2.3: Compliant tower (MOG, 2010)

2.2.2 Floating Offshore Structures

With the preference for increased water depths in oil and gas exploration, fixed offshore structures are becoming uneconomical and unstable. Floating offshore structures are most suitable for deep and ultra-deep water oil and gas exploration. These structures are usually anchored to the sea-bed with wires, chains, or cables, so that, the anchoring system provides the necessary restoring forces. Wang et al. (2011) introduced an efficient approach for choosing floating platforms for specific oil/gas field in deep-water floating platforms all around the world (including Spar, TLP, SEMI and FPSO) using ANN.

2.2.2.1 Semi-submersible

Semi-submersible platforms contain hulls (column and pontoons) which have sufficient buoyancy to help the structure to float (Figure 2.4). These platforms are generally anchored by combinations of cable and tendon during drilling or production operations to keep it in place by the use of dynamic positioning (Sadeghi, 2007). These platforms can be moved from place to place. Semi-submersibles can be used in water depths from 60 m to 3,000 m (Marshall, 2005).

Figure 2.4: Semi-submersible offshore platform (Blushoes, 2010)

2.2.2.2 Tension Leg Platform

A Tension-leg platform (TLP) is a vertically moored floating structure usually used for oil, gas extraction and wind turbines (Figure 2.5). TLP is compatible for water depths greater than 300 m and less than 1500 m (D'Souza et al., 1993). The mooring system is a set of tension legs or tendons attached to the platform and connected to a template or foundation on the seafloor (Blog, 2011).

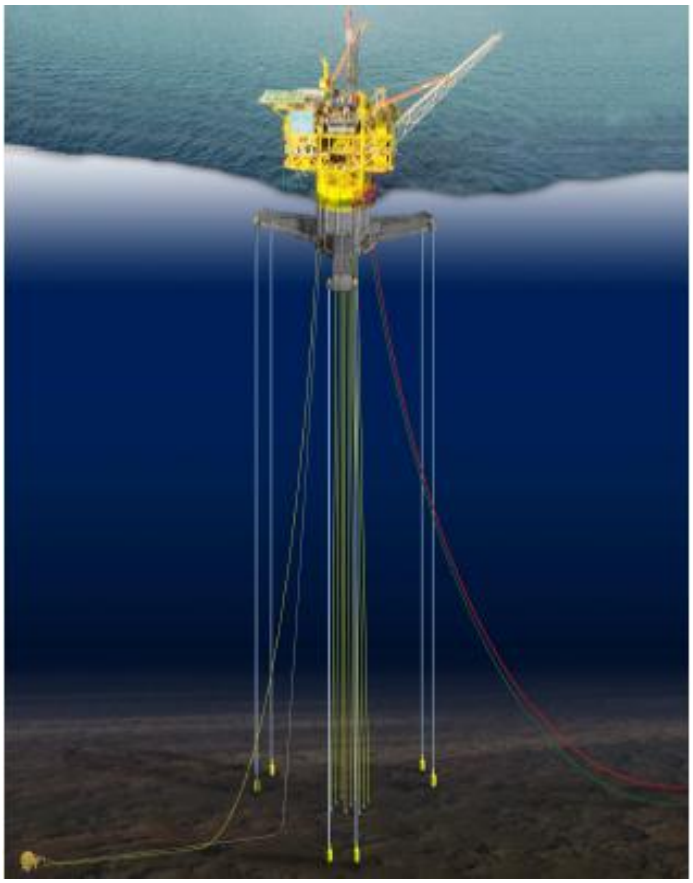

Figure 2.5: Tension leg platform (TLP) (Nallayarasu, 2009)

2.2.2.3 Floating Production, Storage and Offloading (FPSO)

An FPSO system is one of the deep water offshore structures. The FPSO system is widely used for the purpose of processing and storage of oil and gas. FPSO is a suitable mobile offshore structure that can easily be shifted to a new location (Figure 2.6). FPSOs are easy to install at the desired location and do not need a local extra pipeline to export oil. FPSO generally consist of a floating hull combined with pontoons and columns which support a large working deck with drilling and production systems (Weggel, 1997). The station is held in place by catenary mooring systems or by dynamic positioning.

Figure 2.6: Floating production storage and offloading (FPSO) (MacGregor et al., 2000)

2.2.2.4 Spar Platform

Spar platform is one of the floating structures used for deep and ultra-deep water applications of drilling, production, storage, and offloading of ocean deposits by GOM (2000). The spar is the latest among this new generation of floating offshore structures suitable for ocean drilling, production, and storage of oil in deep water (Glanville et al., 1991; Horton and Halkyard, 1992).

2.3 Components of Spar Platform

The central concept behind the spar platform is a cylindrical deep draft floating hull, which allows the structure to buoy and be held in place by mooring lines. The classic spar (Figure 2.7) configuration consists of a deep draft cylindrical hull that provides excellent motion characteristic even in rough seas. This favorable motion characteristic reduces the cost for the mooring system, which is an important factor in deep water installations.

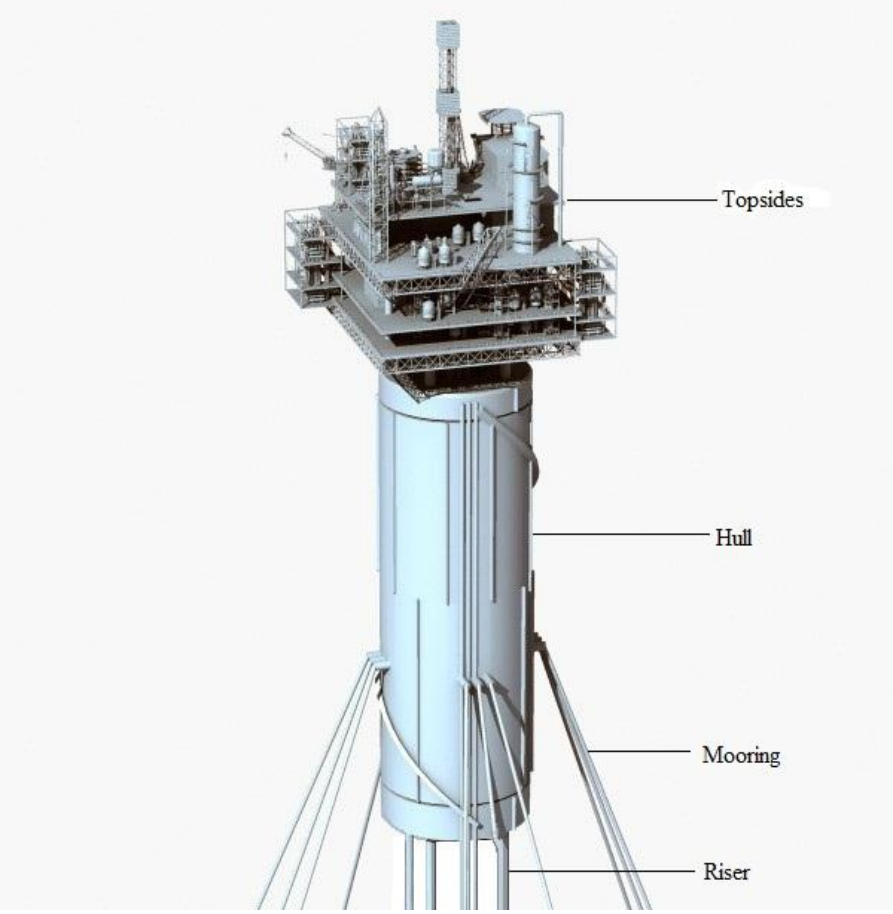

Figure 2.7: Classic spar platform (QLEE, 2011)

The classical spar, as the ones described above, consists of a large circular steel hull, stiffened plate with longitudinal stringers, and deep frames. About 90% of the structure is under-water. The upper part of the hull is responsible for the buoyancy and the midsection contains ample room for oil storage. The lower compartments hold the ballast, which controls the trim for the spar. Spiral strakes are fitted to the underwater part of the hull to prevent vortex induced vibrations. To reduce the wave induced motion, these offshore structures are so designed that their natural frequencies are far away from the peak frequencies of the force spectra. The structure is made stable by maintaining the center bouncy above the center of gravity. Station keeping in position is done by catenary mooring lines which are attached to the hull near the center of pitch.

2.3.1 Hull

Normal marine and shipyard fabrication methods are used for fabricating the hull. The center well size and the hull diameter are considered on the basis of the number of well, surface wellhead spacing, and facilities weight. Different types of risers are attached with top section of a flooded center-well of the cylindrical spar hull. This portion provides the bouncy for the spar. The bottom portion of the hull, named the keel, participates in buoyancy during transport, field installed, and fixed ballast.

2.3.2 Topsides

The topsides of the spar platform are designed comparable to the typical fixed offshore structural concept. This component of spar platform houses a full drilling rig or a work over rig desirable full production equipment. The oil and gas exploration operations directly influence the basis of deck size. The bigger topsides provide drilling, production, and processing quarter's facilities.

2.3.3 Risers

There are mainly two types of risers, such as production and drilling.

Production- Vertical riser participates to explore the oil and gas from seabed to flooded center-well. Vertical production riser is tensioned with floating cylinder which is connected to one or two springs of center-well.

Drilling- The drilling riser participate to drill in to the seabed. The drilling riser is also a top-tensioned casing with a surface drilling, which allows a platform-type rig to be used.

2.3.4 Mooring Lines

A catenary mooring system of 4 to 16 lines holds onto the spar at the designated location. The mooring line is made up of chains in the top and bottom segment and spiral strand wire or polyester rope in the intermediate portion. Each mooring line is anchored to the seafloor with a driven or suction pile. The hull bottom level of the line passes through a fairlead fixed on the hull below the water surface, then extends up the outside of the hull to chain jacks at the top.

2.4 Response Analysis of Spar Platform

Spar platform is a very compliant floating structure used for deep water applications of drilling, production, processing, storage, and off-loading of ocean deposits. Analysis of spar platform is complex due to various nonlinearities such as geometric, variable submergence, varying pretention etc. FEM is an important technique to cope with this kind of analysis. A number of studies have recently been performed in spar platform analysis employing FEM, such: as prediction of extreme response (Low, 2008), nonlinear coupled analysis (Ma et al., 2000), nonlinear coupled dynamic response under regular wave (Agarwal and Jain, 2003), dynamic analysis of spar (Sarkar and Roesset, 2004), coupling effect between spar and mooring (Chen et al., 2001), and time-domain and frequency-domain analysis of spar (Anam et al., 2003; Chen et al., 1999; Low and Langley, 2008). However, response analysis of spar platform by these methods is time-consuming.

The use of ANNs has been established as an alternative approach of FEM (Boom et al., 2009; Cardozo et al., 2011; Javadi et al., 2003; Mingui et al., 2003; Umbrello et al., 2008) to solve various types of engineering problems. ANN exhibits good performance in offshore engineering for damage detection, time series prediction, and controlling in

cases where formal analysis is time consuming. The FEM-ANN based approaches have been studied by a number of other researchers (Fedi et al., 2002; Ji and Zhou, 2011; Kadi, 2006; Lefik and Schrefler, 2003). It is observed that ANNs provide fairly accurate results compared to the FEM. As per the literature reviews on spar platforms, a considerable amount of research and analysis has been done by FEM unlike ANN.

2.5 Artificial Neural Network

Artificial neural networks (ANNs) are an information-processing system encouraged by biological nervous systems, such as the human brain. ANNs are able to learn from experience just like people. An ANN is a combination of artificial neurons namely processing elements, nodes, or units. Each processing element is fully interconnected to the other processing elements by its connection weights. Processing element accepts its weighted inputs, which are summed with adjustable unit bias. The bias unit is utilized to scale up the input to develop the convergence properties of the neural network. The result of this combined summation is passed through the transfer function to produce the output of the processing element.

2.5.1 Artificial Neuron Model

The artificial neurons may have single input or multiple inputs as described below.

Single Input Neuron- Figure 2.8 shows a single input artificial neuron model in its simplified mathematical model from, which has been extracted with some modification from Shahin et al. (2008).

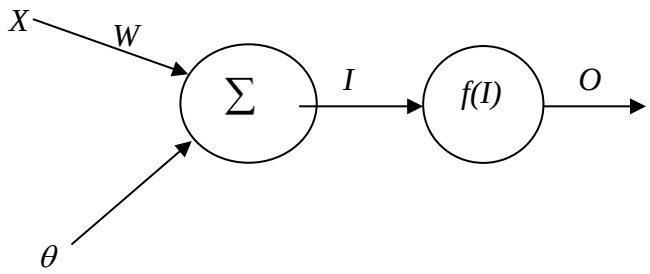

Figure 2.8: Single Input Artificial Neuron Model

$$I = \theta + WX \tag{2.1}$$

where

X=the input;

W= the connection weight;

θ = the bias;

I = the produced response;

$f(.)$ = the transfer function; and

O = the output.

As Figure 2.8 shows, the input neuron X is multiplied by connection weight W to form WX. The bias θ is passed into the summing junction and the produced response I which is shown in Equation 2.1. The produced response I goes into the transfer function $f(I)$ and produces an output O.

Multiple Input Neuron- A typical multiple input neuron with a transfer (activation) function which has been extracted with some modification from Shahin et al. (2008) is shown in Figure 2.9. Neurons usually have more than one input which is multiplied with its own weight. The adjustable unit bias is passed into the summing junction and

produce response which is shown in Equation 2.2. The produced response transfers through the activation function and produces outputs.

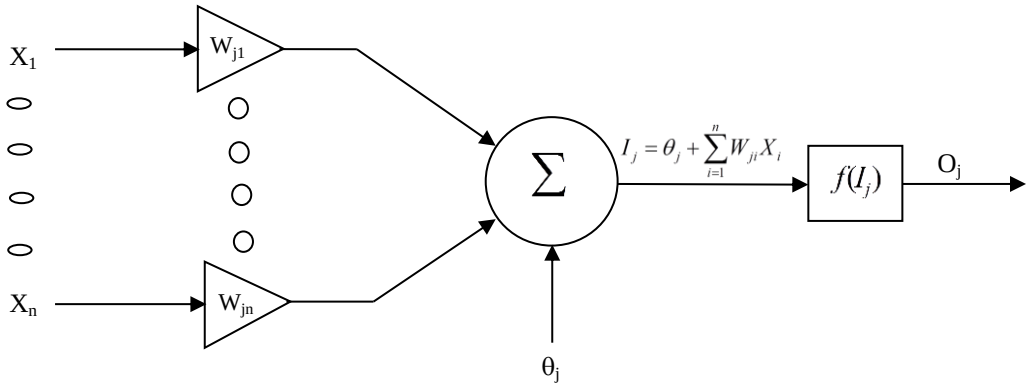

Figure 2.9: Multiple Inputs Artificial Neuron Model

$$I_j = \theta_j + \sum_{i=1}^{n} W_{ji} X_i \qquad (2.2)$$

where,

X_i = the input from node i, i = 0, 1, …, n;

W_{ij}= the connection weight between nodes j and i;

θ_j = the bias for node j;

I = the produced response;

f(.) = the transfer function; and

O_j = the output.

2.5.2 Transfer (Activation) Function

Activation function is contained in hidden layer in between inputs and outputs. This function is also called transfer function. Finally, an activation function controls the amplitude of the output. Needless to say, each transfer function has its own formula which is shown in Table 2.1.

Table 2.1: Different types of transfer (activation) function

Function		Mathematical Representation
Threshold (hard-limit)	Binary	$f(I) = \begin{cases} 1 & if \quad i \geq 0 \\ 0 & if \quad i < 0 \end{cases}$
	Bipolar	$f(I) = \begin{cases} +1 & if \quad i \geq 0 \\ -1 & if \quad i < 0 \end{cases}$
Sigmoid		$f(I) = \frac{1}{1 + e^{-\alpha i}}, \alpha > 0$
Hyperbolic Tangent		$f(I) = \tanh(vi) = \frac{1 - e^{-vi}}{1 + e^{-vi}}, v > 0$
Gaussian		$f(I) = \frac{1}{\sqrt{2\pi\sigma^2}} e^{\left[\frac{(i-\mu)^2}{2\sigma^2}\right]}$

Here α is the slope parameter also called shape parameter; v is also used for the same representation.

2.5.3 Classification of ANNs

ANNs can roughly be divided into the following three categories, based on the arrangement of neurons and the connection patterns of the layers: Feed-forward neural networks, Feed-back neural networks, and Self-organizing maps.

2.5.3.1 Feed-forward Neural Network

A feed-forward neural network is a standard type of neural network that might be used for such applications as prediction, control, and monitoring. Feed-forward neural networks are one-way connections (weights) from input to output layers through the hidden layer (Beale et al., 2010). Feed-forward networks often have one or more hidden layers followed by an output layer. This network propagates in a forward direction; it never goes in backward direction. In a feed-forward neural network, the input numbers are served to input nodes, after multiplying by a weight it's in go pass them on the

hidden layer nodes. A hidden layer node receives the weighted input from each input node and bias connection with it. Then the result passes through the nonlinear transfer function. The output nodes come from the hidden layer node. The network is trained by trial and error, the target output at each output node is compared with the network output and the difference (error) is minimized by adjusting the weights and biases though training algorithms. The optimum network can be applied for a multitude of problem solving purposes (Rai and Mathur, 2008).

Multilayer Perceptron-Multilayer perceptron (MLP) is a feed-forward artificial neural network model that transforms sets of input signals into sets of output signals through hidden layer (Manik et al., 2008). The hidden layer and nodes play significant roles in many successful applications of neural networks (Zhang and Eddy Patuwo, 1998). In MLP, the input signal on a layer-by-layer basis propagates in a forward direction through the network. The network is trained in supervised learning method with error back propagation algorithm.

2.5.3.2 Feed-back Neural Network

A feed-back network is a network with connections from the output of a layer to its input. The feed-back connection can be direct or can pass through several layers. In feed-back networks, the output information defines the initial activity state of a feed-back system, and after the state transitions to the asymptote, final state is identified as the outcome of the computation. The networks known as recurrent networks are also feed-back networks.

2.5.3.3 Self-Organising Maps

The self-organising map describes a mapping from a high dimensional input space to a low dimensional map space and is trained using unsupervised learning. Self-organising maps are different from other artificial neural networks in the sense that they use a neighborhood function to preserve the topological properties of the input space. An ANN can also be self-organising which means that it can create its own organisation or representation of the information it receives during learning time without any intervention from the outside world.

2.5.4 Learning Algorithm

The neural network is trained to adjust the values of the connections (weights) to execute a particular function between an exact input response and a precise target output. This process is known as learning. There are three basic types of learning methods in neural networks, such as supervised, unsupervised, and reinforced learning, which are shown in Figure 2.10. Among them supervised and unsupervised learning algorithm are most popular.

In supervised learning, the target response of the network is compared to a desired output response. If the real target response differs from the desired output response, the network generates an error. This error is utilized to adjust the connection weights between the model target response and output response due to matches with actual outputs, and those predicted by the ANN (Lefik and Schrefler, 2003).

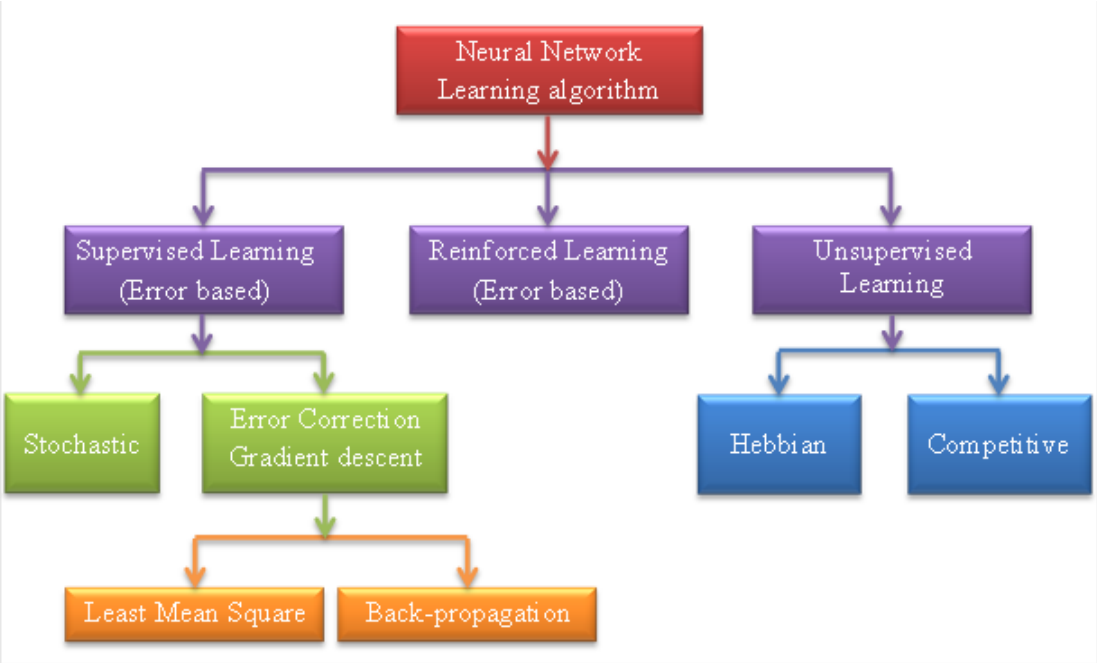

Figure 2.10: Classification of learning algorithms (Chakraborty, 2010)

Unsupervised learning does not require desired target response. The connection weights are adjusted with network according to the input values. In reinforced learning, the target response of the network is not compared to a desired output response. It only indicates whether the computed output is correct or incorrect. The information provided helps the network in its learning process.

2.5.5 Back-propagation Algorithm

Back-propagation algorithm is most popular for training neural networks. It requires lower memory than other algorithms and commonly makes acceptable error levels. This algorithm could be used in various types of networks even though it is usually suitable for training MLPs (Dikmen and Sonmez, 2011). It was developed by simplifying the Widrow-Hoff learning rule to multiple-layer networks and nonlinear differentiate transfer functions (Ruck et al., 1990). Input and the corresponding target are used to train the network until it can function fairly accurately. The back-propagation algorithm

from the details that results are passed forward from input nodes to output nodes. Calculated errors are passed forward from input nodes to output nodes.

2.5.6 Performance Functions

The performance function is used to compute network performance in training. This is useful for many algorithms, such as back-propagation, which operates by adjusting network weights and biases to improve performance. The following functions are conventional performance functions:

MAE: mean absolute error

MSE: mean of squared errors

SSE: sum of squared errors

2.6 Environmental Force on Offshore Structures

Human activities are increasing gradually in offshore environment due to exploration of oil and gas. Sometimes unexpected situations may occur due to environmental phenomena during offshore activities. Considering safety of life and prevention of economic losses, the prediction of wave parameters is an important prerequisite for oil and gas explorations associated with offshore engineering. Waves are generally generated by wind forces in oceanic environment. Meteorological departments usually forecast wind forces and not waves. There are lots of empirical methods today for predicting wave height and wave period from wind force (Günther et al., 1997; Krogstad and F. Barstow, 1999; Muzathik et al., 2011; Tolman et al., 2005; Tolman et al., 2002). ANN can predict waves more accurately than the existing empirical formulae. Several studies have been done for predicting significant wave height and

mean-zero-up-crossing wave period time history for various seas using ANN. Two different neural network approaches have been used by Makarynskyy et al. (2004; 2005) to predict significant wave heights and zero-up-crossing wave periods 3, 6, 12, and 24 h in advance. The simulations have been evaluated for the time histories of these wave parameters in the region off the west coast of Portugal. The main time histories of significant wave height have been disintegrated to multi resolution time histories using wavelet transformation which is hybridized with ANN and wavelet transforms (Deka and Prahlada, 2012). The multi resolution time histories have been used as input of the ANN to predict the significant wave height at unlike multistep lead time near Mangalore, west coast of India. Mandal et al. (2006) predicted significant wave heights from measured ocean waves off Marmugao, west coast of India. Recurrent neural networks with Rprop update algorithm have been applied for prediction of wave height.

The significant wave height and mean-zero-up-crossing wave period time histories have been predicted using locally available wind data. Improvement of the prediction accuracy has been tried by applying various types of neural network models. Paplińska-Swerpel (2006) predicted significant wave height from wind speed using ANN at 10 selected location in the Baltic Sea.. The time history of hindcast wave data originated from the WAM4 wave model. On the basis of Radial Basis Function (RBF), and Feed-forward Back-propagation (FFBP) neural network approach has been developed for predicting significant wave heights at a specified coastal sites in deeper offshore locations (Kalra et al., 2005). Significant wave height, average wave period, and wind speed data have been collected from satellite-sensed data at the west coast of India. The ANN with back-propagation algorithm has been used for prediction of wave height and wave periods from the wind information based on wind-wave relationship (Londhe and Panchang, 2006) which is reported by Tsai et al. (2002). Time histories of waves at any

station can be anticipated on the basis of neighbourhood station's data. Deo et al. (2001) developed a variety of deterministic neural network models to predict significant wave height and wave periods from generating wind speeds. The network could provide satisfactory results in deep water and in open wider areas, and prediction intervals are large, such as one week. The response prediction of spar hull and mooring line, by FEM and ANN, requires maximum wave height and wave period.

For this purpose, the study is carried out to predict maximum wave height and wave period from wind force of Malaysian sea that can be used for predicting response of offshore platform for both cases. Recurrent neural networks and back-propagation neural network have been used in the present study for prediction of wave parameter with the goal of getting more accurate results.

2.7 Finite Element Analysis of Offshore Structures

Spar platform is a compliant floating structure which is used for exploration of oil and gas from deep and ultra-deep water. Spar platform is a cost effective solution to counter lateral and vertical forces while fulfilling the basic oil field requirements like drilling, production support, storage etc., and without any operational limitations posed by water depth. Spars are found to be an economical and efficient type of offshore platform. It is a neutrally-buoyant, fully compliant, floating system of large cylindrical shape, with six degrees of freedom, moored by a semi-taut spread mooring system. The superstructure comprises of derrick and other drilling and production facilities with the provision for a helipad. On the basis of popularity of spar platform, several researchers have studied it to make cost effective and reliable design and installation guide line as well as to ensure safety from catastrophic failure.

Tahar and Kim (2008) have developed a theory and numerical tool for coupled dynamic analysis of deep-water structure like spar and buoy with polyester mooring lines. The static and dynamic behaviour of a buoy and spar were studied. The time domain and frequency domain analyses of mooring line and riser of cell truss spar platform in deep-water have been studied (Zhang et al., 2008). The experimental results were compared with three methods namely quasi-static, semi-coupled, and fully-coupled. The response characteristics of a slack-mooring spar platform were investigated by Ran et al. (1996) under regular waves, unidirectional irregular waves and bichromatic waves with or without currents. Again, Ran et al. (1999) investigated in both time domain and frequency domain analysis of nonlinear coupled response of spar mooring in random waves with and without currents. The difference between time domain and frequency domain analysis of spar platform using Morison's equation were investigated by Anam, et al. (2003). Chen et al. (2001; 1999) studied the response of a slack-mooring line of spar platform subjected to steep ocean waves by a quasi-static and a coupled dynamic method to reveal coupling effect between spar hull and mooring lines. Consistent analytical methods have been presented (Ma et al., 2000) for the prediction of nonlinear-coupled effects among hull, mooring lines, and risers. This method was applied to spar and TLP for different depths up to ultra-deep water. Low and Langley (2008) developed hybrid method for efficient fully coupled analysis of floating structure like vessel, mooring, and risers. The method was found to be in good performance with fully coupled frequency domain analysis for ultra-deep water and time domain analysis for intermediate water depths. The same hybrid method was used to predict extreme response of platform and moorings/risers (Low, 2008). Agarwal and Jain (2003) studied nonlinear coupled dynamic analysis of spar platforms subjected to regular waves. The spar hull was modeled as a rigid body with six-degrees-of-freedom which is attached at the fairlead position and anchored to the seabed with catenary mooring lines. The time

domain response analysis was performed under unidirectional wave by Newmark's Beta approach. The wave forces were estimated by Morison's equation using Airy's wave theory. The Mathieu instability for the spar platform was investigated by Koo et al. (2004) for long period regular wave environment and swell condition. The damping effects of spar hull, mooring lines, and risers were evaluated. Jameel et al. (2011) studied nonlinear fully coupled analysis of integrated spar and mooring lines. The behaviour of spar platform after long period of wave hitting was assessed.

The analysis of conventional processes states that, the force and displacement of mooring heads and vessel fairleads are iteratively matched at every instant of time marching scheme while solving the equilibrium equations. In this process the major contribution of moorings in terms of drag, inertia, and damping due to their longer lengths, larger sizes, and heavier weights are not fully incorporated. This effect is more prominent in deep water conditions. The conduct at longer time state on spar-mooring system may be severe. Hence, the objective of present study is the prediction of nonlinear fully coupled analysis of spar hull and mooring line response subjected to waves with or without current. The present study is also observed the damping effects on mooring lines and the importance of coupling effect on spar platform during long period of wave hitting.

2.8 Artificial Neural Network in Offshore Structure

Artificial Neural Networks (ANNs) are widely used across all disciplines of coastal, ocean, marine, and offshore engineering. Several researchers who did their work using ANN, such as Mahfouz (2007), presented a method of predicting the capability-polar-plots for dynamic positioning systems for offshore platforms, stability analysis of the rubble mound breakwater (Mandal et al., 2007), estimating the cost, uncertainties and

risk analysis of floating structures (Cocodia, 2008), identifying the crack extent and location of damage on the longitudinal faceplate of ship's structure (Zubaydi et al., 2002). ANN was also used to predict the risk of different pipe sticking in the Iranian offshore oil field (Miri et al., 2007). The researchers used neural network for offshore structures to solve their problems during 1996-2012 (Table 2.2).

Table 2.2 Summary of offshore structural research using ANN

Researchers	Types of work	Types of offshore structure	Input variable	No. of hidden layer/ neuron	Transfer fun. hidden: output	Training Algorithm	Outputs
Mangal et al. (1996)	Damage Detection	Jacket platform	Varies on networks	3/NA	hard limiters, sigmoid: hyperbolic tan	BPN and ART	1
Lopes and Ebecken (1997)	Fatigue monitoring	Jacket platform	14	2/8	Sigmoid: sigmoid	FFBPN	1
Diao et al. (2005)	Damage localiza-tion	Jacket platform	3	3/NA	Sigmoid: sigmoid	BPN and PNN	1
Elshafey et al. (2010)	Damage detection	Jacket platform	2	1/NA	Sigmoid: sigmoid	BPN	1
Chang et al. (2009)	Response control	Jacket platform	2	1/ 5	NA	MLPBPN	1
Yan-jun et al. (2010)	Vibration control	Jacket platform	3	NA	NA	FFOC	1
Ma et al. (2006)	Optimal control	Jacket platform	1	NA	NA	FFOC	1
Elshafey et al. (2011)	Prediction of force and moment	Jacket platform	3	1/50	hyperbolic tangent: sigmoid, linear	FFN	2
Mazaheri et al. (2005)	Prediction of response	FPSO	6	1/10	Sigmoid: sigmoid	MLFFN	3
Mazaheri (2006)	Prediction of response	FPSO	6	1/10	Sigmoid: sigmoid	MLFFN	3
Haddara et	Response	Ship	4	1/5	Sigmoid:	MLPNN	1

al. (1999)	prediction				sigmoid		
Xu and Haddara (2001)	Estimating bending moment	Ship	6	1/24	Sigmoid: linear	MLPNN, BP	1
Guarize et al. (2007)	Response prediction	FPSO	3	1/ 2, 3, 10	hyperbolic tangent: linear	Non-linear differential equation	1
Simoes et al. (2002)	Response prediction	FPSO	6	1/4, 6, 9	NA	MLPBPN	3
Pina et al. (2010)	Response prediction	FPSO	3	1/10	hyperbolic tangent	FFMLP, LMBP	1

NA-Not Available, ART-Adaptive resonance theory; BPN-Back-propagation network; FFBPN-Feed-forward back-propagation network; FFN-Feed-forward network; FFMLP-Feed-forward multilayer perceptron; FFOC-Feed-forward and feedback optimal control; LMBP-Levenberg-Marquardt back-propagation; MLFFN-Multilayer feed-forward network; MLPBPN-Multilayer perceptron back-propagation network; MLPNN-Multilayer perceptron neural network; PNN-Probabilistic neural network;

In the field of offshore engineering, ANN is used for damage detection, time series prediction, and controlling in cases where formal analysis is tough or impossible. ANNs have been used to solve these types of offshore engineering problems which are categorically reviewed below.

2.8.1 Controlling

The safety of offshore structures is of significant concern under the oceanic environmental load. The reduction of the dynamic response of offshore structures subjected to random ocean waves has been a critical issue in terms of serviceability, fatigue life, and safety of the structure. Chang et al. (2009) used modified probabilistic neural network (MPNN) for controlling the response of fixed offshore structures subjected to random ocean waves. Linear quadratic regulator algorithm was used to calculate the control forces and to verify the proposed offshore structural control

method under random ocean wave. Significant decreasing rates for the structural responses proved that the MPNN control algorithm is an effective vibration control technique.

Hong-nan and Lin-sheng (2003) presented the control method for fixed offshore platforms using semi-active tuned liquid column damper (TLCD). Back-propagation neural network (BPNN) was used to adjust the orifice opening of TLCD because of the nonlinear motion of liquid in TLCD. The control method was verified by numerical examples efficiently.

Ya-jun and De-you (2003) proposed a new active control scheme on the basis of neural network for the suppression of oscillation in multiple-degree-of-freedom offshore platforms. After that, Ya-jun et al. (2003) presented classical optimal control using ANN for active structural control of offshore platforms under random waves. BPN algorithm was used for active control according to the robustness, fault tolerance, and generalized capability of ANN. The result shows that active control was feasible, effective, and overcame time delay of classical algorithms.

Wei and Gong-you (2004) investigated the optimal control for linear systems affected by external harmonic disturbance and applied it to vibration control systems of offshore steel jacket platforms using ANN. It was established that the control scheme was useful in reducing the displacement response of these platforms.

Ma et al. (2006); Ma et al. (2009) studied the vibration control with an active mass damper of a jacket-type offshore platform and presented a feed-forward and feed-back optimal control (FFOC) law under irregular waves. The reductions of the lateral deck motion under different control laws were compared. The simulation shows that the

FFOC law was more efficient and robust than the classical-state feed-back optimal control (CFOC) law.

Cui and Zhao (2007) proposed a rough neural network, as an adaptive predictive inverse controller, for active control of offshore platform under the combined action of random waves and winds. The result showed that the proposed networks had high training speed and enhanced robustness. The displacement response of top platform was effectively controlled and the time delay was sufficiently suppressed. This method also possesses strong anti-disturbance capability.

Hong-yu et al. (2009) proposed an adaptive inverse control method on the basis of novel rough neural networks (RNN) to control the harmful vibration of the jacket platform. The jacket platform model was established by dynamic stiffness matrix method. The constructed novel RNN has advantages such as clear structure, fast training speed, and strong error-tolerance ability.

Kim et al. (2009) applied a new neuro-control scheme to the vibration control of a fixed offshore platform under random wave loads to examine the applicability of the Lattice Probabilistic Neural Network (LPNN). The results of LPNN showed better performance in effectively suppressing the structural responses in a shorter computational time.

According to Yan-Jun et al. (2010), the nonlinear pile-soil interactions were strongly influenced by the wave load disturbances of jacket platform. The Morison equation was used to estimate the wave load disturbances. Results of feed-forward and feed-back vibration control for a 7 lumped masses jacket-type offshore platform was significantly effective.

Hong-yu and De-you (2010) proposed a grey neural network and its application, as an adaptive predictive inverse controller, which was implemented to vibration control of

jacket offshore platform. The simulation results show that the grey neural network has strong robustness and can effectively control the displacement of jacket offshore platform under the random loads.

Lin (2010), Ma et al. (2009a; 2009b) utilized the neural network to identify the loads and measure the vibration of WZ12-1 offshore platform. A three-layer BP network has been trained up to the state when the data obtained from ANSYS were converged. The result shows that the neural network method could gain a great advantage over the traditional techniques in these large and complex problems.

2.8.2 Prediction

Offshore structures are subjected to environmental loads such as wind loads, wind generated wave excitations, and current forces. The dynamic response prediction of offshore structures in a random environment is a significant aspect of design.

Yun and Bahng (1997) presented a method for sub-structural identification of offshore structure using ANN. BPNN was used to estimate the number of unknown parameters of jacket platform. The result shows that the proposed method effectively demonstrated the identification of the sub-structure.

Mandal et al. (2004) addressed the prediction of stress resultant deflection of fixed offshore platform under varying sea environment using neural networks. With the data of deck displacements at various loading state, a BPNN was first trained and later prediction of the deck displacements were obtained for any loading condition. The result showed that prediction of deck displacement was significantly accurate.

Yasseri et al. (2010) proposed a predictive method for identifying the range of sea-states considered safe for the installation of offshore structures using FEM and ANN. A finite element dynamic analysis on a table of some safe and unsafe sea-states has been prepared based on the pile allowable stress. MLFFNNs were used to determine whether the predicted sea-state is safe or not.

Simoes et al. (2002) developed a neural network for prediction of mooring forces and analysis of the dynamic behaviour of FPSO and a shuttle ship in tandem configuration. MLPBP algorithm was used for developing the neural network. This approach was suitable for preventing collisions of the ships and maintenance of mooring line.

Mazaheri et al. (2005; 2003) proposed the response-based hydrodynamic model named SAMRES to calculate responses of a floating offshore platform subjected to arbitrary wind, wave, and current loads. SAMRES model was written in MATLAB to determine the loads and motions of a turret-moored FPSO over a reasonable period of environmental data (e.g. 5 years). Multilayer feed-forward algorithm was used in ANN model to predict the platform's responses subjected to metocean parameters. The resulting vessel response predicts the extreme excursion and mooring force over an N-year life period. After that, Mazaheri (2006) applied mooring force of floating offshore structures on his SAMRES model as an example.

Guarize et al. (2007) proposed hybrid ANN – Finite Element Method (FEM) approach for the prediction response (top tension) of mooring line and risers of FPSO. A quite short FEM-based time domain response of slender marine structure was trained by ANN. Hyperbolic tangent function was used for non-linear dynamic response prediction of mooring line and riser for long time. It was observed that the proposed ANN–FEM methodology was about 20 times faster than a full FEM-based analysis for a 3 h long dynamic response simulation.

Pina et al. (2010) developed a model with application of surrogate models on the basis of ANN to predict response of offshore structures, replacing dynamic analyses with FEM. FEM analysis time series data were used in nonlinear autoregressive model (NARX) and prescribed motion inputs (PMI). For the testing model, the authors used mooring line of FPSO. Results have shown that ANNs are very efficient in predicting response accurately in considerably less time.

Elshafey et al. (2011) provided a deck acceleration measurement tool to predict the value of the force and moment acting on the offshore structure's foundation subjected to wind generated wave excitations. Neural networks and Fokker-Planck formulation methods were used to determine the relationship between the force and moment acting on the foundation and deck acceleration. The total virtual mass of the equivalent single degree of freedom formulation of the structure was determined at different deck masses.

2.8.3 Damage Detection

Offshore structures subjected to hostile environmental loads can experience critical damage due to fatigue and ship collision. All kinds of damage should be identified quickly so that corrective actions can be taken to overcome disastrous failures. As a result, it is customary to ensure reliable monitoring and competent system for such structures.

Wu et al. (1992) developed automatic monitoring methods using neural network for the detection of structural damage. BPNN was used to recognize the behaviour of an undamaged structure and observed the behaviour of the structure with different probable damage states. It was found that the network had the potential to detect any existing damage.

Mangal et al. (1996) proposed a theory named Adaptive resonance theory (ART) for online monitoring of damage detection and its location for jacket platforms. BPN and ART networks were used for comparison of damage detection. ART networks work on the principle of pattern recognition. It has the ability to be trained with new data or to adapt itself to new conditions. Speech recognition and object identification problems can be easily explained with BPN. It was suitable to use both BPNs and ART simultaneously for good results.

Banerji and Datta (1997); Idichandy and Mangal (2001) used ANN for monitoring the integrity of an offshore structure. Feed forward neural network algorithm was used for pattern recognition and comparing RMS displacement responses at different elevations of the structure for various sea states.

Lopes and Ebecken (1997) proposed a method using neural network for fatigue monitoring of jacket platform. Automatic fatigue data is being gained on board and performed in-time on the actual loading condition. Finite element method and stochastic fatigue analysis were used for fatigue damage calculation. The results clearly indicated that the fully connected network produced smaller errors and better performance.

Mangal et al. (2001) investigated a laboratory jacket platform model to access the feasibility of adapting vibration responses due to impulse and relaxation for on-line structural monitoring. Effects of damage in six members of the platform and changes in deck masses were studied. A finite-element model of the structure was used to analyze all the cases for comparison of the results and system identification.

Fathi and Aghakouchak (2007) developed four MLP networks to predict weld magnification factor for weld toe cracks in T-butt joints under membrane and bending loading for offshore structure. The training data for these networks were obtained from

results of finite element modeling. The comparison between network results and fatigue life was reported in experiments, which shows that neural network is a successful prediction technique if properly used in this area.

Moghim et al. (2007); Shafiefar et al. (2011); Shafiefar and Moghim (2005); Zhou and Luan (2009) used ANNs to predict hydrodynamic forces generated by waves and current forces on slender cylinders. The laboratory experimental data was used to train and evaluate the prediction performance of the ANNs. Results indicated that ANN is able to efficiently predict the waves and current forces on slender cylinders after performing proper training.

Zeng et al. (2001); Diao et al. (2005); Diao and Li (2006) proposed a method named probabilistic neural networks (PNN) for the damage localization of fixed platform. The members of offshore platform structure were classified and separated into several layers. And the decision system for the type and layer of damaged members was established using the BPN. The experimental results show that the trained neural networks are able to detect the damages with reasonable accuracy.

Elshafey (2009, 2010) evaluated the behaviours of damage detection in random loading by the combined method of random decrement signature and neural networks. The random decrement technique was used to extract the free decay of the structure from its online response while the structure was in service. The free decay and its time derivative were used as inputs for a neural network. The output of the neural network was used as an index for damage detection. It has been shown that function N (number of segments) was effective in damage detection in the members of an offshore structure.

Zhen and Zhigao (2010) proposed the time-domain response data with noise measurement, under random loading, for detecting damage of offshore platforms. A

sensitivity matrix consisting of the first differential of the autoregressive coefficients of the time-series models with respect to the stiffness of the structural elements was then obtained based on-time domain response data. Numerical simulation showed that with only a handful of sensors, acceleration time history data with a certain level measurement noises is capable of detecting damages efficiently, and that an increase in the number of sensors helped in improving the diagnosis success rate.

2.8.4 Other Application

ANNs can provide meaningful solutions and can process information in extremely rapid mode ensure high accuracy of prediction. A great deal of research has been carried out using ANN to solve offshore Engineering problem.

Xu and Haddara (2001) developed the time-domain technique for estimating the wave-induced vertical bending moment from coupled heave and pitch motions of ship hull. A MLPNN was employed and a back-propagation learning algorithm was used for the network training. The training results show that the computational time was significantly reduced and the accuracy was improved.

Haddara et al. (1999) studied the derivation of partial differential equations describing the free response of a heaving and pitching ship from its stationary response to random ocean waves. The coupled heave–pitch motion of a ship in random seas was modeled as a multi-dimensional Markov process. The method has shown good results when the system is lightly damped.

Yamamoto et al. (2002) described new dynamic positioning technology for a tandem type floating offloading system using a neural network. The effects on total operation

performance resulting from this technology were evaluated by simulation for the northern area of the North Sea, i.e. the area offshore of Borneo and Pearl River Basin.

Cepowski (2010); Islam et al. (2001) used artifical intelligence techniques for automatic hull form generation of ships with some desired performances. Genetic Algorithm is one of the important elements for design and implementation of hull. Neural network is a very good tool for readjusting the dimensions of hull. In this process hull form was generated automatically and accurately.

A dynamic position controller was designed using a neural network, and several model experiments under beam sea conditions were carried out to verify its ability (Nakamura et al., 2003). The calculated results were in good agreement with experimental results.

CHAPTER 3.0 RESEARCH METHODOLOGY

3.1 Introduction

This chapter discusses environmental force prediction by neural network and the use of the predicted values for response prediction of spar platform using FEM and ANN. The fully coupled dynamic analysis of spar platform subjected to regular wave has been discussed in this chapter. These FEM results are used to train the Resp-Pred network and then to predict the response of spar platform to environmental forces.

3.2 Environmental Forces

Environmental force is a natural phenomenon, which may lead to structural damage, operation disturbance and loss of life. The important phenomena for offshore structures are wind, wave, and currents. The large waves are usually generated by winds associated with storms passing over the surface of the sea. However, the complexity and uncertainty of the wave generation phenomenon is such that even with significant advances in computational methods, the solutions obtained are neither exact nor uniformly applicable. Prediction of wave height and period from wind is basically an unreliable and random practice and hence difficult to model by using deterministic equations. Neural networks are suitable to model a random input with the corresponding random output and their application does not require knowledge of the underlying physical process as a necessity. This attainment of reliable wave height and wave period is used for the purpose of response prediction of offshore structures by FEM and ANN.

3.2.1 Data Collection

The location of offshore Sarawak (longitude 111°E, latitude 6°N) (Jameel et al., 2012), Malaysia is selected on the basis of possible existing as well as future oil and gas exploration and production activities. The locations of these data are illustrated in Figure 3.1. The environmental data is collected from this location due to monitor of existing offshore structures and possible future installation of offshore structure for the purpose of oil and gas exploration.

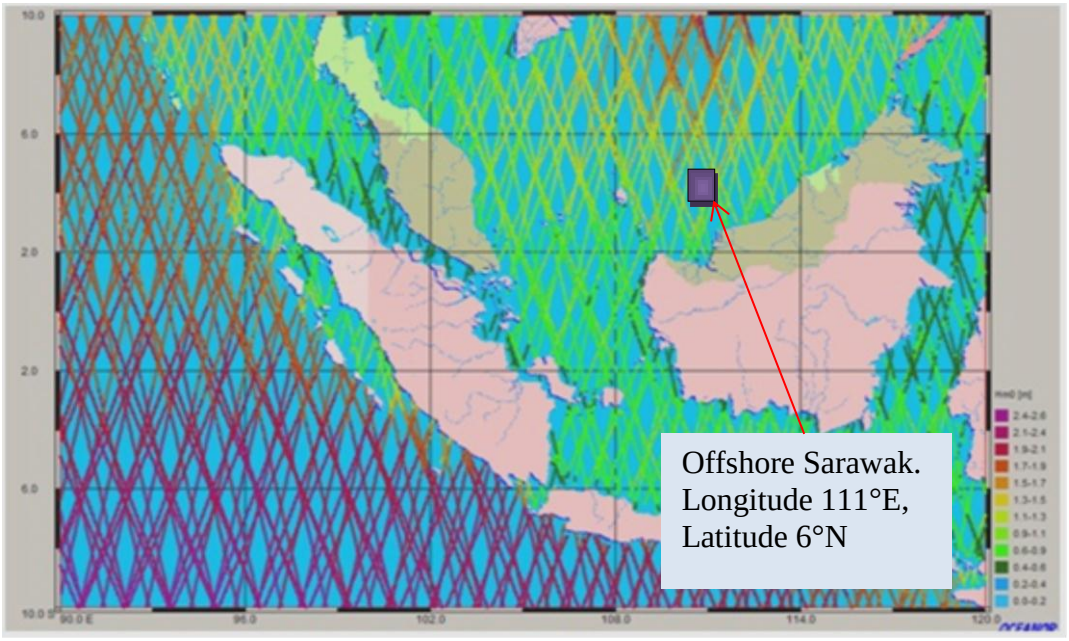

Figure 3.1: Data collection location of the South China Sea, Projecting Malaysia (WAM data from ECMWF)

In this study, high quality met-ocean data have been collected from WAM data from ECMWF which is calibrated against satellite data. These data have been acquired at 6-hour intervals for the period of January 1997 to December 1997. The wind force at 10 m height of sea surface and wave height, as well as wave period, have been collected from the South China Sea which is around Malaysia.

3.2.2 ANN Architecture for Environmental Forces

This study is carried out to predict maximum wave height and period from wind force of Malaysian sea using ANN. There are three layers of the ANN architecture, namely input, output, and hidden layer. The wind force is used as input and the wave height as well as wave period are used as output for training the network. The total number of data set is 1460, among them 992 number of data are used for training, 234 number of data are used for validation and 234 number of data are used for testing. This approach is schematically shown in Figure 3.2.

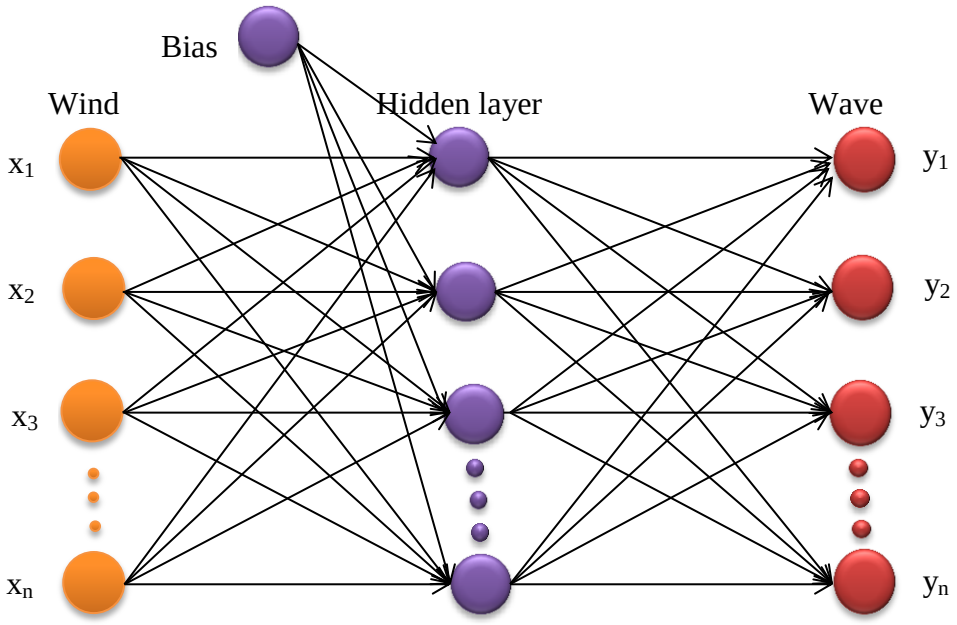

Figure 3.2: ANN architecture for environmental force.

Two models are considered for achieving better performance of the network. The first one uses a neural network as a nonlinear auto regressive network model (NARX) which has exogenous input. The network consists of a Multilayer Perceptron which takes input of past input and output values and computes the current output. The input to the feed-forward network is more accurate. In this network 5 neurons are used in hidden layer with sigmoidal activation function and 2 steps delay are used. The network weights and bias are randomly adjusted and the training algorithm used is the Levenberg-Marquardt

back-propagation (Hagan et al., 1996; Hagan and Menhaj, 1994). The resulting network has purely feed-forward architecture, and static back-propagation can be used for training.

The second one uses a neural network as a feed-forward back-propagation neural network model (NEWFF) which is most widely used in offshore engineering problems. In this network, 30 neurons are used in the hidden layer with tangent sigmoid activation function, and pure linear activation function is used in the output layer. The network weight and bias values are randomly initialized and the training algorithm used is the Levenberg-Marquardt back-propagation. This algorithm is considered the fastest for training feed-forward neural networks and it does not require more memory.

The expected outputs are in difference with the network output and generate error which is minimized by adjusting the weights and biases though training algorithms. The network is found by trial and error method. After training the network, ANN is used to predict wave height and wave period from randomly selected wind force.

The validation of the ANNs is performed in terms of the root mean square error RMSE, scatter index SI, and correlation coefficient R, computed as follows:

$$Bias = \frac{1}{N}\sum_{i=1}^{N}(y_i - x_i) = \bar{y} - \bar{x} \tag{3.1}$$

$$RMSE = \sqrt{\frac{\sum_{i=1}^{N}(y_i - x_i)^2}{N}} \tag{3.2}$$

$$SI = \frac{RMSE}{\bar{x}} \tag{3.3}$$

$$R = \frac{\sum_{i=1}^{N}(x_i - \bar{x})(y_i - \bar{y})}{\sqrt{\sum_{i=1}^{N}(x_i - \bar{x})^2 \sum_{i=1}^{N}(y_i - \bar{y})^2}} \tag{3.4}$$

where x_i is the value observed at the i^{th} step, y_i is the value simulated at the same point, N is the number of increments, $\bar{x}$ is the mean value of observations, and $\bar{y}$ is the mean value of simulations.

3.3 Finite Element Method

3.3.1 Model of Spar Platform

For this study, a spar platform is selected in 1018 m deep water. Spar platform consist of three major parts, i.e. spar hull, mooring line, and riser. The mechanical and geometrical properties of the spar mooring system are given in Table 3.1. Table 3.2 illustrates the hydrodynamic characteristics of the sea environment.

The spar hull is modeled as rigid beam which is anchored at fair lead position and seabed by mooring lines. The rigid Spar platform has been connected to the elastic mooring lines by means of six springs (three for translations like surge, sway, heave, and three for rotations such as roll, pitch, yaw). The individual stiffness of the translation springs is very high, whereas those of the rotational springs are very low, simulating a hinge connection.

The mooring lines are modeled such that they can incorporate all types of significant nonlinearities. It includes the nonlinearities due to low strain large deformation and fluctuating pretension. Hybrid beam element is used to model the mooring lines. It is hybrid because it employs two shape functions one for simulating elastic behaviour while the other for simulating the axial tension to maintain the catenary shape of mooring line. The hybrid beam element is selected for easy convergence, other elements such as linear or nonlinear truss elements can also be considered.

Seabed is modeled as a rigid plate. The contact between mooring lines and seabed is such that, the mooring lines will not penetrate the seabed. The contact is modeled as surface to surface and friction-less. Circumferential surface of mooring line and surface of seabed are selected for contact interaction. The integrated spar hull and mooring line have been modeled in finite element code ABAQUS (Figure 3.3).

Table 3.1: Mechanical and geometrical properties of spar and moorings (Jameel et al., 2011)

Description		Unit	Value
Sea-bed size		m^2	5000 × 5000
Spar (Classic JIP Spar)	Length	m	213.044
	Diameter	m	40.54
	Draft	m	198.12
	Mass	kg	2.515276E8
	Mooring Point	m	106.62
	No. of Nodes		17
	No. of Elements		16
	Type of Element		Rigid beam element
Water Depth		m	1018
Mooring	No. of Moorings		4
	Stiffness (EA)	N	1.50E9
	Length	m	2000.0
	Mass	Kg/m	1100
	Mooring line pretension	N	1.625E7
	No. of Nodes		101
	Element Type		Hybrid beam element

Table 3.2: Hydrodynamic properties (Jameel et al., 2011)

Description	Coefficient	Value
Spar	Drag	0.6
	Inertia	2.0
	Added mass	1.0
Mooring line	Drag	1.0
	Inertia	2.2
	Added mass	1.2

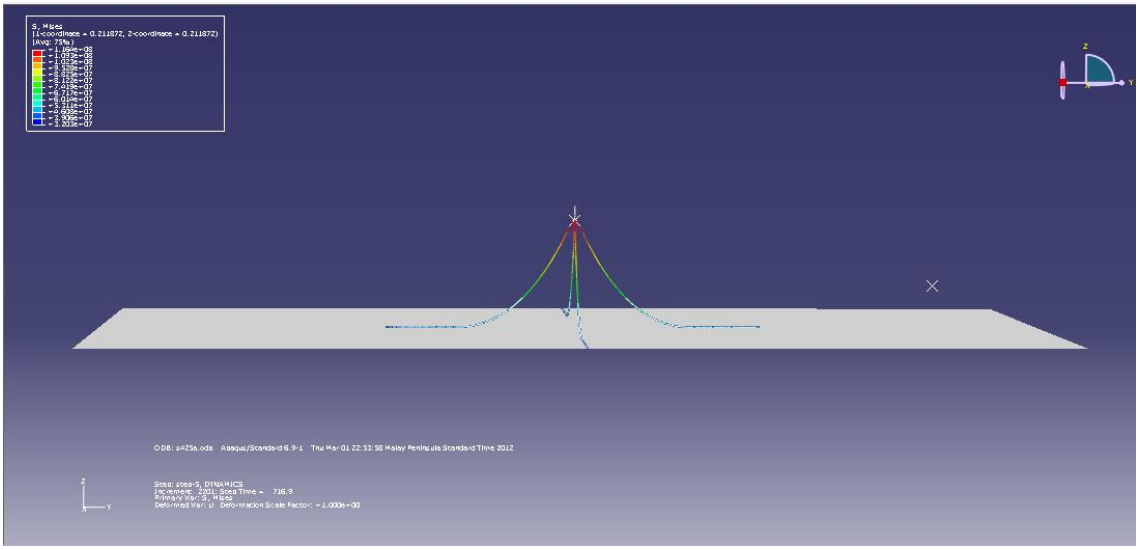

Figure 3.3: Finite element model of Spar platform in ABAQUS

3.3.2 Finite Element Analysis

The finite element model is used to implement the fully coupled integrated spar hull and mooring line under regular waves and current forces. The analysis of spar platform is considered actual physical coupling between the rigid vertical floating hull and mooring lines. This model can handle all nonlinearities, loading, and boundary conditions (Jameel, 2008). The effect of integrated coupling, employed in the present study is investigated to show the importance of drag damping of mooring systems in deep-sea

conditions. The finite element code ABAQUS/AQUA is used to obtain the response of spar platform.

The basic aim of this analysis is to obtain the proper catenary shape of mooring line under self-weight, axial tension, and stiffness associated with its mean curvature. The state of equilibrium is finally achieved when spar cylinder is slowly released under buoyancy. The dynamic analysis is carried out under regular sea. The most common approach for solving the dynamics of spar platform is to employ a decoupled quasi-static method, which ignores all or part of the interaction effects between the platform and mooring lines. To obtain the mooring line responses, the motions of the platform are applied as external loading in terms of forced boundary conditions in a separate detailed finite element model of catenary mooring line. Therefore, the dynamic interaction among platform and mooring lines are not properly modeled in the conventional uncoupled analysis. For platform in deeper waters, mooring lines generally contribute significant inertia and damping due to their longer lengths, larger sizes, and heavier weights. Accurate motion analysis of platform in deep waters requires that these damping values be included.

Coupling analysis, which includes the mooring lines and platform in a single integrated model, is a realistic way to capture the damping due to mooring lines in a consistent manner. This approach yields dynamic equilibrium between the forces acting on the platform and the mooring line at every time station. The outputs from such analyses will be platform motions as well as a detailed mooring line response. The computational efforts required for the coupled system analysis considering a complete model including all mooring lines are substantial and should, therefore, be considered as a tool for final verification purposes. The ability for more accurate prediction of platform motions by coupled analysis approach may consequently contribute to a smaller and less expensive

mooring and riser system, and hence, a lighter spar platform through a reduction in payload requirements.

The static and dynamic loads are applied, as required by the analysis. This technique is more accurate because the stress and stiffness associated with the mean curvature are automatically included in the model. Wave and current loads on the mooring lines are completed at each time step. The wave height and wave period are specified in the numerical data of published literature (Jameel and Ahmad, 2011).

3.3.3 Nonlinearities

The analysis of spar platform turns out to be a complex procedure, primarily because of the uncertainties associated with the environmental loads and system configuration. The problem is further compounded by the nonlinearities in the system, leading in some cases, to resonant slow drift and high frequency responses. The non-linear behaviour is due to the variable submergence, added mass variation, damping, geometric non-linearity, interaction of mooring line with seabed, and forces acting on the structure.

3.3.4 Mathematical Formulation

In this section, the dynamic equations for catenary mooring lines and spar hull have been derived. Combined equations of motion of spar hull and mooring lines have been generated accordingly. Three dimensional models of spar-mooring line system have been considered.

The formation of a nonlinear deterministic model for coupled dynamic analysis includes the formulation of a nonlinear stiffness matrix allowing for mooring line tension fluctuations subjected to variable buoyancy as well as structural and environmental

nonlinearities. The model involves selection and solution of Airy wave theory that reasonably represents the water particle kinematics to estimate the drag and inertia for all the six degrees of freedom. The static coupled problem is solved by Newton's method. In order to incorporate high degrees of nonlinearities, an iterative time domain numerical integration is required to solve the equation of motion and to obtain the response time histories. The Newmark-β time integration scheme with iterative convergence has been adopted for solving the coupled dynamic model. The equation of motion describing the spar hull- catenary mooring lines equilibrium between inertia, damping, restoring, and exciting forces can be assembled as follows:

$$[M]\{\ddot{X}\}+[C]\{\dot{X}\}+[K]\{X\}=\{F(t)\} \tag{3.5}$$

Where

$\{X\}$ = 6 DOF structural displacements at each node

$\{\dot{X}\}$ = Structural velocity vector

$\{\ddot{X}\}$ =Structural acceleration vector

[M] =Total mass matrix= [M] Spar+ Mooring lines + [M] Added mass

[C] = Damping Matrix= [C] Structural damping+[C] Hydrodynamic damping

[K] =Stiffness matrix= [K] Elastic+ [K] Geometric

Total force on the spar hull and mooring lines is denoted by $\{F(t)\}$. The dot symbolizes differentiation with respect to time. The total spar platform mass matrix of the system consists of structural mass and added mass components. The structural mass of the spar platform is made up of elemental consistent mass matrices of the moorings and lumped mass properties of the rigid spar hull. The lumped mass properties are assumed to be

concentrated at the Center of Gravity (CG) of spar hull. The added mass of the structure occurs due to the water surrounding the entire structure. Considering the oscillation of the free surface, this effect of variable submergence is simulated as per Wheeler's approach.

The total stiffness matrix element [K] consists of two parts, the elastic stiffness matrix [KE] and the geometrical stiffness matrix [KG]. The major damping is induced due to the hydrodynamic effects. It may be obtained if the structure velocity term in the Morison equation is transferred from the force vector on right hand side to the damping term on the left hand side in the governing equation of motion. The structural damping is simulated by Rayleigh damping. It follows the following equation (3.6) in which ξ is the structural damping ratio, Φ is modal matrix, ω_i is natural frequency, and m_i is generalized mass.

$$\Phi^T [C]^{Structural} \Phi = [2\xi\omega_i m_i] \tag{3.6}$$

Morison's equation is considered to be adequate in calculating hydrodynamic forces. For mooring line element, the ratio of the structure dimension to peak wave length is small. The wave loads on a structure are computed by integrating forces along the free surface centerline from the bottom to the instant free surface at the displaced position. As the diameter of the mooring line is small in comparison to the length of the wave encountered, the distortion of the waves by the structure is negligible.

3.4 Resp-Pred ANN Approach

The main idea is to generate a Resp-Pred approach using ANN to predict response of the spar platform. This approach predicts surge, heave, and pitch responses of spar hull and top tension of mooring line from environmental and structural parameters. The

network is created separately for each response. The response network architecture and activation function is same. There are 10-18 sets of data train in these networks. Each set of input data having 22 numbers of environmental and structural parameters (Table 3.1 and Table 3.2). The wave height and wave period of environmental force are variable, structural parameters are kept unchanged. The responses of surge, heave, pitch and top tension are used as target which is obtained from FEM. Each set of target data contains 3000 sec time histories of response that are used for training the network. The data is randomly divided, 70% for training, 15% for validation, and 15% for testing. It is noted that the input and target data are normalized within the range -1 to 1 by the function *mapminmax*, before training the network. The equation is as follows:

$$y = \frac{(y_{\max} - y_{\min}).(x - x_{\min})}{x_{\max} - x_{\min}} + y_{\min} \tag{3.7}$$

where *y* is the normalized value, *x* is the measured value, *ymax*, *ymin*, *xmax*, *xmin* are the maximum and the minimum values of environmental and structural parameters. Finally, input and target data are arranged for the neural network by the following format:

$$[y_{11} \quad y_{12} \quad y_{13} \quad \cdots \quad y_{1\times n}]$$

$$= \begin{bmatrix} x_{11} & x_{12} & x_{13} & \cdots & x_{1\times n} \\ x_{21} & x_{22} & x_{23} & \cdots & x_{2\times n} \\ x_{31} & x_{32} & x_{33} & \cdots & x_{3\times n} \\ \vdots & \vdots & \vdots & \ddots & \vdots \\ x_{22\times 1} & x_{22\times 2} & x_{22\times 3} & \cdots & x_{22\times n} \end{bmatrix} \begin{bmatrix} w_{11} & w_{12} & w_{13} & \cdots & w_{1\times 22} \\ w_{21} & w_{22} & w_{23} & \cdots & w_{2\times 22} \\ w_{31} & w_{32} & w_{33} & \cdots & w_{3\times 22} \\ \vdots & \vdots & \vdots & \ddots & \vdots \\ w_{n\times 1} & w_{n\times 2} & w_{n\times 3} & \cdots & w_{n\times 22} \end{bmatrix} \tag{3.8}$$

where x is the input matrix, and w is the weight matrix, and y is the target matrix.

A feed-forward back-propagation neural network with an input layer, one hidden layer having 20 neurons with hyperbolic tangent sigmoid activation function, and output layer with pure linear activation function, is used. The network weight and bias values are randomly initialized and the training algorithm used is the Levenberg-Marquardt back-

propagation. If the ANN result differs from the desired output response, the network generates an error. This error is utilized to adjust the connection weights between the target response and output response. The network is developed by trial and error method and the weights are calculated on the basis of gradient optimization method. Subsequently, the network performance is measured by the mean square error (MSE).

3.5 Hybrid FEM-ANN Approach

This study predicts mooring line response long time history from hull response short time history of spar platform using hybrid FEM-ANN approach, which was used by Guarize, et al. (2007) and Pina, et al. (2010). There are three layers of neural network having input, hidden layer with hyperbolic tangent function, and output using pure linear function, which is considered in the present study (Figure 3.4).

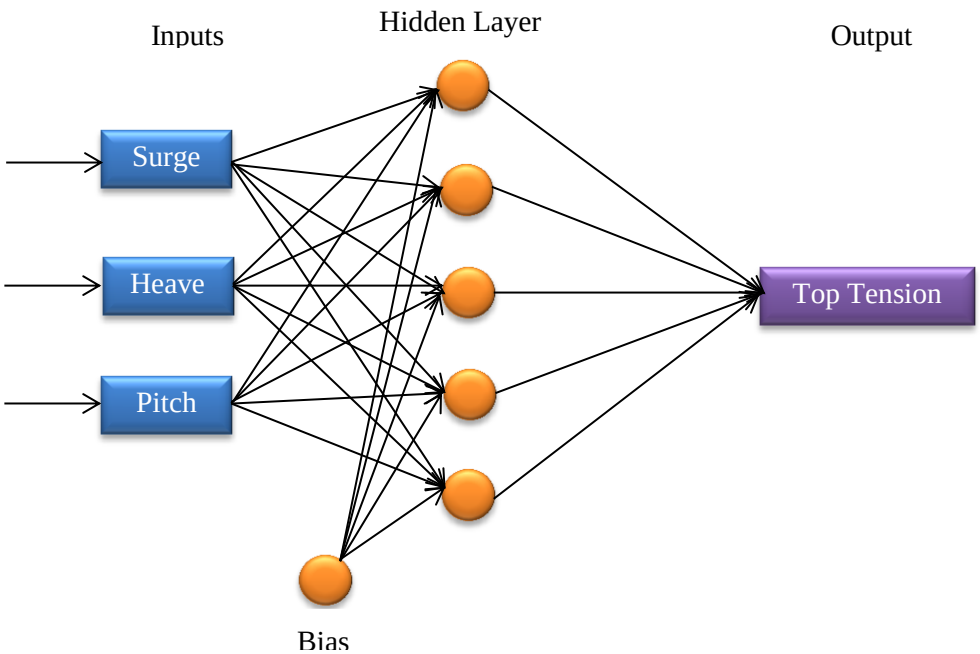

Figure 3.4: Neural Network Architecture

The responses such as surge, heave, and pitch of spar hull are obtained from FEM. Non-linear dynamic response time histories are used as input in ANN for training the network. Mooring line top tension time history is used in ANN as target for training, which is obtained from FEM. In this study FEM based response is trained by ANN for short simulation length. The ANN is capable of predicting long response time histories in dynamic analysis of spar mooring lines. The hybrid approach is schematically shown in Figure 3.5.

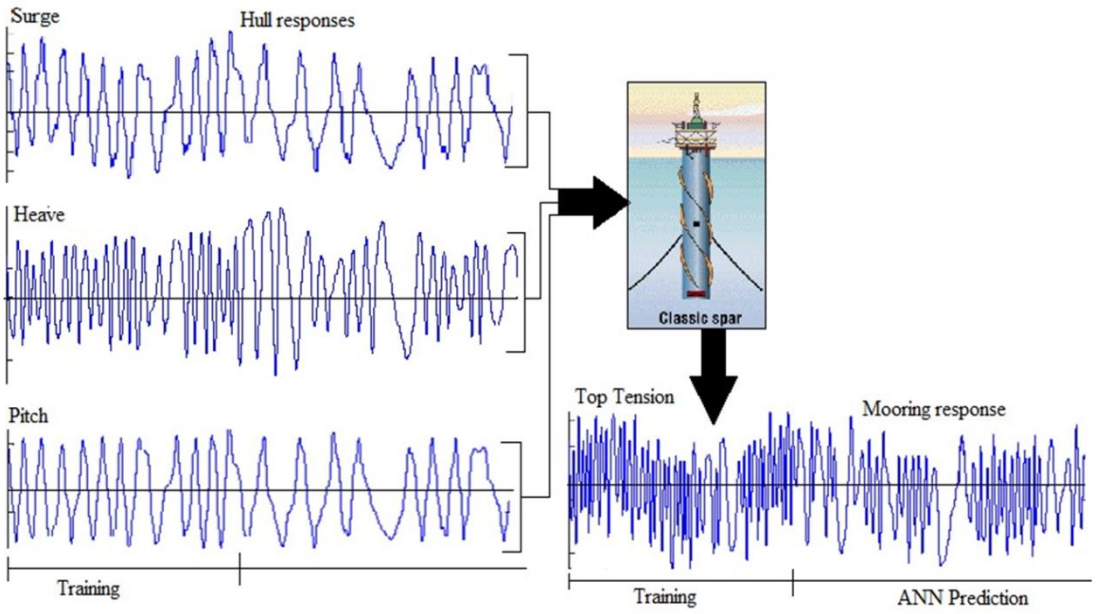

Figure 3.5: Hybrid FEM-ANN approach

In a dynamic analysis, output response depends not only upon their current values but also on their previous values. The input for the ANN is formed as follows:

$$r(t) = f(x(t), x(t-\Delta t), \ldots\ldots x(t-N_x\Delta t),$$
$$y(t), y(t-\Delta t), \ldots\ldots y(t-N_y\Delta t),$$
$$z(t), z(t-\Delta t), \ldots\ldots z(t-N_z\Delta t) \qquad (3.9)$$

where r(.) is the top tension response estimated by ANN; x*(t),* y*(t),* and z*(t)* are surge, heave and pitch response time histories, Δt is the time step, and N_x, N_y, and N_z are the number of delays for surge, heave, and pitch.

Nonlinear auto regressive network model algorithm (NARX) is used to train ANN architecture. If the response of top tension differs from the desired output response, the network generates an error. This error is utilized to adjust the connection weights between the target response and the output response. The network is developed by trial and error method and the weights are calculated on the basis of gradient optimization method.

CHAPTER 4.0 RESULTS AND DISCUSSIONS

4.1 Introduction

This chapter presents the technique of how ANN is applied to predict environmental forces like maximum wave heights and wave periods from wind speeds of Malaysian sea. The environmental forces are used to analyze of spar platform by using FEM commercial software ABAQUS/AQUA. For this analysis, a classical spar platform is considered in 1018 m water depth. Response time history of spar and mooring lines under regular waves as well as with currents are obtained by FEM. The obtained results of spar platform responses are used to train the network and predict responses from new environmental forces. Also, presented in this chapter is long time history response prediction of spar mooring line from short time history response of spar hull using ANN.

4.2 Prediction of Environmental Forces by ANN

The present study involves the prediction of wave parameters from randomly selected wind force using ANN. The wind force at 10 m height of sea surface and wave height as well as wave period are collected from the South China Sea which is projecting Malaysia (WAM data from ECMWF). Maximum wave height and wave period are predicted using ANN and wind force is used as input. The training data set consists of approximately 1460 samples. Two types of algorithms of ANN are used to create network, there are nonlinear autoregressive network with exogenous inputs (NARX) and feed-forward back-propagation network (NEWFF). The wave parameters of ocean and wind force are used to train NARX and NEWFF networks with 3 and 30 neurons in

hidden layer respectively. The number of hidden neurons is obtained by trials and it is expected to get a minimum value of means square error (MSE) at the end of a sufficiently large number of training iterations.

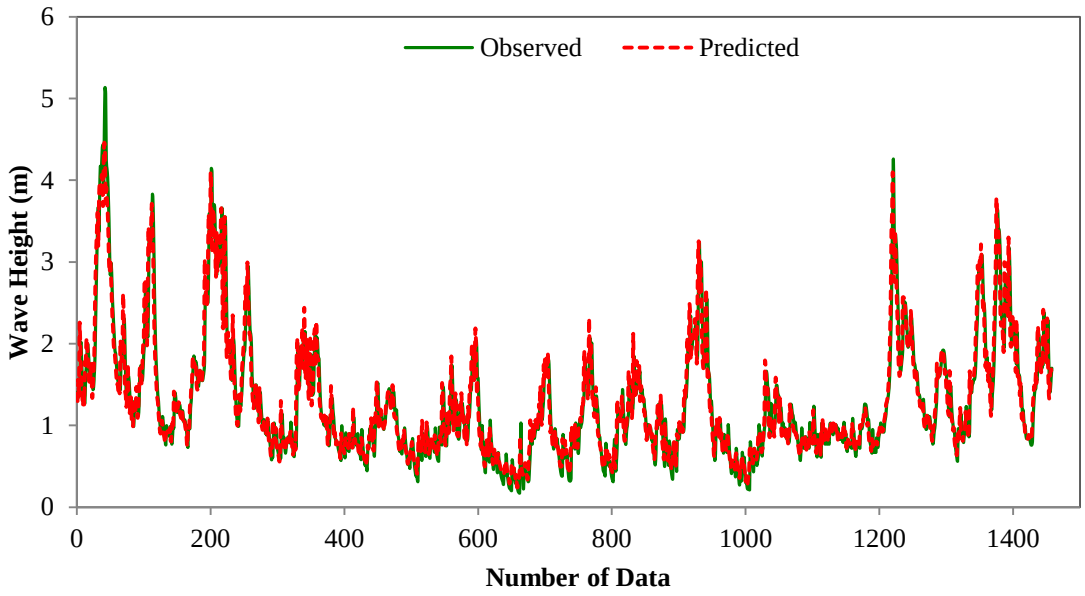

Figure 4.1: Maximum observed and predicted wave height by NARX network, from training data.

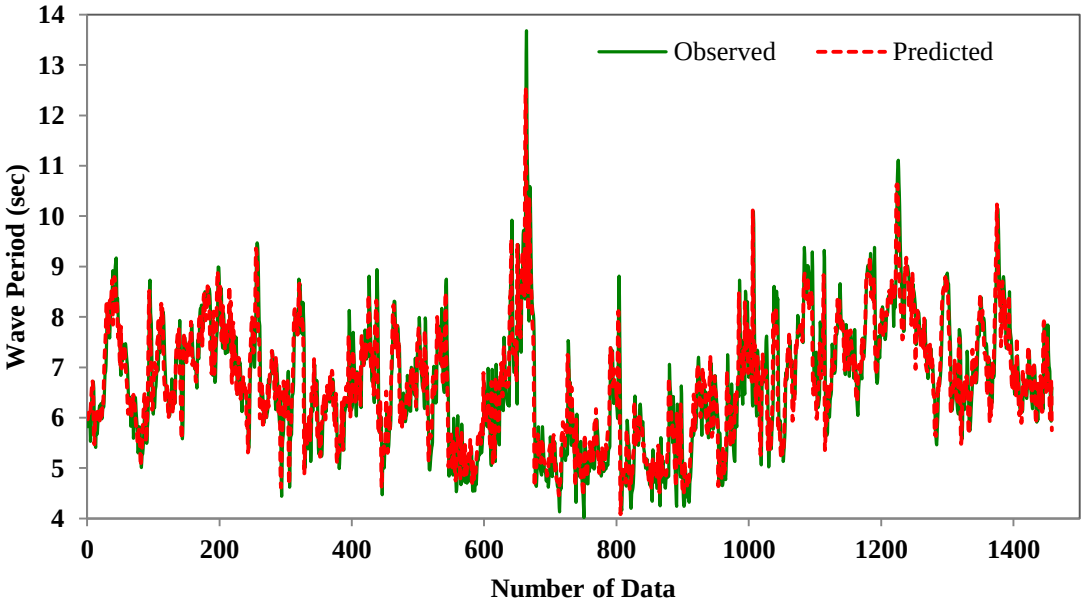

Figure 4.2: Maximum observed and predicted wave period by NARX network, from training data.

An NARX network employed in this study is trained in 436 training epochs. The gradient of the performance function is close to 0 after 436 training epochs. Figures 4.1 and 4.2 shows that well convergence of observed maximum wave height and wave period with respect to the predicted wave height and wave period by using NARX network respectively. It may be seen that the network's predictions are close to their observed values. In order for the parallel response (iterated prediction) to be accurate, it is important that the network be trained so that the errors in the series-parallel configuration are very small. Average prediction error is less than ±1% and this model can also predict wave parameters with reference to randomly selected wind forces.

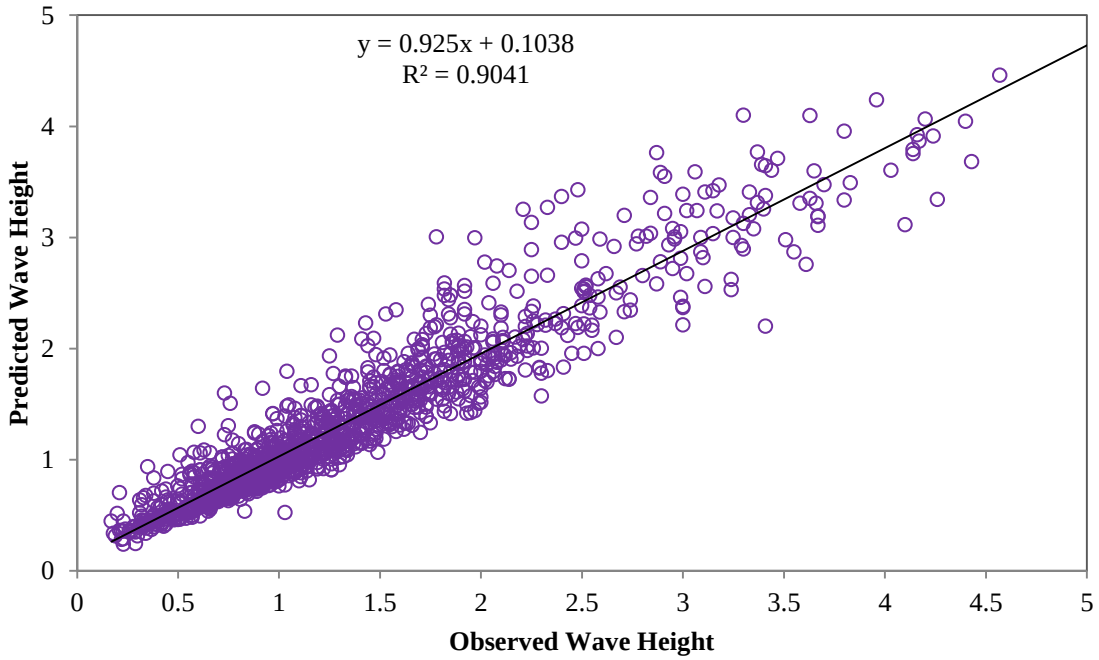

Figure 4.3: Comparison between the observed and NARX network predicted wave height, from training data.

A comparison between the observed and nonlinear dynamic network predicted wave height and wave period are shown in Figure 4.3 and 4.4, respectively. In these figures, training data is plotted for the network outputs and the expected outputs of wave

parameters. In Figures 4.3 and 4.4, the results of Y factors predicted by this NARX network versus observed values and the corresponding trend lines are shown.

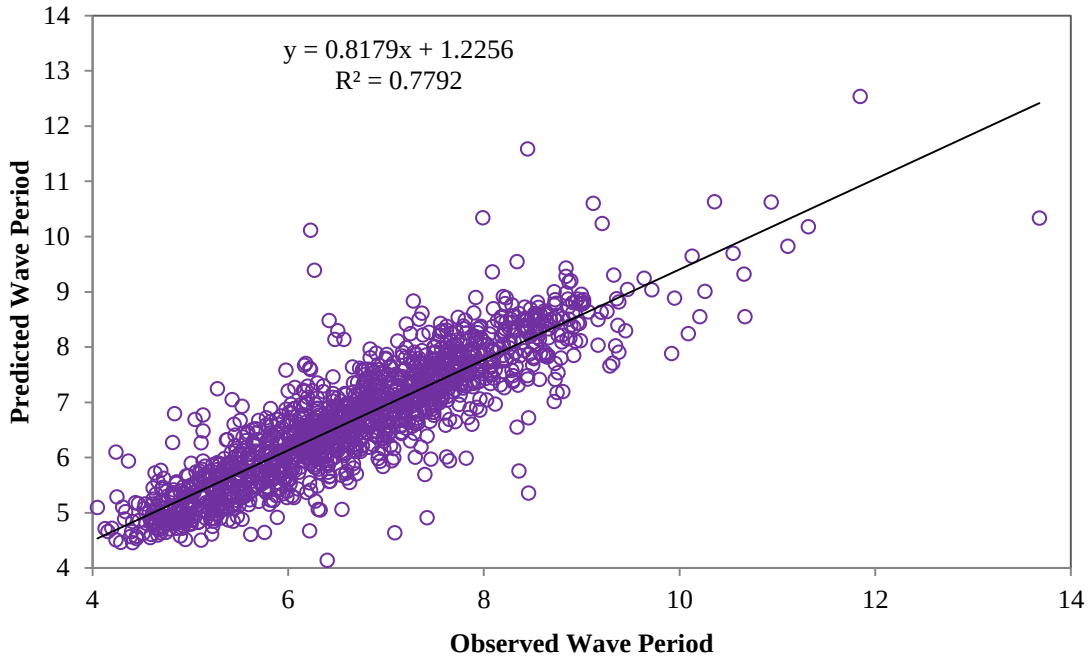

Figure 4.4: Comparison between observed and NARX network predicted wave period from training data.

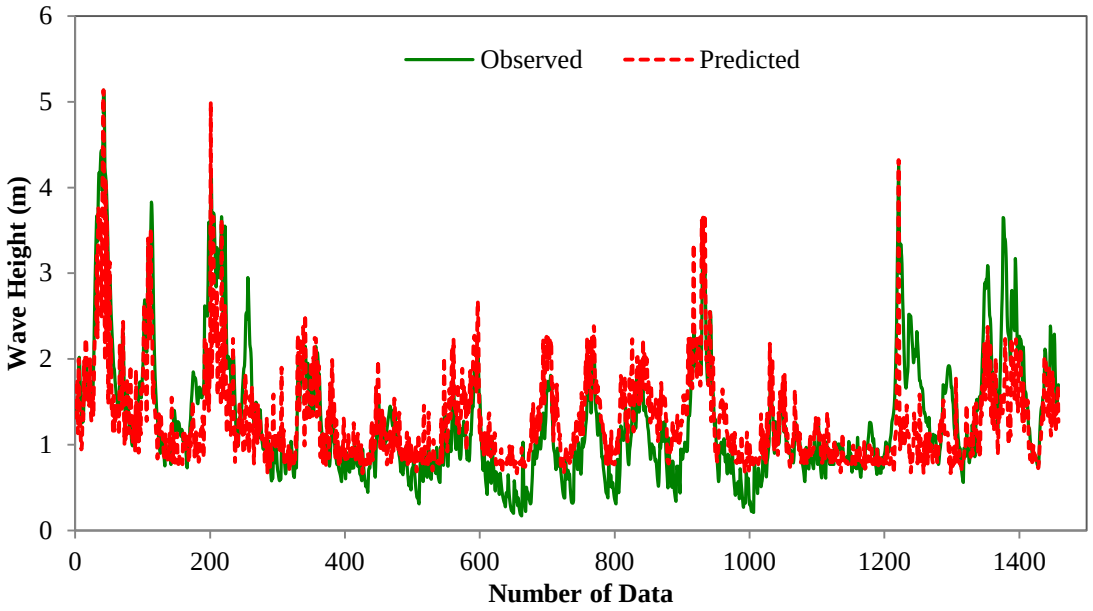

Figure 4.5: Maximum observed and NEWFF network predicted wave height from training data.

In the current research, a feed-forward back-propagation neural network is introduced, which is trained in 364 training epochs. After 364 training epochs, gradient of the performance function is adjacent to 0. The convergence of observed maximum wave height and wave period with respect to the predicted wave height and wave period by using NEWFF network is shown in Figure 4.5 and 4.6, respectively. For this case, NEWFF network predicted results are close to observed wave height and wave period, although the precision obtained is a little bit poorer than NARX network predicted results. This model is able to predict wave parameters with reference to randomly selected wind forces.

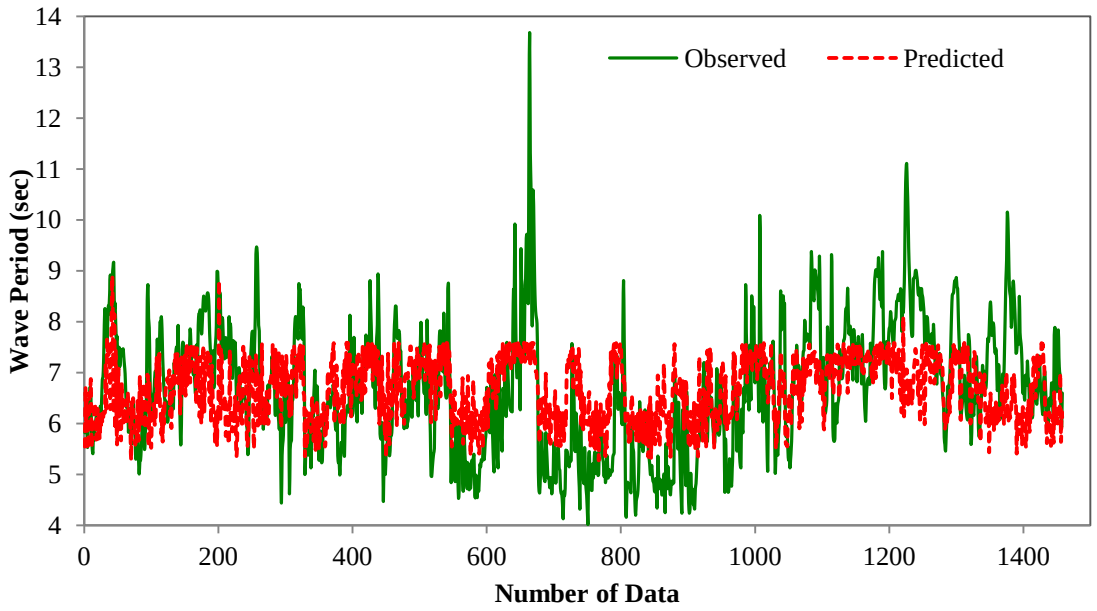

Figure 4.6: Maximum observed and predicted wave period by NEWFF network, from training data.

The comparison between the observed and NEWFF network predicted wave height and wave period is explained in Figure 4.7 and 4.8 respectively. In these figures, training data is plotted for the network outputs and the expected outputs of wave parameters. The results of Y factors predicted by this NEWFF network versus observed values and the corresponding trend lines are plotted in Figure 4.7 and 4.8.

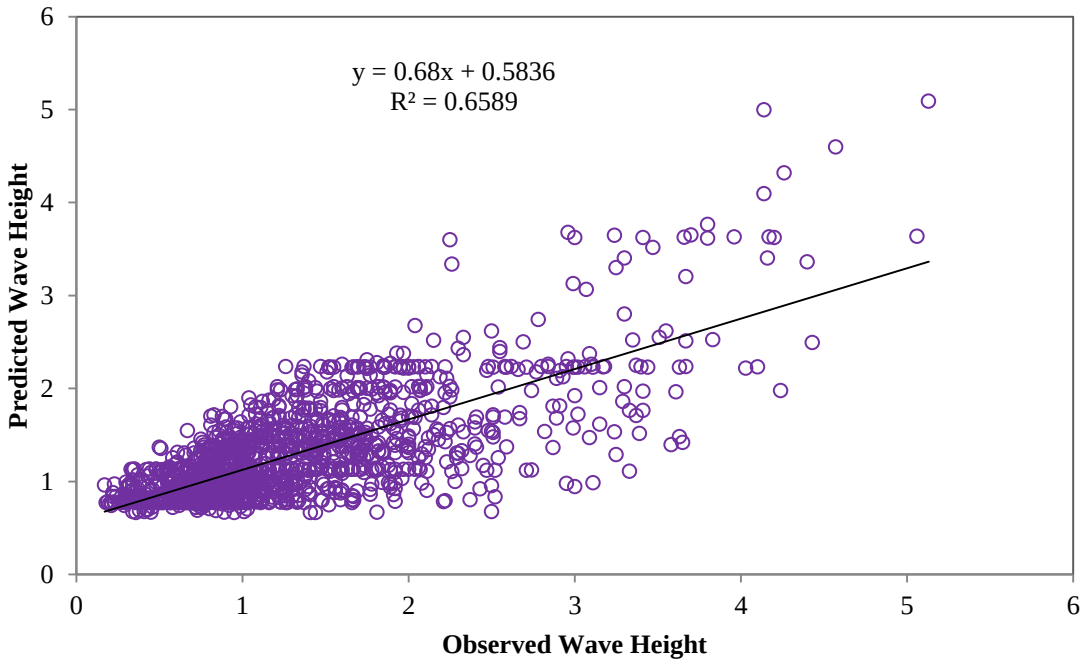

Figure 4.7: Comparison between observed and NEWFF network predicted wave height, from training data.

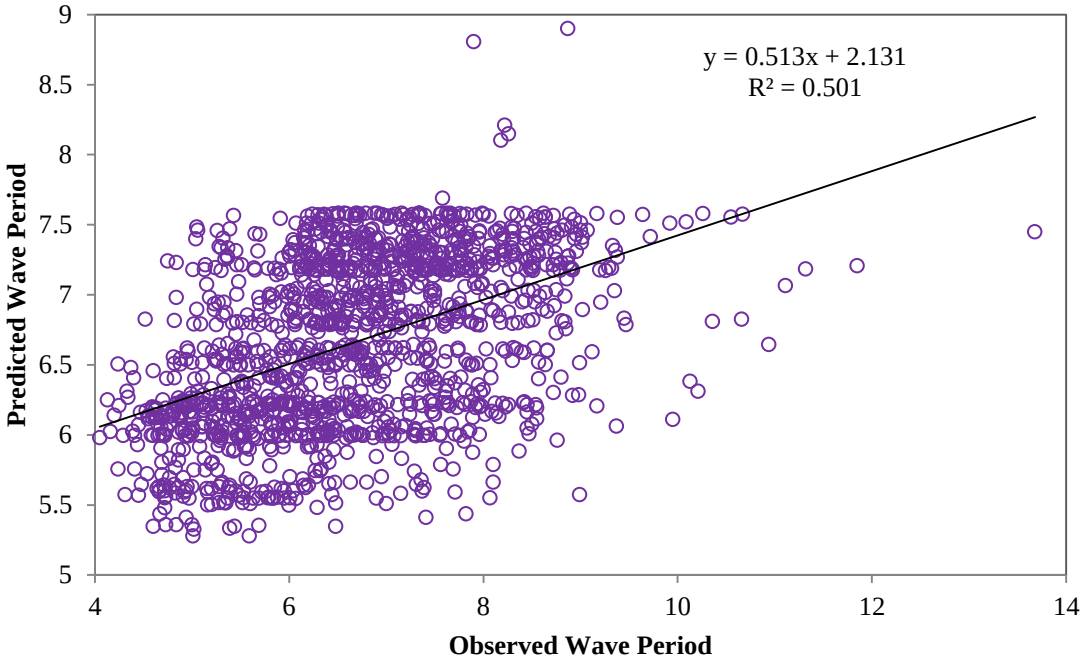

Figure 4.8: Comparison between observed and NEWFF network predicted wave period from training data.

The overall accuracies of the predictions are found to be good both cases, NARX and NEWFF networks. Error criteria are evaluated which are shown in Table 4.1 as statistical parameters of the network outputs and the expected outputs, from the training data. The NARX network results are better compared to the NEWFF network predictions of wave height and wave period as revealed in the higher value of the correlation coefficient 0.996 and 0.989, respectively. Correlation coefficient of NEWFF network predicted wave height and wave period is 0.741 and 0.731, respectively.

Table 4.1 Statistical Comparison between predicted and observed wave parameters incorporating different algorithms

Algorithm	Parameter	MaxE	MinE	StdevE	RMSE	Bias	SI	R
NARX	Wave Height (m)	0.3368	-0.4832	0.0662	0.0673	0.0123	0.052	0.996
	Wave Period (sec)	0.6969	-2.1046	0.2078	0.2106	0.0344	0.032	0.989
NEWFF	Wave Height (m)	2.403	-1.3215	0.5058	0.5057	0.0009	0.393	0.741
	Wave Period (sec)	5.6458	-2.5775	0.8469	0.8466	0.0024	0.127	0.731

Here RMSE is root mean square error, SI is scatter index, R is correlation coefficient.

Table 4.2 shows that prediction of wave parameter from randomly selected wind force in different algorithms. From Table 4.1, and Figures 4.9 and 4.10 display that predictions of wave height and wave period for NARX network showed good statistical performance, despite some discrepancies between the predicted and observed wave height and wave period from new randomly selected wind force. On the other hand, a NEWFF network result of statistical performance is not good, but prediction of wave height and wave period from new randomly selected wind force is show good performance.

Table 4.2: Prediction of wave parameters from randomly selected wind force by incorporating different algorithms

Wind Force (m/sec)	Wave Height (m) (NEWFF)	Wave Height (m) (NARX)	Wave Height (m) (Observe)	Wave Period (sec) (NEWFF)	Wave Period (sec) (NARX)	Wave Period (sec) (Observe)
11.25	1.977	2.746	1.89	5.549	6.008	5.53
10.57	2.230	2.872	1.86	6.215	6.591	5.67
10.04	2.234	2.865	2	6.406	6.250	5.83
14.43	3.766	2.875	3.8	7.689	8.094	7.58
13.86	3.633	2.790	4.17	7.456	7.431	7.96
12.52	2.619	2.689	2.5	6.267	7.030	6.2
11.73	2.502	2.590	2.69	6.289	6.791	6.55
10.98	2.400	2.610	2.55	6.378	6.962	6.62
13.93	3.653	2.643	3.7	7.469	7.194	7.38
13.47	3.623	2.570	3	7.450	6.843	6.19
9.86	2.194	2.475	2.47	6.337	6.568	7.5
8.03	3.482	3.584	3.63	9.109	9.852	9.95
9.79	2.107	2.518	2.23	6.193	7.201	6.46
5.04	1.146	2.609	1.63	6.235	7.490	7.01
8.7	1.899	1.642	1.74	6.143	6.826	6.23
14.22	4.097	3.744	4.14	8.149	8.045	8.26
10.27	2.736	2.675	2.95	7.354	7.387	7.34
10.51	3.231	2.979	3.02	7.218	7.466	7.49
11.23	3.008	2.704	3.15	7.597	7.511	7.37
13.8	3.627	3.735	3.66	7.452	7.532	7.62

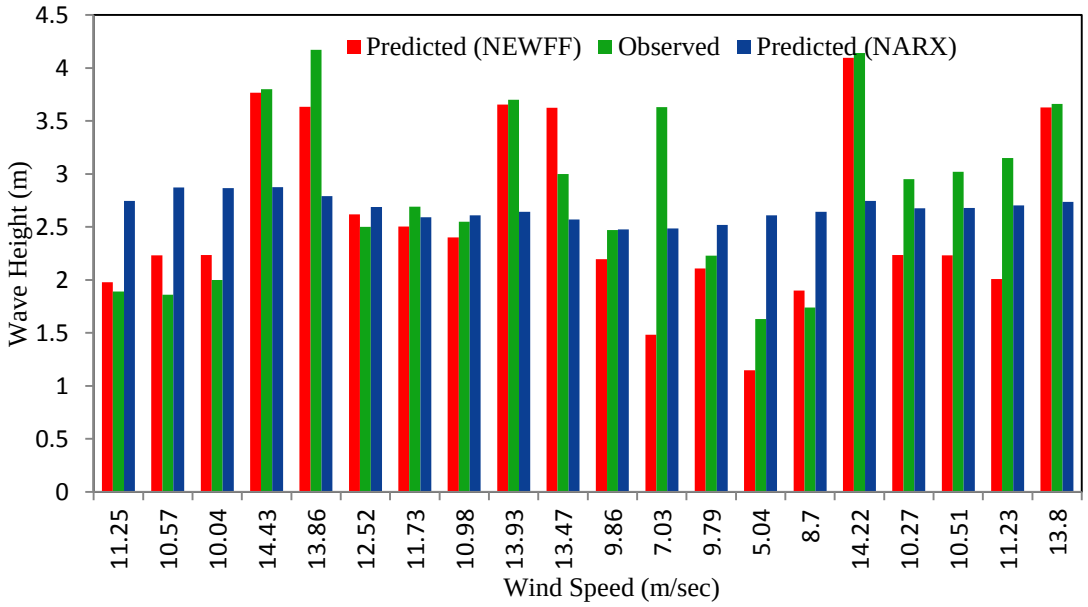

Figure 4.9: Variation of observed and predicted wave height from randomly selected wind force.

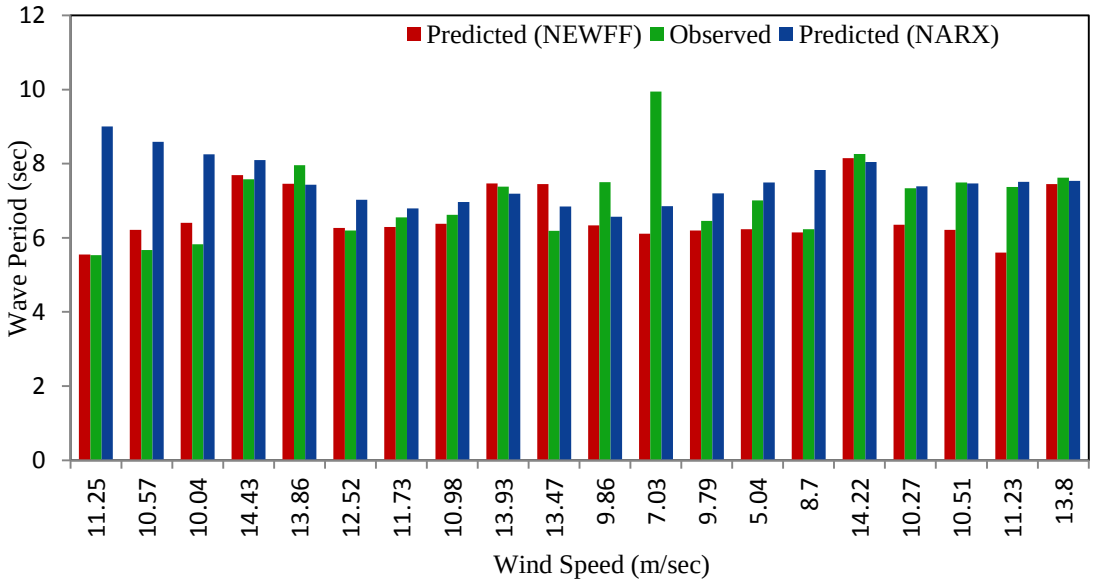

Figure 4.10: Variation of observed and predicted wave period from randomly selected wind force.

4.3 Finite Element Analysis of Spar Platform

In this part of the study, a fully coupled analysis of spar hull and mooring line as a single integrated model is performed. This approach carries dynamic equilibrium between the forces acting on the spar hull and the mooring line at every time step. It gives true behaviour of spar hull and mooring line system and an accurate way to capture the damping. The ability for more accurate prediction of spar platform motions can be obtained by fully coupled analysis approach. The selected configuration of the spar platform is analysed under loading by regular wave as well as regular wave plus current and its structural response behaviour is studied. Integrated fully coupled analysis of spar hull and mooring line system is performed for 1018 m water depth. The application example is associated with the prediction of response of spar hull and mooring line, wave height 7.0 m and wave period 12.5 sec is considered for both cases and current speed is 0.9 m/sec. The wave data is considered for the response analysis in the Morison's regime and the small time step is considered to ensure statistical stability of the structure and accuracy of the solution (Jameel et al., 2011).

4.3.1 Dynamic Response in Regular Wave

The response analysis of spar hull and mooring lines subjected to regular wave in deep water conditions have been performed by FEM. The results are obtained at deck level which is plotted at both the time history 5000 to 6000 sec and up to 12000 sec. Relative valuation for surge, heave, pitch motion responses as well as top tension are carried out in terms of time history and spectral density. Statistical analysis results in terms of max, min, mean and standard deviation are given in Table 4.3.

Table 4.3: Statistical response of spar hull and mooring lines

Wave Ht.=7.0 m Wave Pr.=12.50 sec	Max	Min	Mean	Standard deviation
Surge (m)	+18.09	-17.25	0.41	4.66
Heave (m)	+1.56	-1.87	0.03	0.38
Pitch (rad)	+0.12	-0.11	-0.00004	0.04
Mooring line Tension (N)	1.70E+07	1.12E+07	1.62E+07	3.08E+05

4.3.1.1 Surge Response

The surge response of spar platform under regular waves is intensely influenced at the deck level. The surge response time history at the deck level is shown in Figures 4.11 and 4.13. The peak of surge response ranges from +18.09 m to -17.25 m for wave height 7.0 m and wave period 12.5 m which is shown in Table 4.3.

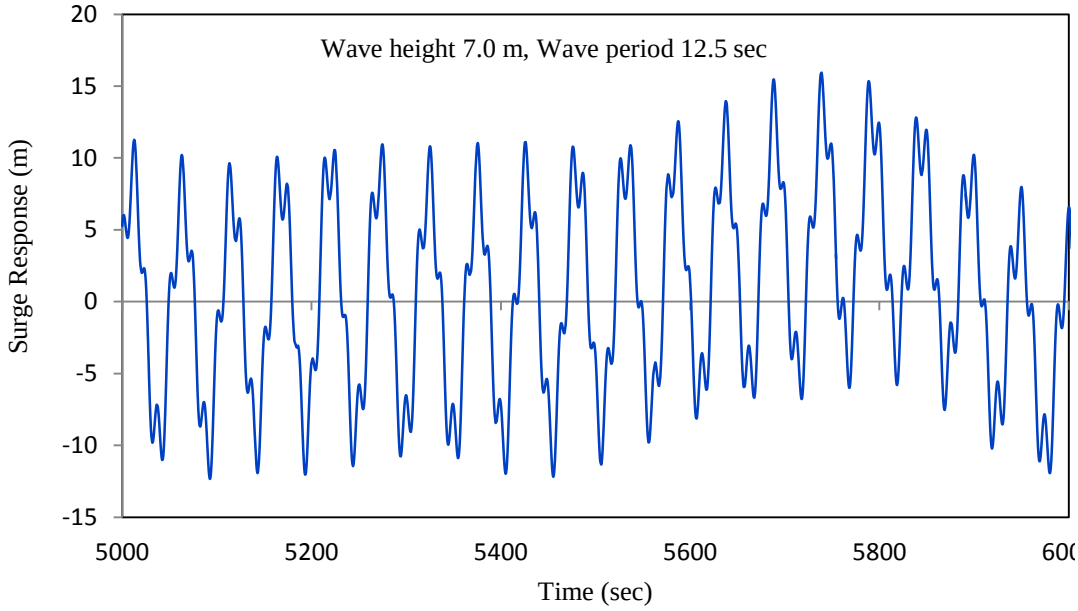

Figure 4.11: Surge response time history (5000-6000 sec)

At the deck level, the behaviour of surge is found to be mostly periodic. Hence a single dominant peak arises in surge response at pitching frequency which can be observed from Figure 4.12. The surge and pitch response occur simultaneously and attracts wave energy similar to the pitch frequency. The surge response at the deck level is principally controlled by the pitching motion of the hull with insignificant excitation of surge mode. It is mainly due to coupling of surge and pitch.

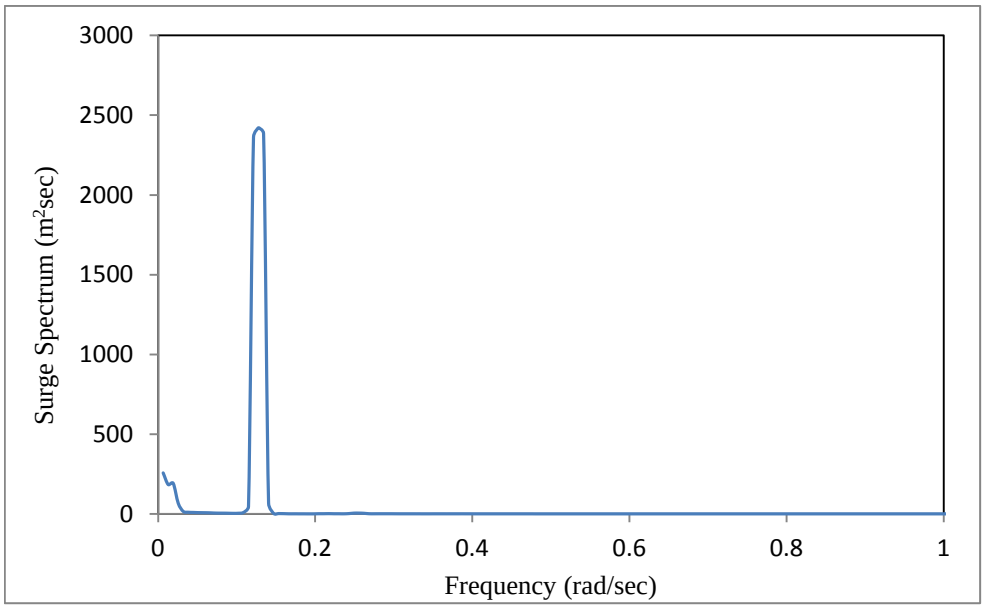

Figure 4.12: Surge spectral density for 5000-6000 sec

The spectral density as shown in Figure 4.12 shows the contribution of two frequencies. At a frequency of 0.01 rad/sec, the small oscillation of the harmonic response takes place due to the natural frequency. The spectral density shows clearly peak frequency at 0.14 rad/sec. It is clear that effect of non-linearity is not so strong on surge response. Figure 4.13 shows that 0 to 12000 sec time history of surge response behaviour is typically regular. At the end of 9000 sec of surge response time history, the platform oscillations takes place in regular intervals with maximum and minimum values of +5.09 and -4.84 m, respectively.

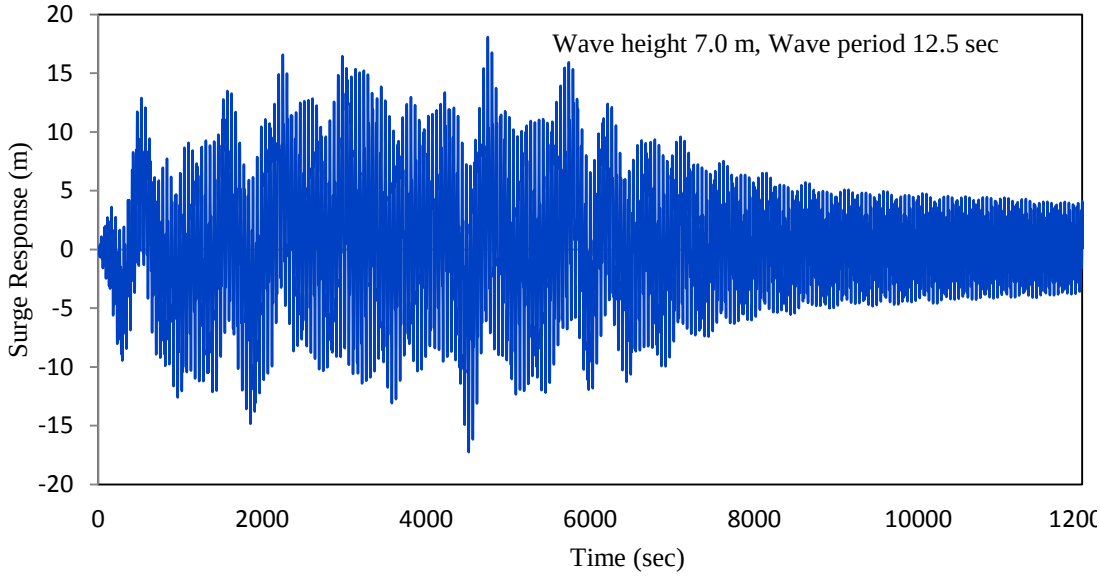

Figure 4.13: Surge response time history (0-12000 sec)

The spectral density of the surge time history from 9000 to 10000 sec shows one peak (Figure 4.14) at 0.128 rad/sec. This peak frequency occurred due to natural frequency of surge. While the spar hull undergoes a static off-set at time state 9000 sec, the coupled stiffness matrix of the spar mooring system significantly changes. The forces in the mooring lines and their geometry changes substantially. It does happen so that the mooring lines become taut, when the system oscillates about the static off-set position. As a result nonlinearities and regularity are more appreciable.

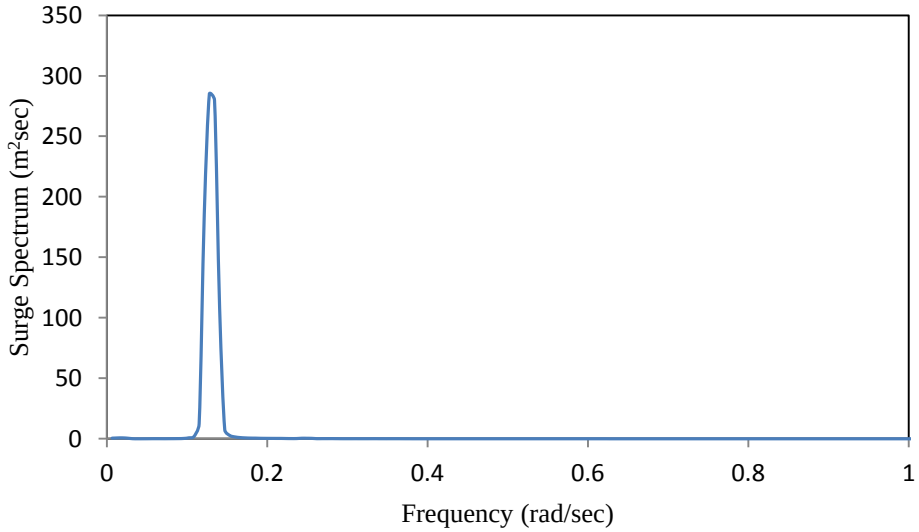

Figure 4.14: Surge spectral density for 9000-10000 sec

4.3.1.2 Heave Response

The spar mooring lines are directly affected by heave (vertical motion) response. Figure 4.15 shows the heave responses time history (5000-6000 sec) under regular wave. The time history shows a regular phenomenon with the cluster of reversals occurring at fluctuating time intervals. The statistical summary of heave response, which is shown in Table 4.3, illustrates that the maximum and minimum responses are 1.56 m and –1.87 m, whereas the mean value is 0.03 and standard deviation is 0.38. Fluctuation of heave response from small to large amplitude with respect to the mean position and iteration of the similar trend forwards all through the time history is shown in Figure 4.15. The fluctuations in amplitude of the heave response gradually increases and decreases from tapered to wider shape by 30 % and vice versa.

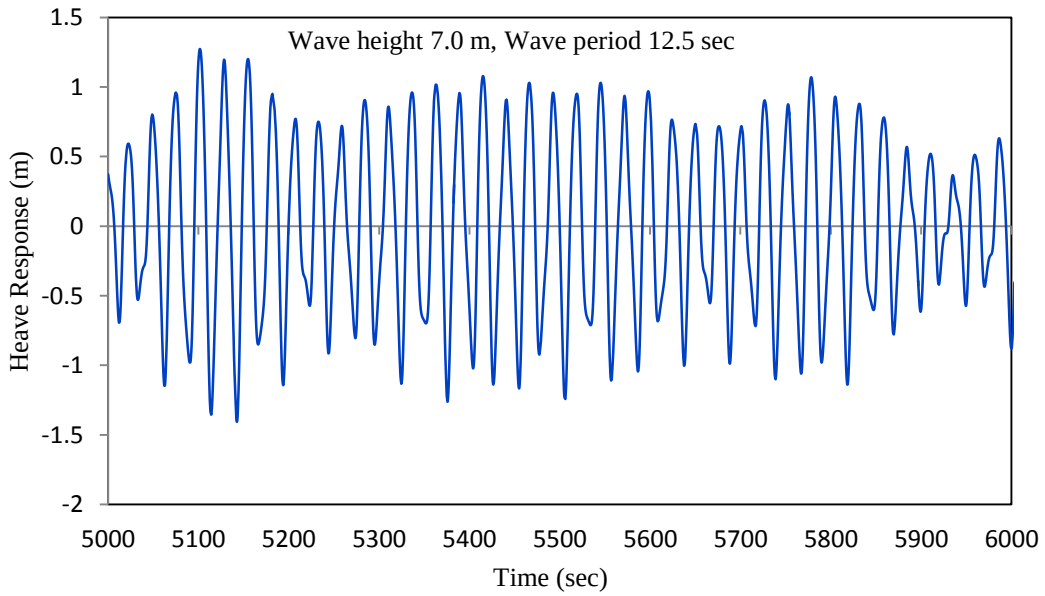

Figure 4.15: Heave response time history (5000-6000 sec)

Figure 4.16 shows the spectral density of the coupled heave from 5000-6000 sec time history under regular wave. The spectral density of heave response shows a peak at 0.262 rad/sec and the natural frequency of heave at 0.384 rad/sec.

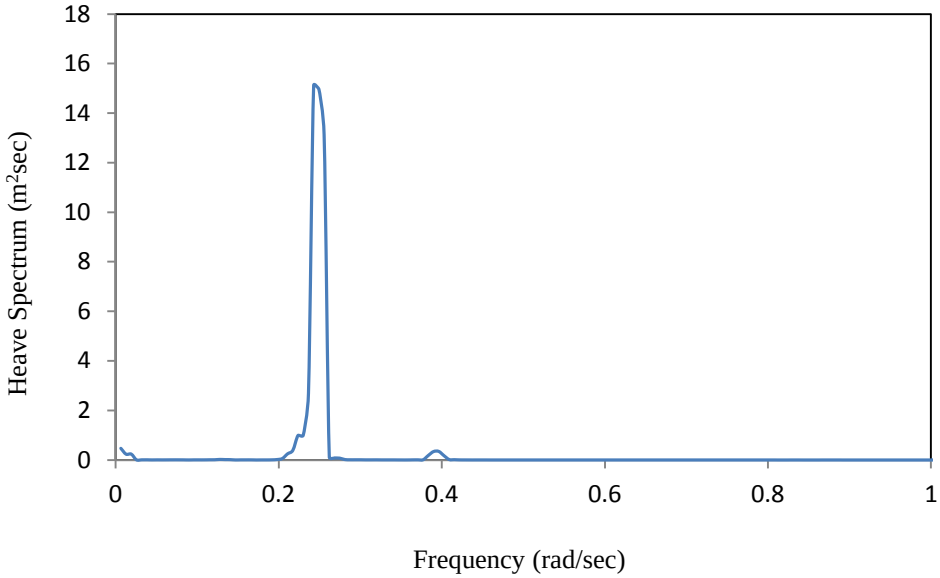

Figure 4.16: Heave spectral density for 5000-6000 sec

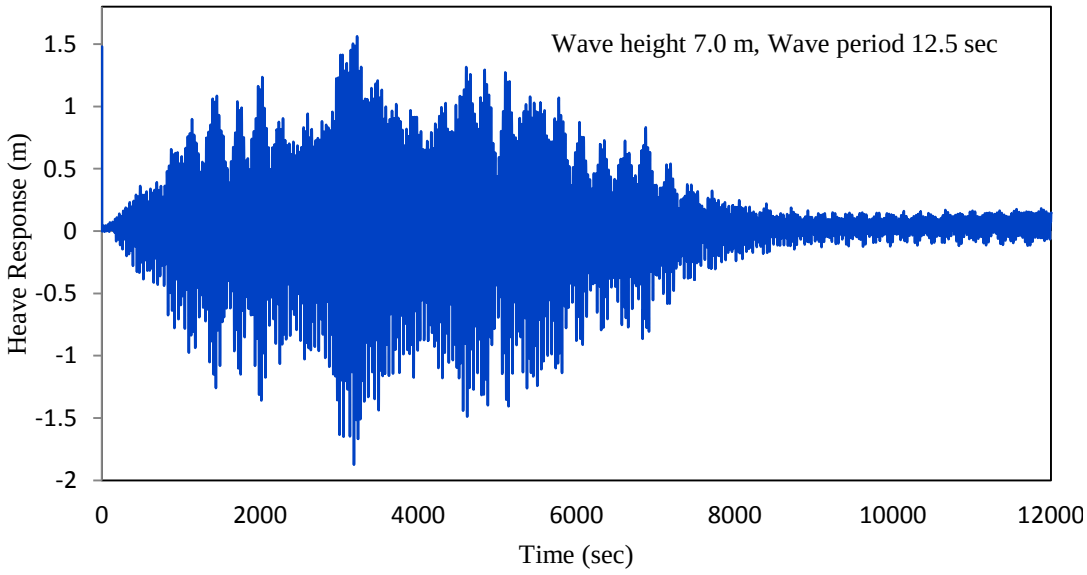

Figure 4.17: Heave response time history (0-12000 sec)

Figure 4.17 shows the entire time history of heave response under unidirectional regular waves. According to the figure, the platform oscillation occurs in regular intervals and from the qualitative diagram it is seen that the time histories of heave response gradually increase and decrease until 5000 sec. After this time period, the values significantly decrease due to damping of mooring lines. From 8500 sec onward the time

history goes to steady state condition, where the maximum and minimum values are of +0.19 and -0.15 m, respectively.

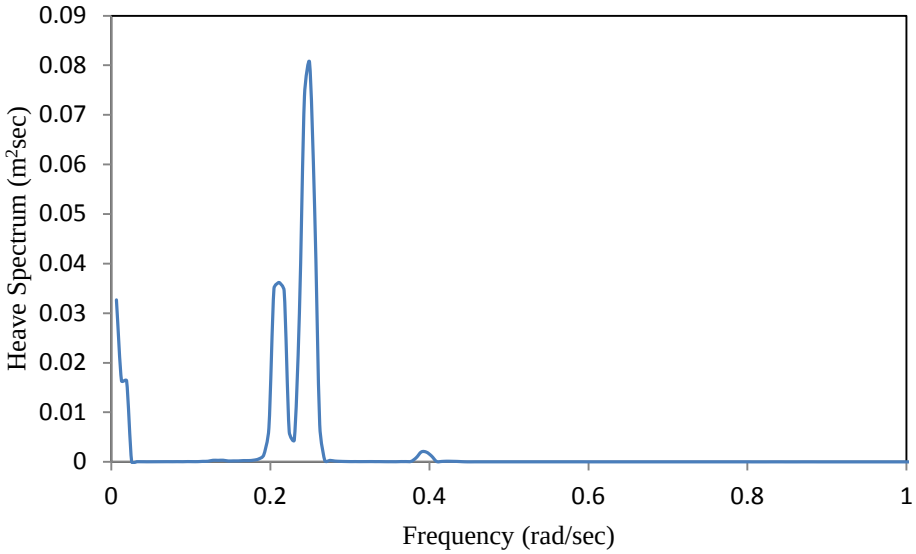

Figure 4.18: Heave spectral density for 9000-10000 sec

The spectral density of heave response from 9000-10000 sec time history is shown in Figure 4.18. It is noted that there is a solitary peak at the system's natural frequency. The peak occurs at 0.25 rad/sec which is close to another peak at 0.205 rad/sec and the natural frequency at 0.384 rad/sec.

4.3.1.3 Pitch Response

The pitch (rotational) response of coupled spar platform under regular wave is shown in Figure 4.19. The time history from 5000-6000 sec shows regular oscillations ranging from ± 0.09 rad and reducing to small ordinates of ± 0.06 rad. The pitch response is less sensitive to the form of damping as shown in the figure 4.19. The statistical summary of pitch response is shown in Table 4.3. The maximum and minimum values are +0.12 and -0.11 rad respectively. The mean value is almost zero and the standard deviation is 0.04 rad. The value of mean close to zero indicates the spar platforms

regular fluctuations about the middle position. The surge and pitch response are significantly affected at the deck level.

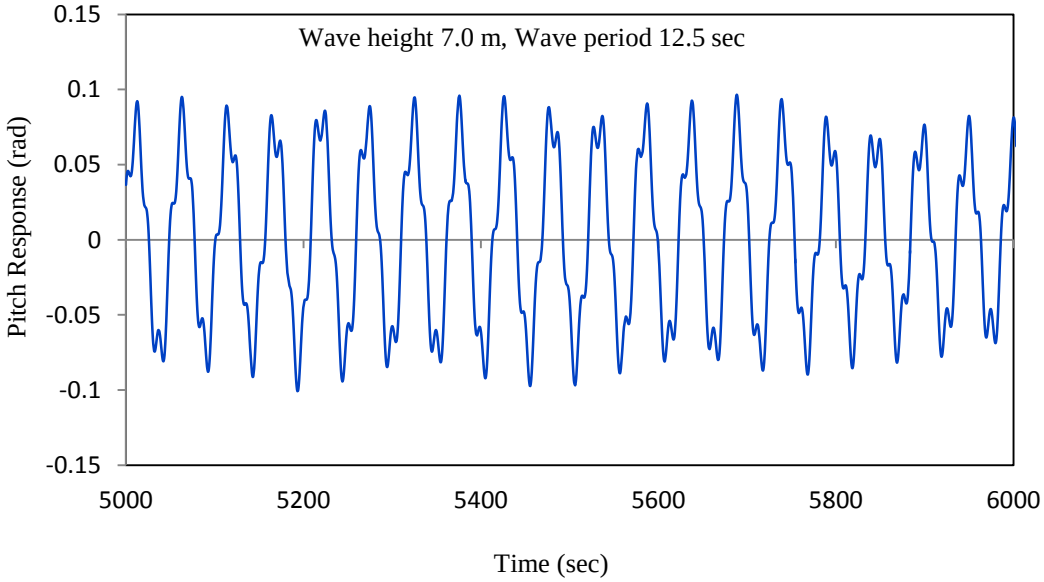

Figure 4.19: Pitch response time history (5000-6000 sec)

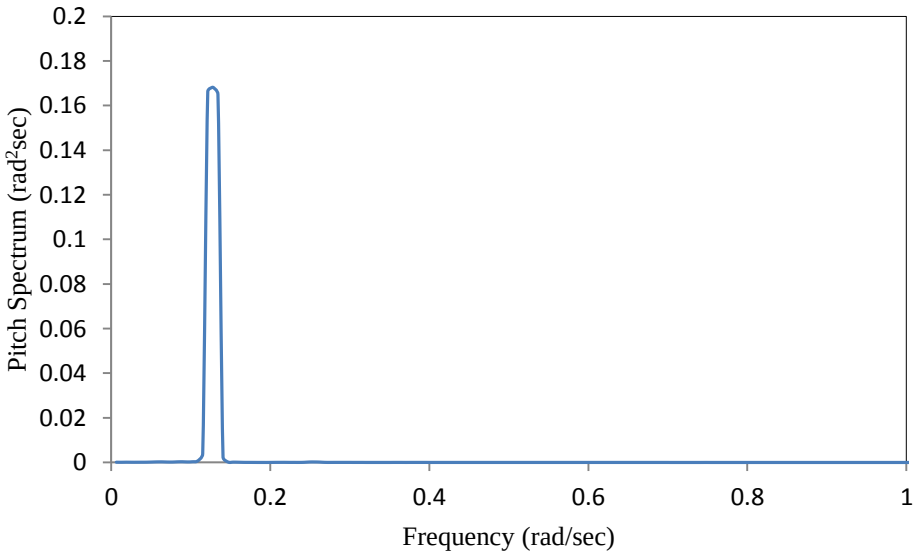

Figure 4.20: Pitch spectral density for 5000-6000 sec

Figure 4.20 shows the spectral density of pitch response 5000-6000 sec time history at deck level. The pitch response behaviour is similar to the surge response time history.

The spectral density of pitch response shows a peak at 0.121 rad/sec, which is the same for surge response caused by wave force on the spar platform.

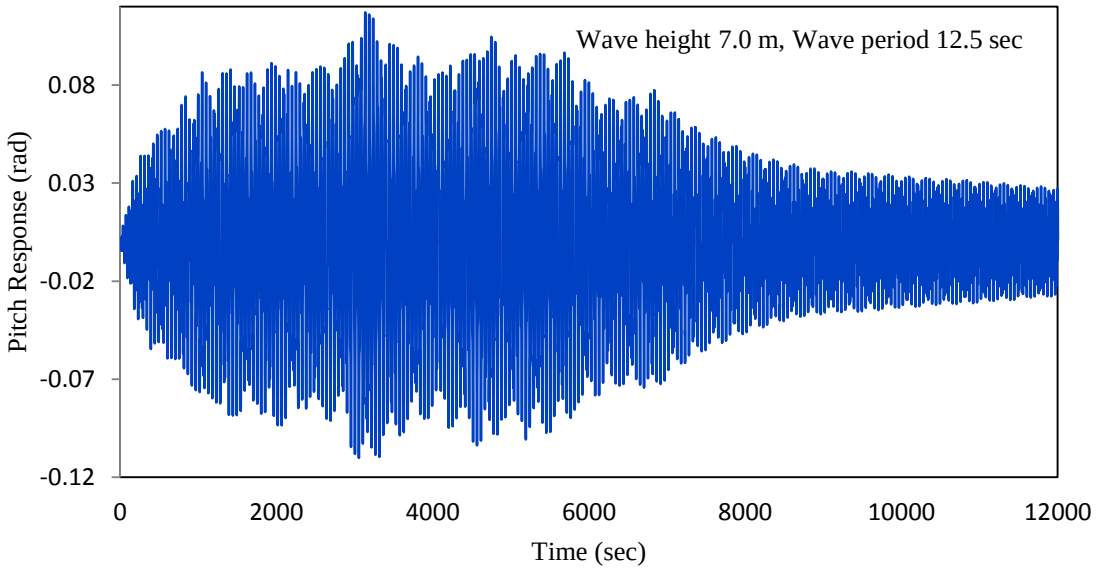

Figure 4.21: Pitch response time history (0-12000 sec)

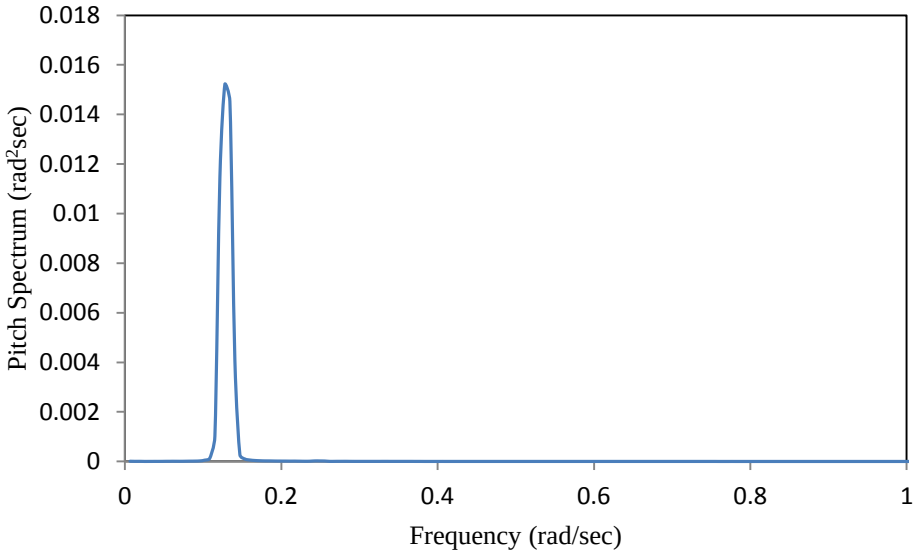

Figure 4.22: Pitch spectral density for 9000-10000 sec

Figure 4.21 shows the total time history of pitch response under regular wave. Fluctuation of the pitch response is in regular amplitude about the mean position and iterating the same trends. On the view of schematic, fluctuating response increases until 6000 sec due to wave loading. After the time stated, the values significantly reduce due to damping of the mooring lines. The damping variations produce changes in the pitch response similar to those in the surge response predictions. From 9000 sec onwards, the time history moves to the steady state condition, where the maximum and minimum pitch responses are +0.04 and -0.04 respectively. The spectral density of pitch response time history under regular wave from 9000-10000 sec is shown in Figure 4.22. The peak arises at 0.128 rad/sec which is similar to the surge response spectral density as shown in figure 4.14.

4.3.1.4 Top Tension Response

The spar mooring lines have a significant function in the nonlinear coupled dynamic analysis. In the finite element model, 4 catenary mooring lines are connected at the fairlead position of the spar hull and attached to the seabed. The spar hull and mooring lines are significantly affected due to the regular wave loads. Table 4.3 shows statistical responses where it is seen that the maximum and minimum tensions on the mooring lines are 1.70E07 N and 1.12E07 N, respectively. The top tension time history of mooring line 1 under regular waves is influenced by surge and heave response, (Figure 4.23). Mooring line 1 and 3 are located opposite to the direction of wave propagation. Mooring line 1 potentials the maximum tension to tolerate surge response in the onward direction, while mooring line 3 releases pretension. For both of these mooring lines under the regular wave, periodic behaviour is dominates. The spectral density of tension 5000-6000 sec time history is shown in Figure 4.24. The peak frequency occurs at 0.128

rad/sec, which is close to the natural frequency at 0.24 rad/sec. It is anticipated that heave may considerably influence the mooring tension response. Surge response also causes increase in tension.

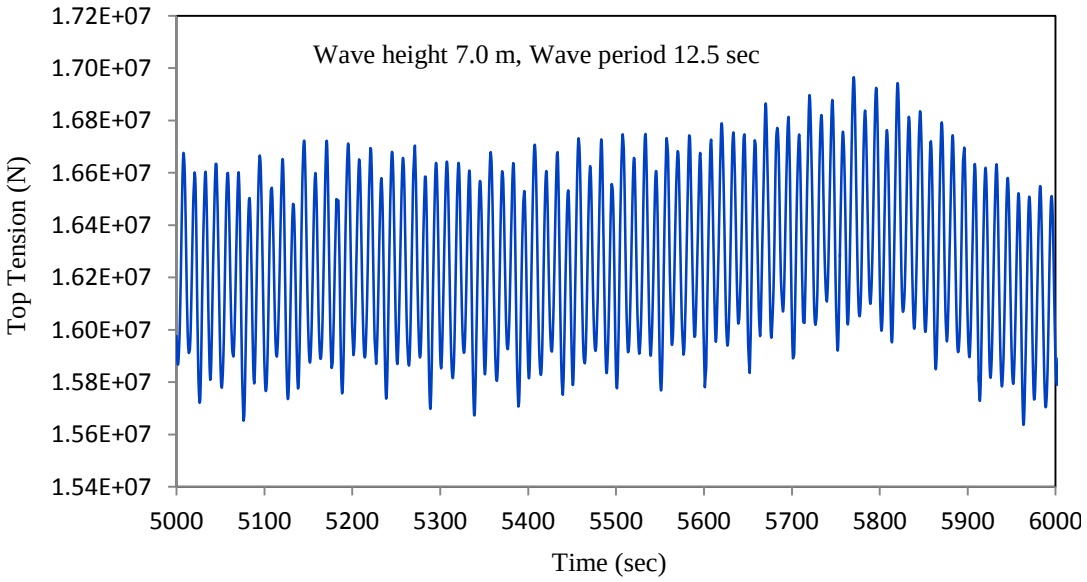

Figure 4.23: Maximum tension time history of mooring line-1 (5000-6000 sec)

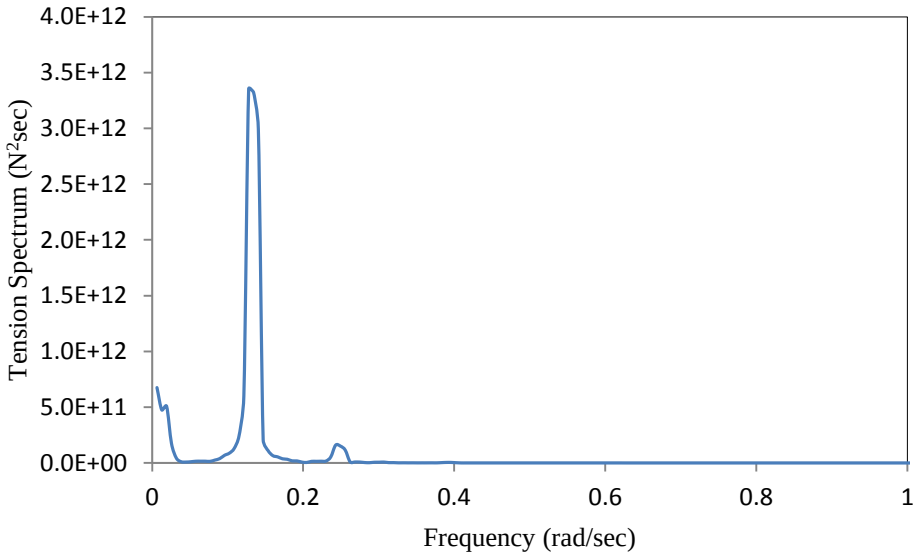

Figure 4.24: Maximum tension spectral density of mooring line-1 for 5000-6000 sec

Figure 4.25 shows the maximum tension of mooring line-1 (0-12000 sec) time history under unidirectional regular waves. According to figure, the mooring line oscillation occurs in regular intervals and on the view of qualitative diagram the time histories of mooring tension high fluctuating occurs up to 7500 sec.

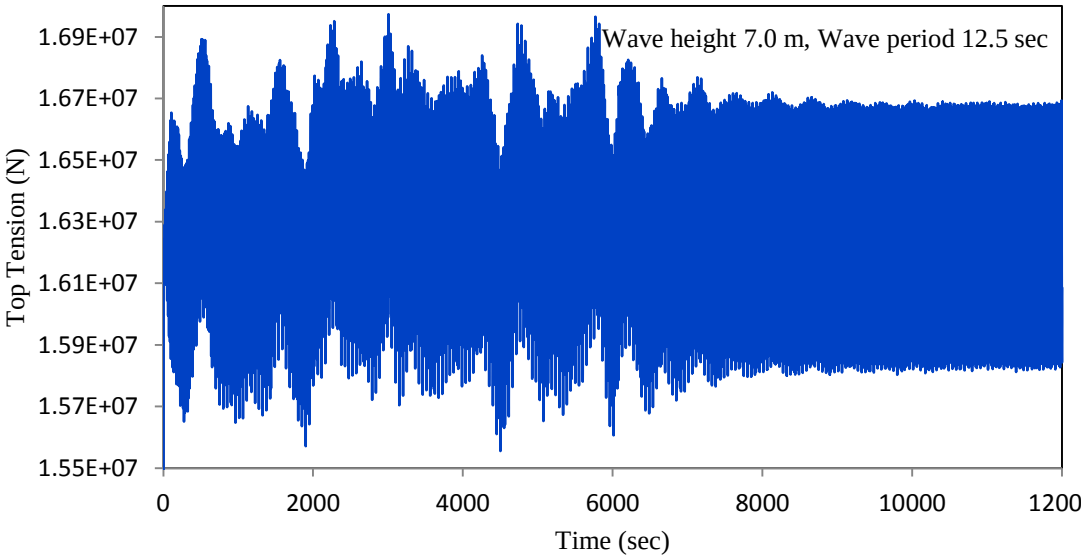

Figure 4.25: Maximum tension time history of mooring line-1 (0-12000 sec)

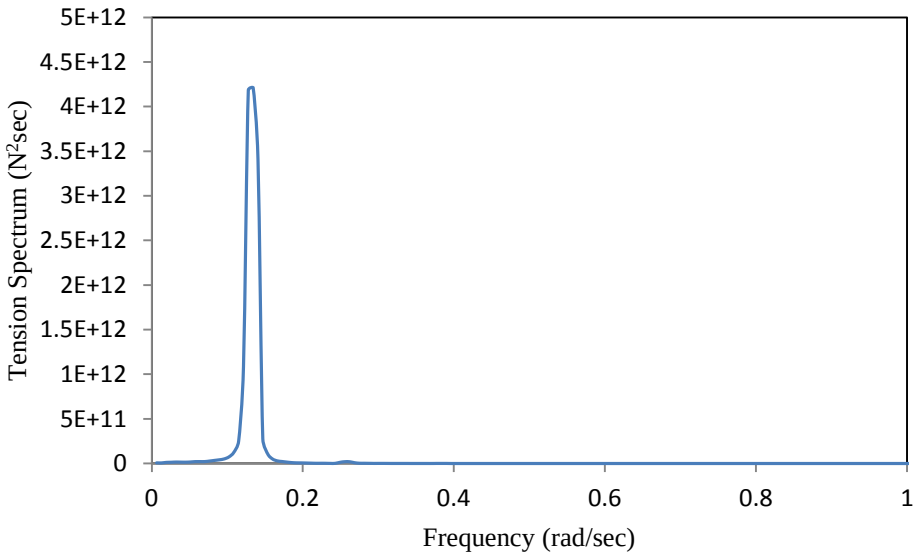

Figure 4.26: Maximum tension spectral density of mooring line-1 for 9000-10000 sec

After the time state, the values fluctuations in the value of tension are regular due to damping provided by the mooring lines. The spectral density of mooring tension 9000-10000 sec time history is shown in Figure 4.26. The peak frequency occurs at 0.128 rad/sec but absence of natural frequency.

4.3.2 Dynamic Response in Regular Wave and Current

The fully coupled dynamic response analysis of spar hull and mooring lines under regular wave and current in deep water conditions have been performed by FEM. Maximum response of the spar platform occurs at the deck level. The obtained results are plotted at both the time histories, i.e. 5000 to 6000 sec and up to 12000 sec, at the same level. Relative valuation for surge, heave, pitch motion responses as well as top tension is carried out in terms of time history and spectral density. Statistical analysis results of spar hull and mooring lines in terms of max, min, mean, and standard deviation are given in Table 4.4.

Table 4.4: Statistical response of spar hull and mooring lines

Wave Ht.=7.0 m Wave Pr.=12.50 sec Current speed =0.9 m/sec	Max	Min	Mean	Standard deviation
Surge (m)	13.85	-9.49	1.36	3.61
Heave (m)	1.48	-0.77	0.04	0.18
Pitch (rad)	0.08	-0.08	-0.001	0.03
Mooring line Tension (N)	1.70E+07	1.12E+07	1.63E+07	3.10E+05

4.3.2.1 Surge Response

The wave loads along with current loads have been considered in the analysis of spar hull and mooring lines. In the Figure 4.27, the surge response (5000-6000 sec) time history is obtained at the deck level. The maximum and minimum surge responses are +13.85 and -9.49 m respectively, as shown in Table 4.4.

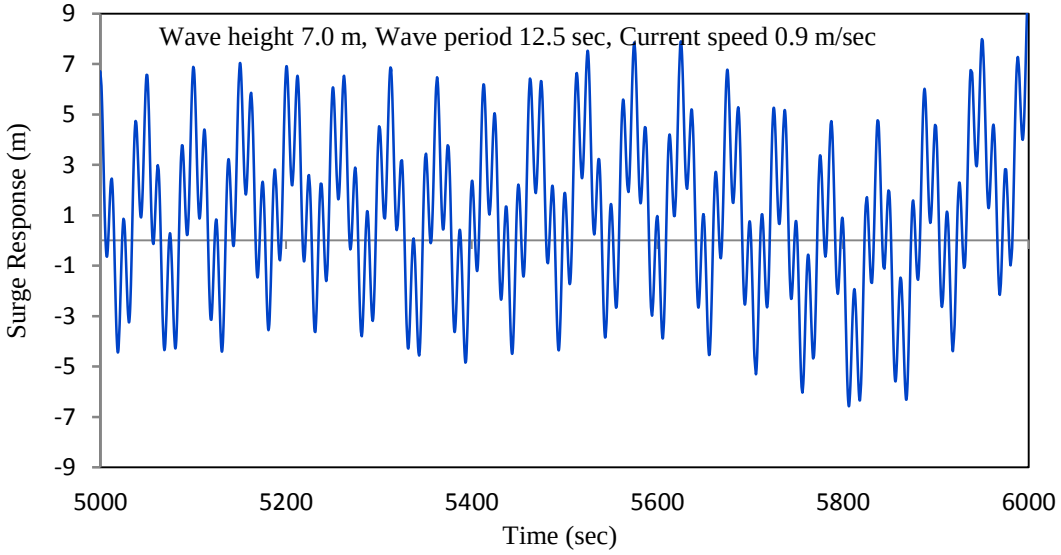

Figure 4.27: Surge response time history (5000-6000 sec)

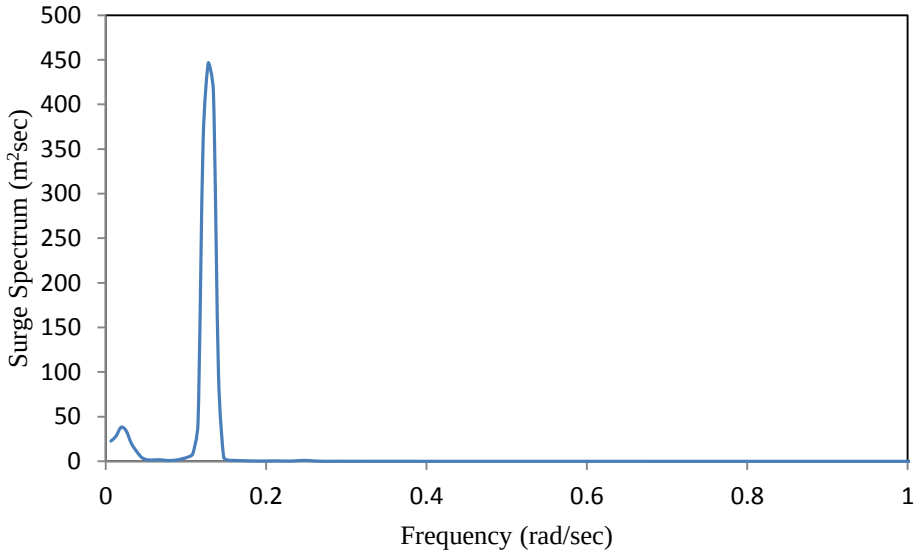

Figure 4.28: Surge spectral density for 5000-6000 sec

The surge response at the deck level is found to be mostly periodic. Hence, a single dominant peak arises in surge response at pitching frequency which can be observed from Figure 4.28. The surge and pitch responses occur simultaneously and attracts wave and current energy similar to the pitch frequency. The surge response at the deck level is principally controlled by the pitching motion of the hull with insignificant excitation of

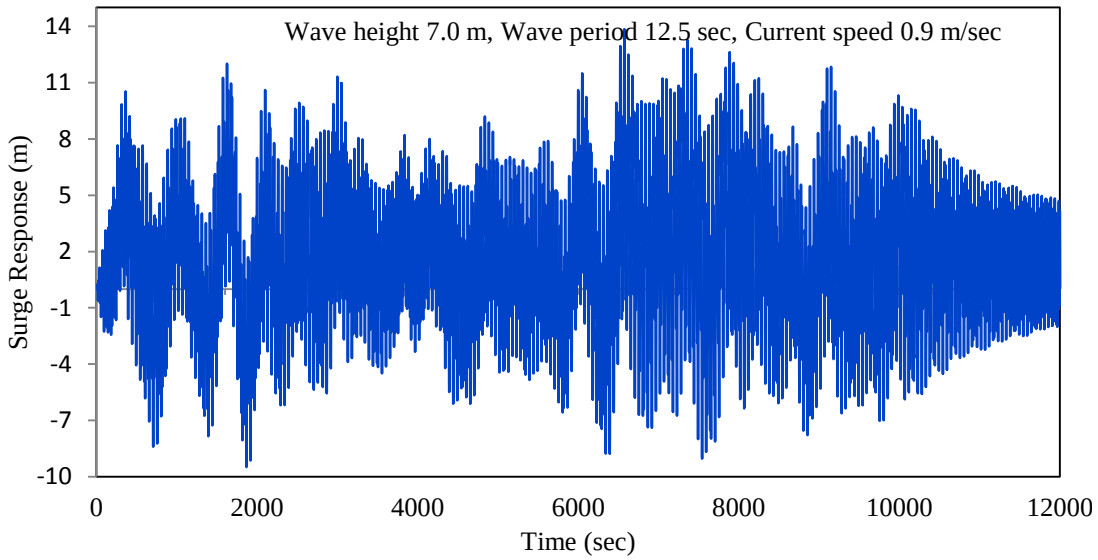

Figure 4.29: Surge response time history (0-12000 sec)

surge mode. It is mainly due to coupling of surge and pitch. Figure 4.28 shows the spectral density of surge response for 5000-6000 sec time history. The spectral density shows clearly peak frequency at 0.128 rad/sec. It is clear that the effect of non-linearity is not so strong on surge response. Figure 4.29 shows that from 0 to 12000 sec time history of surge response, oscillation is regular. The static effect of current diminishes the dynamic fluctuations significantly. This adverse fluctuation continues throughout the time history with mild fluctuations in the mean value. At the end of 12000 sec of surge response time history, the platform oscillations take place in steady state condition due to damping of the mooring line. The spectral density of the surge time history from 9000 to 10000 sec shows one peak (Figure 4.30) at 0.128 rad/sec. The surge response oscillates at frequency equal to that of the wave force. In case of current, mooring lines

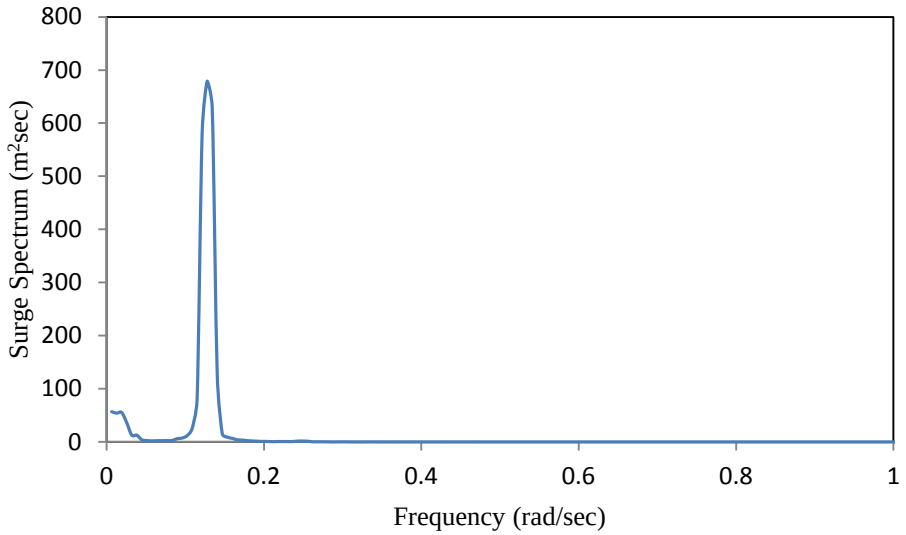

Figure 4.30: Surge spectral density for 9000-10000 sec

get taut and accordingly the stiffness matrix gets modified leading to large number of stress reversals. This is mainly due to the high frequency in surge response.

4.3.2.2 Heave Response

The heave response shows a significant change in behaviour as compared to the case where current is not considered. Figure 4.31 shows the heave responses time history (5000-6000 sec) under regular wave and current loads. The time history shows regular phenomenon with the cluster of reversals occurring at fluctuating time intervals. The statistical summary of heave response which is shown in Table 4.4 shows that the maximum and minimum responses are 1.48 m and –0.77 m, whereas the mean value is 0.04 and standard deviation is 0.18. Fluctuation of heave response from small to large amplitude with respect to the mean position, and iteration of the similar trend forwards all through the time history is shown in Figure 4.31. The fluctuations of heave response gradually increase and decrease from taper to widen by 30 % and vice versa.

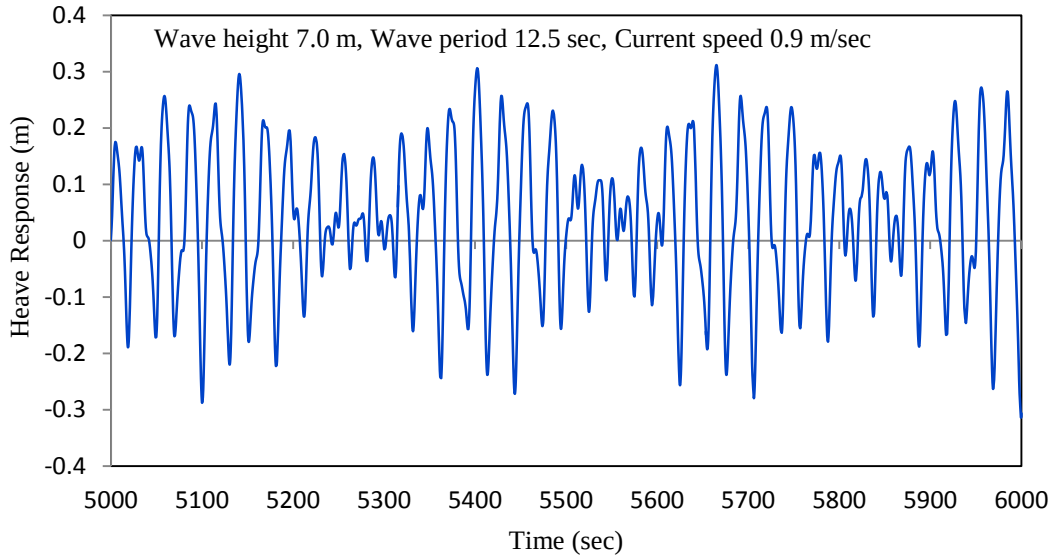

Figure 4.31: Heave response time history (5000-6000 sec)

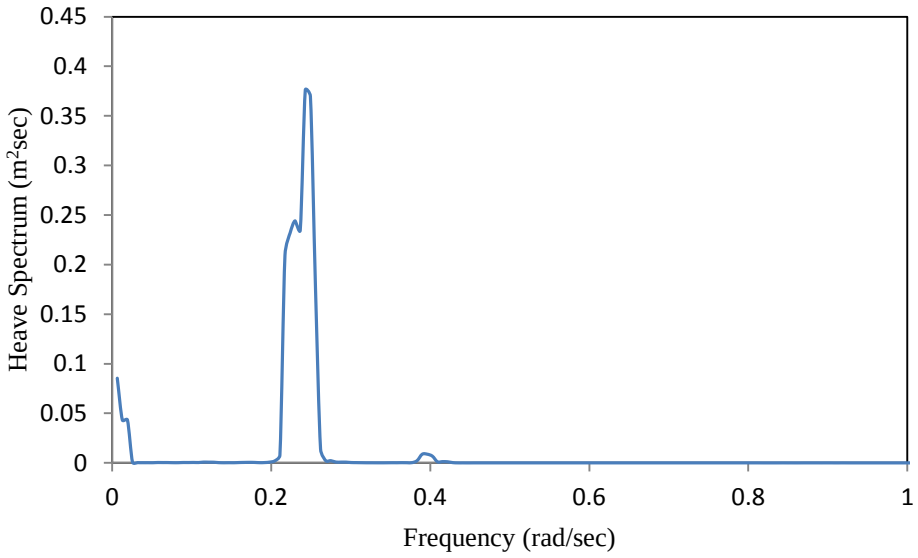

Figure 4.32: Heave spectral density for 5000-6000 sec

Figure 4.32 shows the spectral density of the coupled heave for 5000-6000 sec time history under regular waves and current loads. There are several peaks shown but the maximum peak occurs at 0.24 rad/sec which is close to the other frequency of heave at 0.22 rad/sec. Another small peak occurs at 0.383 rad/sec as a natural frequency. Figure 4.33 shows the entire time history of heave response under unidirectional regular waves. According to the figure, the platform's dynamic oscillation occurs in regular intervals.

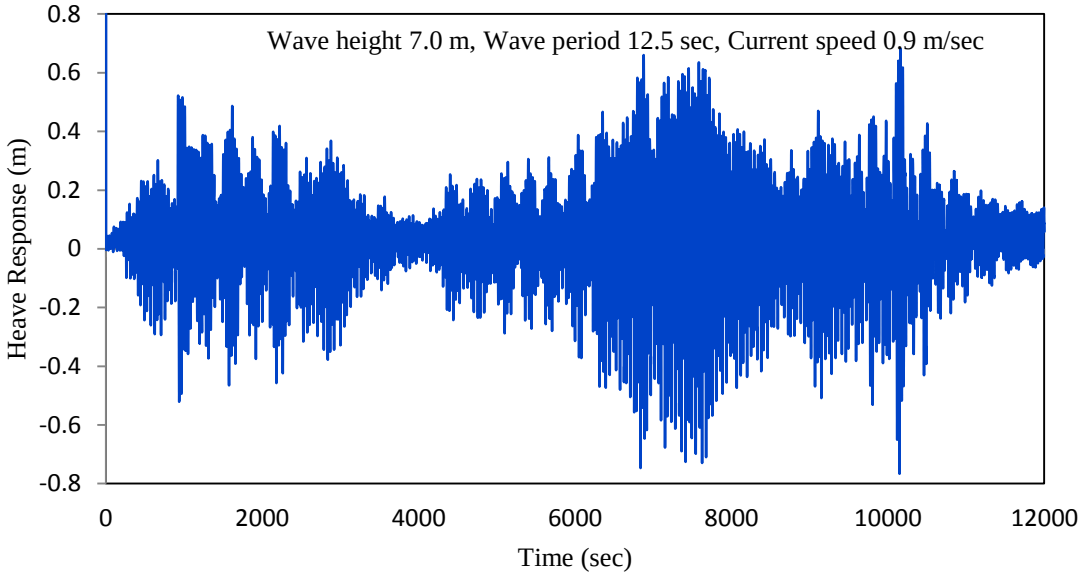

Figure 4.33: Heave response time history (0-12000 sec)

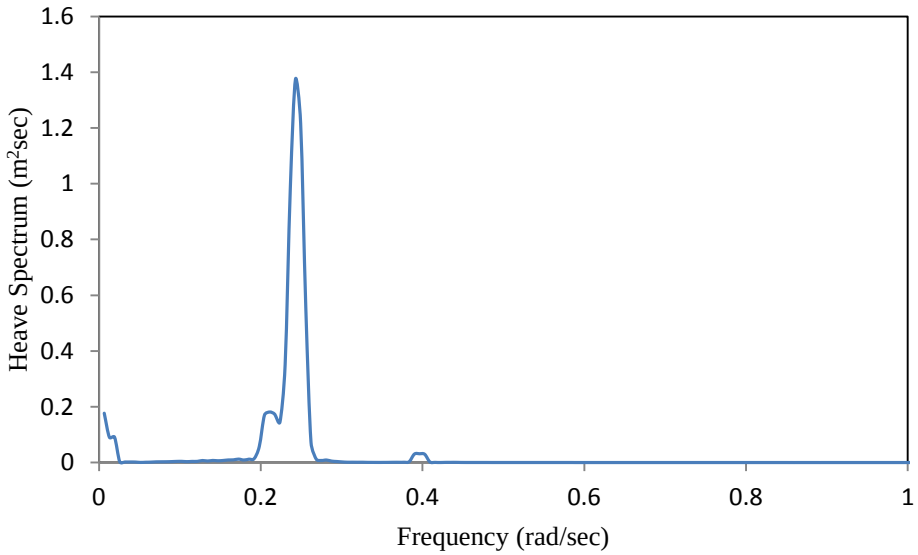

Figure 4.34: Heave spectral density for 9000-10000 sec

After 12000 sec of heave response, the time history moves to steady state condition due to damping provided by the mooring lines. The spectral density of heave response from 9000-10000 sec time history is shown in Figure 4.34. The frequency peak position is same as previous Figure 4.32 but unlike magnitude of spectrum.

4.3.2.3 Pitch Response

The rotational response pitch of spar hull subjected to sea waves and current are illustrated in Figure 4.35. The time history 5000-6000 sec shows regular oscillations ranging from ± 0.07 rad and reducing to small ordinates of ± 0.03 rad. The pitch response is less sensitive to the form of damping as shown in the figure. The statistical summary of pitch response is shown in Table 4.4 with maximum and minimum values of +0.08 and -0.08 rad respectively. The mean value is -0.001 rad and the standard deviation is 0.03 rad. The surge and pitch responses are significantly affected duly at deck level of spar hull, as expected.

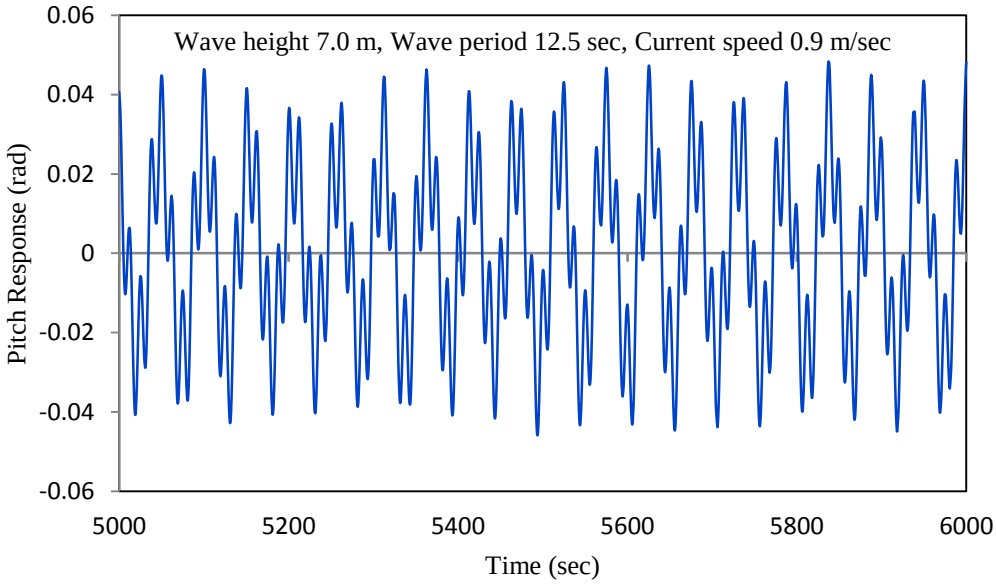

Figure 4.35: Pitch response time history (5000-6000 sec)

Figure 4.36 shows the spectral density of pitch response 5000-6000 sec time history at deck level. The pitch response behaviour is similar to the surge response time history. The spectral density of pitch response shows a peak at 0.128 rad/sec which is the same position of surge response caused by wave and current force on the spar platform. Figure 4.37 shows the total time history of pitch response subjected to wave and current

loads. Fluctuation of the pitch response is irregular in amplitude about the mean position but iterates the same trend.

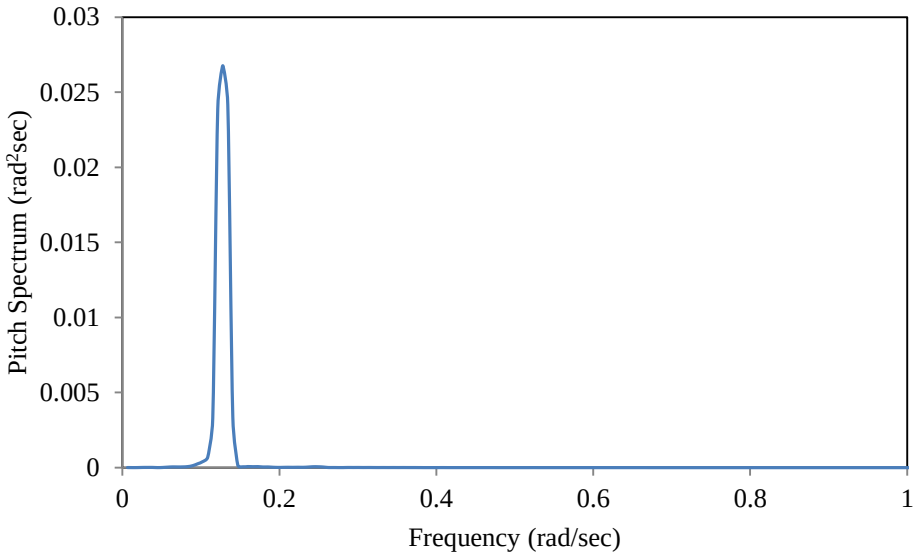

Figure 4.36: Pitch spectral density for 5000-6000 sec

The damping variations produce changes in the pitch response similar to those in the surge response predictions. Onwards of 12000 sec, forwards the time history moves to the steady state condition due to the damping of the mooring lines.

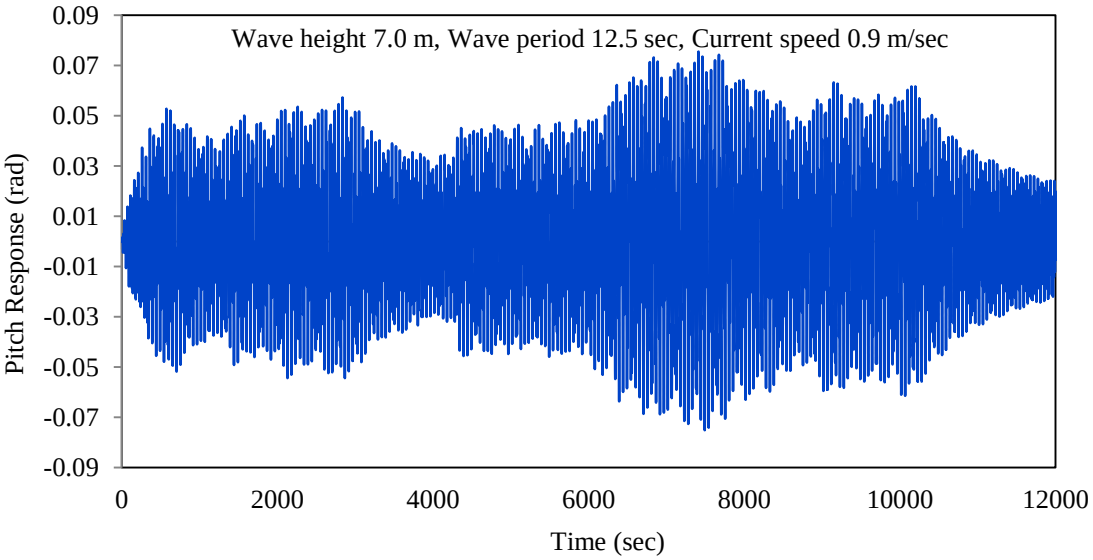

Figure 4.37: Pitch response time history (0-12000 sec)

The spectral density of pitch response time history subjected to wave and current for 9000-10000 sec is shown in Figure 4.38. The peak arises at 0.128 rad/sec which is similar to the surge response spectral density.

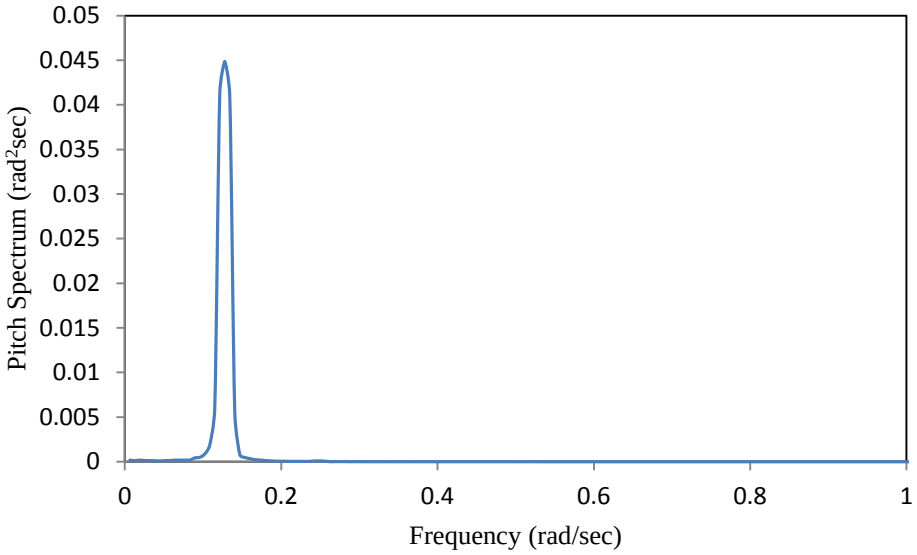

Figure 4.38: Pitch spectral density for 9000-10000 sec

4.3.2.4 Top Tension Response

In the finite element model, 4 numbers of catenary mooring lines are connected at the fairlead position of the spar hull and attached at the seabed. The spar hull and mooring lines are significantly affected by the regular wave and current loads. Table 4.4 shows statistical responses; the maximum and minimum tension of mooring lines are 1.70E07 N and 1.12E07 N respectively. The top tension time history of mooring line 1 under regular waves and current is influenced by surge and heave responses (Figure 4.39). Mooring line 1 and 3 are located opposite the direction of wave propagation. Mooring line 1 potentials the maximum tension to tolerate surge response in the onward direction, while mooring line 3 releases pretension. For both of these mooring lines under the regular wave with current periodic behaviour is dominates.

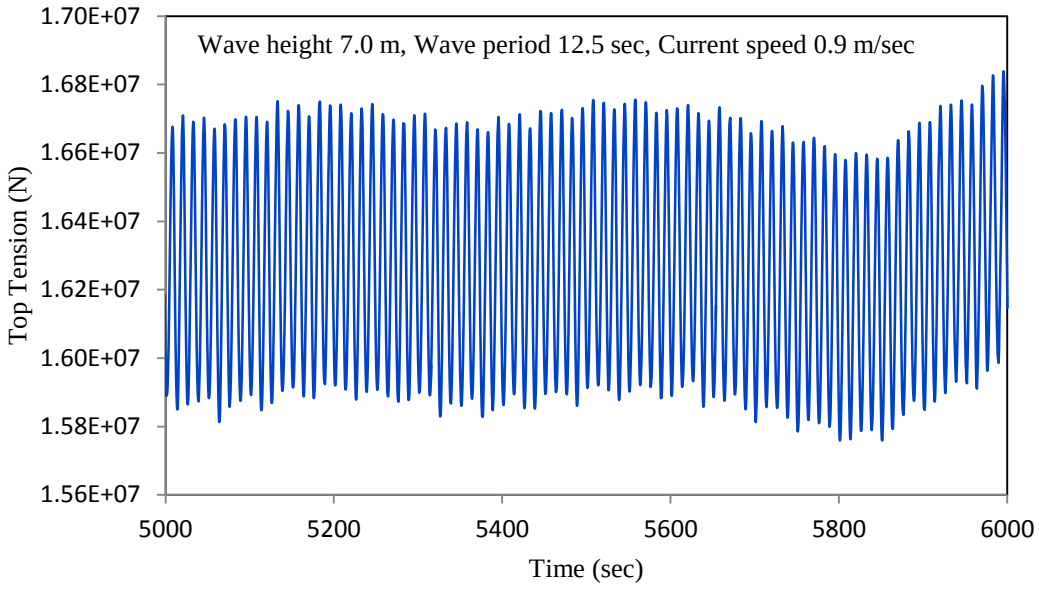

Figure 4.39: Maximum tension time history of mooring line-1 (5000-6000 sec)

The spectral density of tension 5000-6000 sec time history is shown in Figure 4.40. The peak frequency occurs at 0.134 rad/sec but absence of the natural frequency. It is anticipated that heave may considerably influence the mooring tension response. Surge response also causes increase in tension.

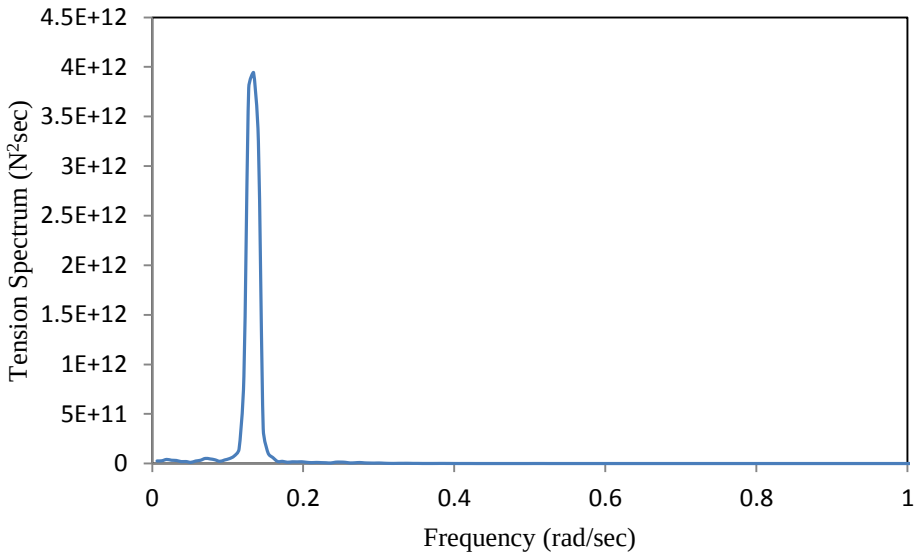

Figure 4.40: Maximum tension spectral density of mooring line-1 for 5000-6000 sec

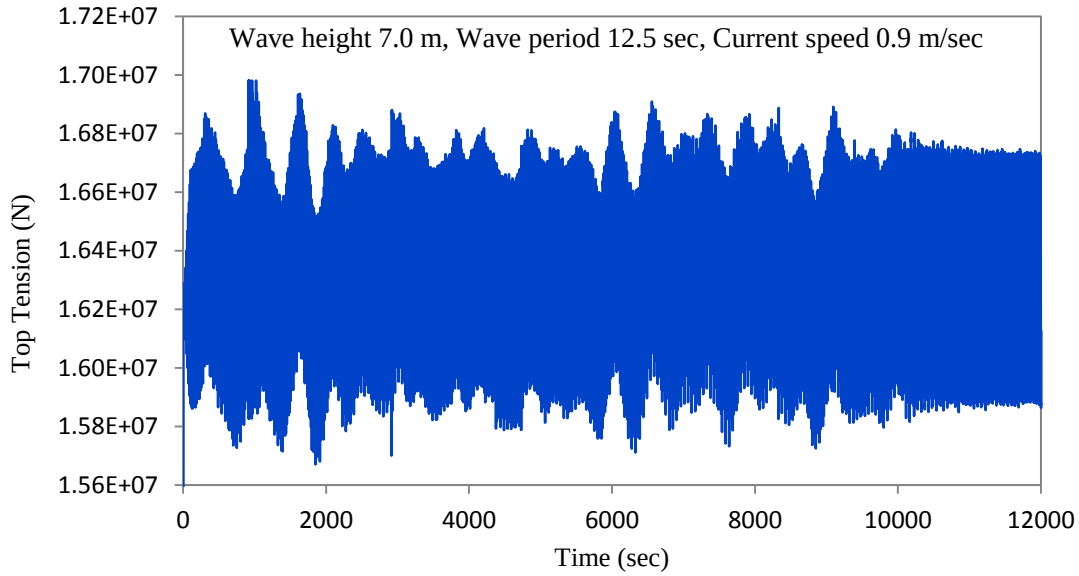

Figure 4.41: Maximum tension time history of mooring line-1 (0-12000 sec)

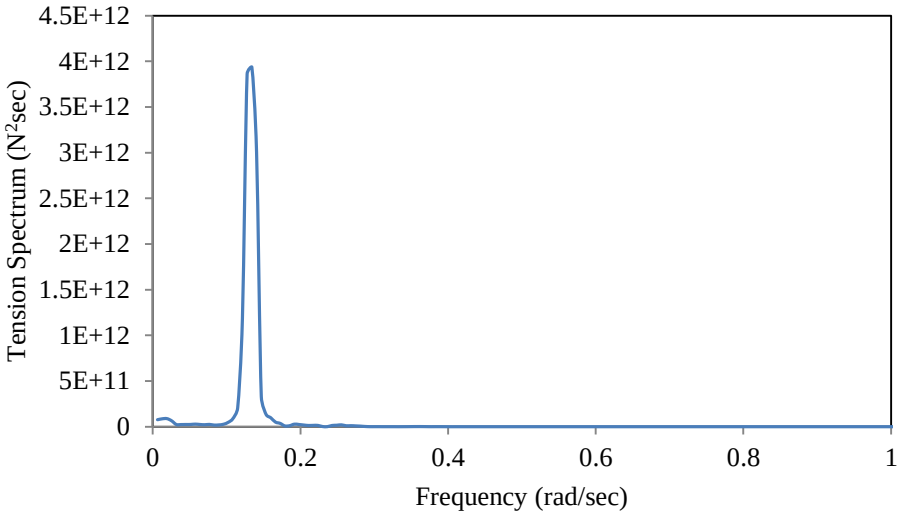

Figure 4.42: Maximum tension spectral density of mooring line-1 for 9000-10000 sec.

Figure 4.41 shows the maximum tension of mooring line-1 (0-12000 sec) time history under unidirectional regular waves and current loads. According to the figure, the mooring line oscillations occur in dynamic in regular intervals due to wave and current loads. At the end of 10000 sec, tension time history oscillation moves to steady state condition due to damping by mooring lines. The spectral density of mooring tension 9000-10000 sec time history is shown in Figure 4.42. The peak frequency occurs at 0.128 rad/sec but absence of natural frequency.

4.4 Resp-Pred ANN Approach for Response Prediction of Spar Platform

The present study involves the response prediction of the spar platform from newly selected environmental forces like wave height and wave period is obtained using ANN. The obtained finite element results are used as target and maximum environmental forces and mechanical parameters are used as inputs in training the network. Different networks are created according to the response of spar platform such as surge, heave, pitch, and top tension response. 10-18 sets of data are used for training the network and each set consists of approximately 3000 sec time history as target as well as 22 mechanical and environmental parameters as inputs. There are three layers of all neural networks consisting of input, target, and hidden layer. In this study, the optimum neurons (3 to 20) in hidden layer of the network are obtained by trial and error method. Feed-forward back-propagation algorithm is used for creating each network and hyperbolic-tangent function is used as activation function in hidden layers. The root mean square error (RMSE) and correlation coefficient (R) are used as error function and predictive ability of the network respectively, which is shown in Table 4.5.

Table 4.5: Statistical comparison between predicted and FEM results of Spar mooring responses

Parameter	MaxE	MinE	StdevE	RMSE	Bias	R
Surge response (m)	2.564	-2.749	0.750	0.757	0.1005	0.9819
Heave response (m)	0.119	-0.128	0.041	0.041	-0.0002	0.9919
Pitch response (rad)	0.004	-0.003	0.001	0.001	0.0001	0.999
Top tension (N)	116230	-88155	35704	35839	3307.5	0.997

4.4.1 Spar Hull Responses

4.4.1.1 Surge Response

The surge response prediction of spar hull to12.65 m wave height and 11.39 sec wave period is considered for validating the network in this study. Figure 4.43 shows that the convergence of the prediction by Resp-Pred approach with respect to FEM results of the surge response of spar hull. It may be seen that prediction response by the Resp-Pred approach is close to the FEM results. A comparison between the FEM and ANN predicted surge response is shown in Figure 4.44. In this figure, the FEM and the predicted results are plotted as scatter plot for 12.65 m wave height and 11.39 sec wave period. The overall Resp-Pred approach performance is found to be good for predicting response. The results of Y factors predicted by the approach versus FEM results and the corresponding trend lines are shown in figure 4.44.

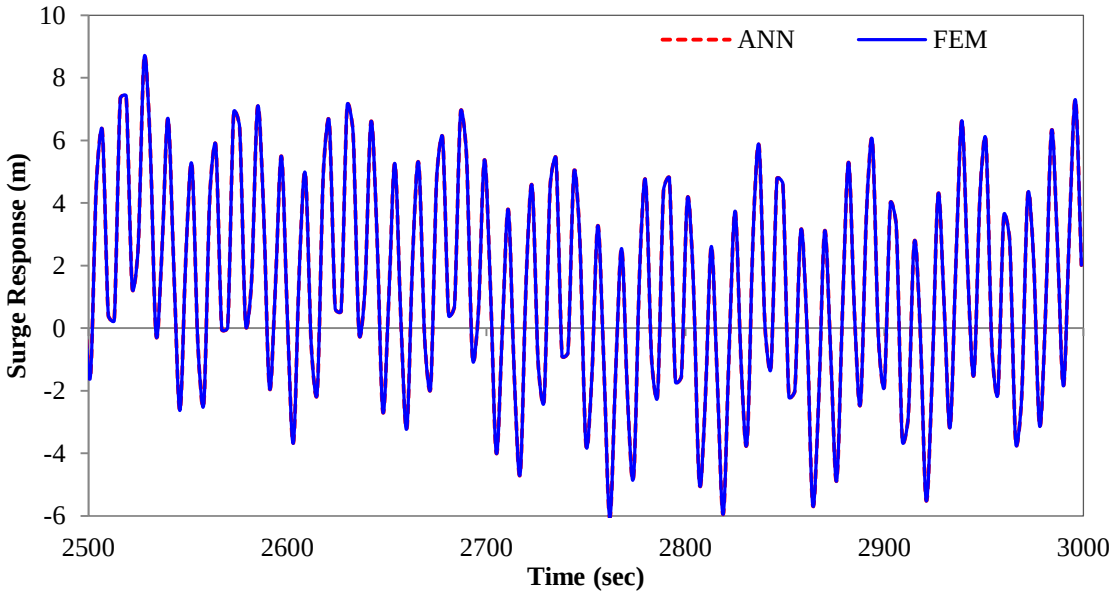

Figure 4.43: Predicted surge response and FEM results time history for 12.65 m wave height and 11.39 sec wave period.

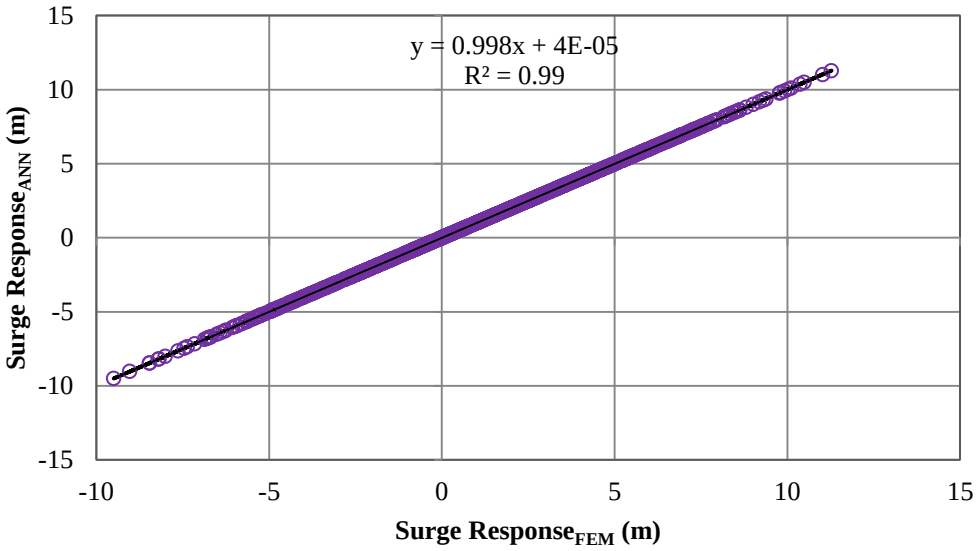

Figure 4.44: Comparison between predicted and FEM results of surge response for 12.65 m wave height and 11.39 sec wave period

Table 4.6 shows the statistical predicted surge response and FEM results for 12.65 m wave height and 11.39 sec wave period. The Resp-Pred approach results are better for predicting surge response as revealed in the higher value of the correlation coefficient 0.9819. This model can also predict surge response from newly selected environmental force and mechanical parameter which is shown in Figure 4.45. Predicted surge response 3000 sec time history by Resp-Pred approach for 9.65 m wave height and 10.10 sec wave period.

Table 4.6: Statistical surge response of ANN and FEM results for 12.65 m wave height and 11.39 sec wave period.

Surge Response (m)	Max	Min	Mean	Standard deviation
FEM	11.279	-9.497	1.017	3.741
Resp-Pred	11.311	-10.154	0.916	3.917
Difference (%)	0.29	6.478	9.93	4.477

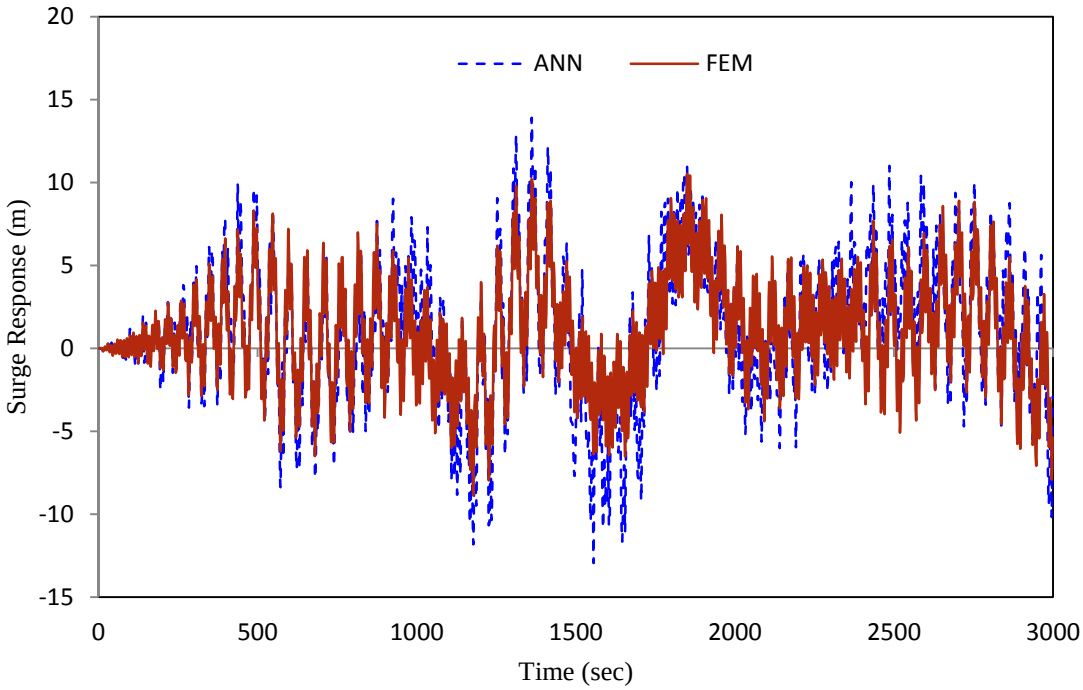

Figure 4.45: Surge response predicted time history for 9.65 m wave height and 10.10 sec wave period.

4.4.1.2 Heave Response

In this study, environmental force like wave height and wave period as well as mechanical parameters are considered to predict heave response of spar hull. Figure 4.46 shows the comparison between heave responses predicted and FEM results for 9.65 m wave height and 9.94 sec wave period. According to the figure it can be explained that the Resp-Pred approach predicted results which are close to the FEM results. Figure 4.47 shows that the scatters plot of heave response for 9.65 m wave height and 9.94 sec wave. Along the horizontal axis FEM results are plotted and the predicted heave response is shown along the vertical axis.

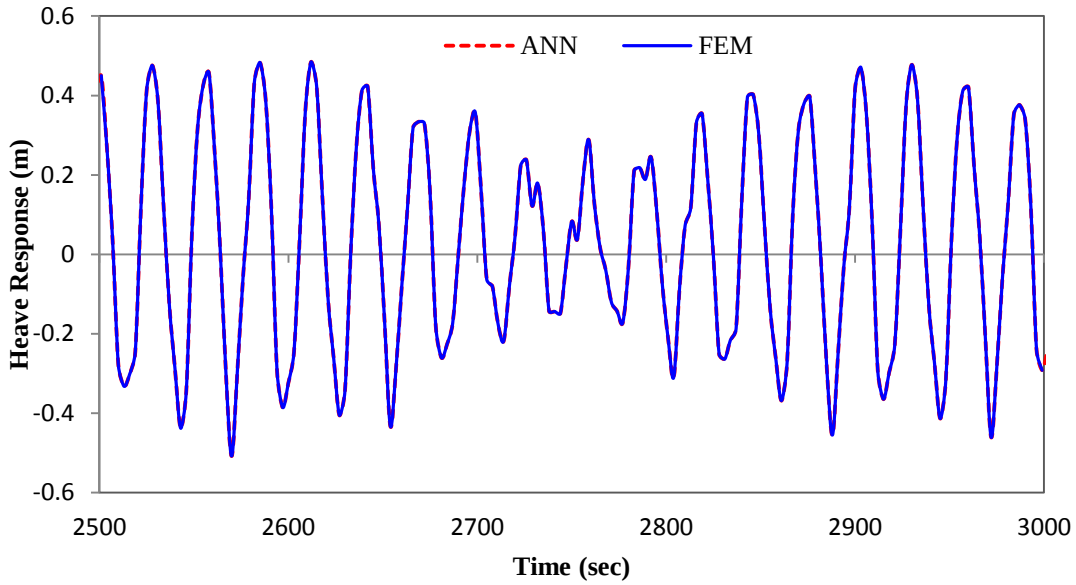

Figure 4.46: Heave response of predicted and FEM time history for 9.65 m wave height and 9.94 sec wave period.

The overall performance of the Resp-Pred approach is found to be good for predicting the response. The results of Y factors predicted by the Resp-Pred approach versus FEM results and the corresponding trend line are shown in figure 4.47.

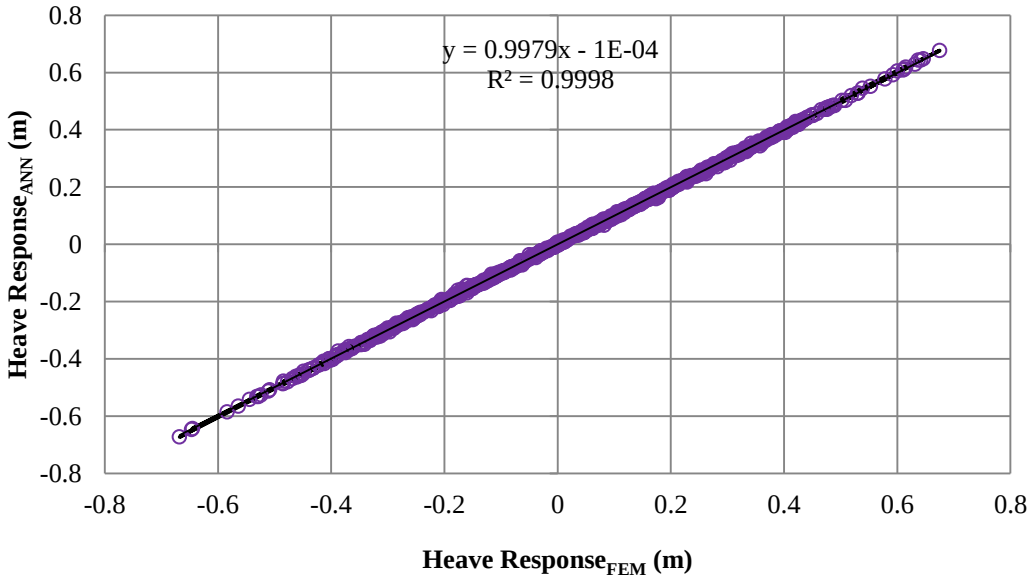

Figure 4.47: Comparison between heave response of predicted and FEM for 9.65 m wave height and 9.94 sec wave period

The statistical heave response for 9.65 m wave height and 9.94 sec wave period is shown in table 4.7, which was predicted by Resp-Pred approach as well as FEM. The Resp-Pred approach results are better for predicting heave response as revealed in the higher value of the correlation coefficient (0.9919). RMSE are used to evaluate performance of this approach and the approach can predict heave response from newly selected environmental force and mechanical parameter as shown in Figure 4.48. The heave response 3000 sec time history is predicted for 6.65 m wave height and 8.25 sec wave period. The heave response fluctuates about the mean position oscillating from smaller to larger amplitudes and repeating the same trend onwards all through the time series. The fluctuations gradually decrease from broad to narrow by 20 %.

Table 4.7: Statistical heave response of ANN and FEM for 9.65 m wave height and 9.94 sec wave period

Heave Response (m)	Max	Min	Mean	Standard deviation
FEM	0.675	-0.668	0.033	0.250
Resp-Pred	0.574	-0.575	0.033	0.222
Difference (%)	14.96	13.92	0.480	11.2

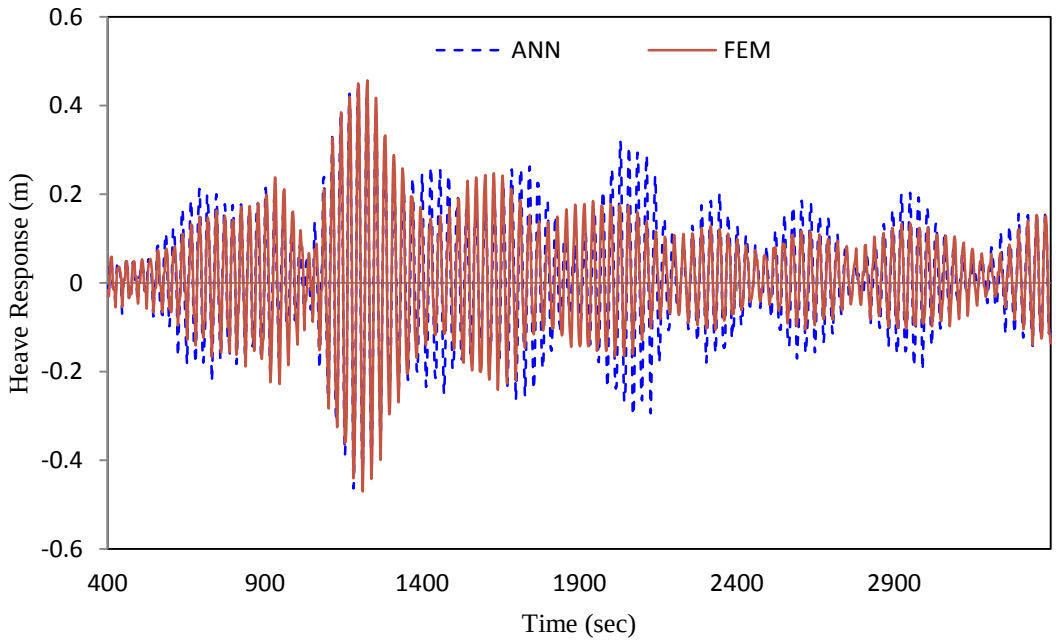

Figure 4.48: Heave response of predicted time history for 6.65 m wave height and 8.25 sec wave period

4.4.1.3 Pitch Response

The Resp-Pred approach is used for validating the pitch response results for 9.65 m wave height and 9.94 sec wave period in this study. Figure 4.49 shows that the convergence of the predicted values by Resp-Pred approach and those by the FEM results of the pitch response of spar hull. As can be observed, the results predicted by Resp-Pred approach converge very well with those obtained from FEM results that are almost unseen in the figure. Figure 4.50 shows that the comparison between predicted and FEM results of pitch response. Along the horizontal axis FEM results are plotted and the predicted pitch response is shown along the vertical axis which is predicted for 9.65 m wave height and 9.94 sec wave period. The overall pitch response network's performance is found to be good for prediction. The results of Y factors predicted by this pitch-network versus FEM results and the corresponding trend line are shown in figure 4.49.

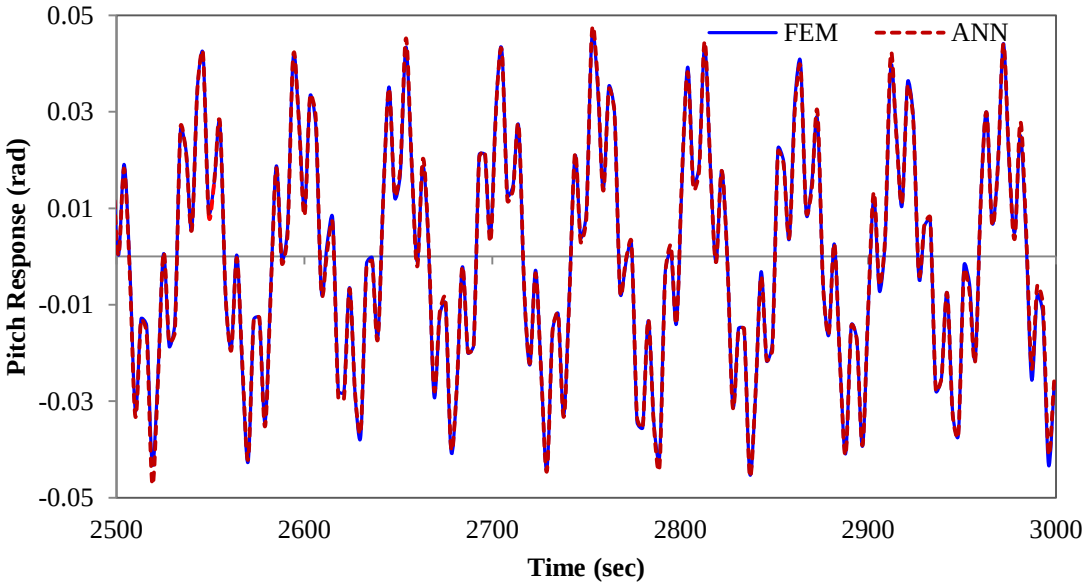

Figure 4.49: Pitch response of predicted and FEM time history for 9.65 m wave height and 9.94 sec wave period

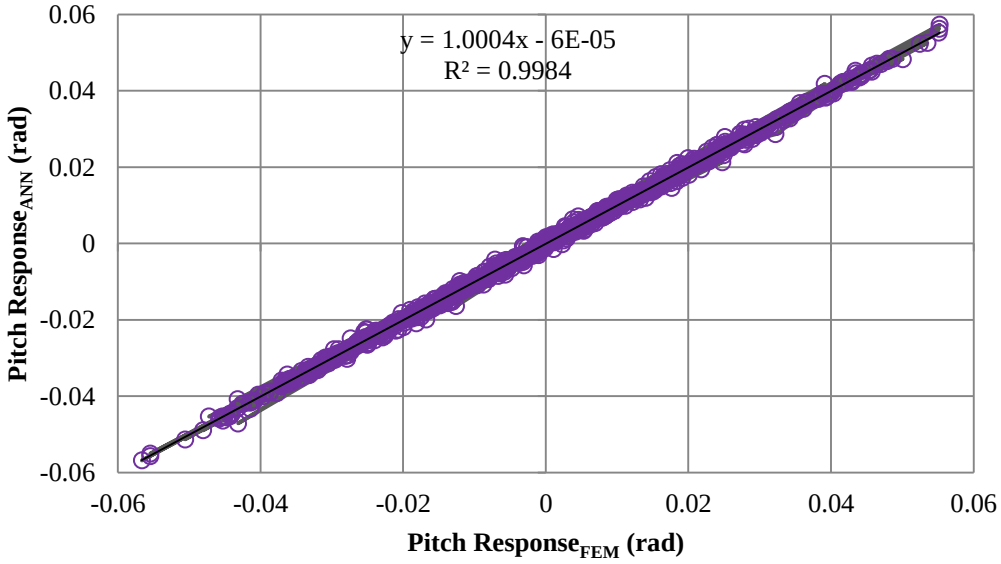

Figure 4.50: Comparison between pitch response of predicted and FEM for 9.65 m wave height and 9.94 sec wave period

Table 4.8 shows the statistical pitch responses of Resp-Prop approach and FEM results for 9.65 m wave height and 9.94 sec wave period. The Resp-Prop approach results are better for predicting pitch response as revealed in the higher value of the correlation coefficient of 0.999. Average prediction error is less than ±1% and this approach can predict pitch response for newly selected environmental force and mechanical

parameter, which is shown in Figure 4.51. The pitch response 3000 sec time history is predicted for 12.65 m wave height and 11.39 sec wave period. The response shows peak value of 0.9 rad.

Table 4.8: Statistical pitch response of ANN and FEM for 9.65 m wave height and 9.94 sec wave period

Pitch Response (m)	Max	Min	Mean	Standard deviation
FEM	0.055	-0.057	0.00026	0.021
Resp-Pred	0.057	-0.057	0.00019	0.021
Difference (%)	3.56	0.287	24.038	0.173

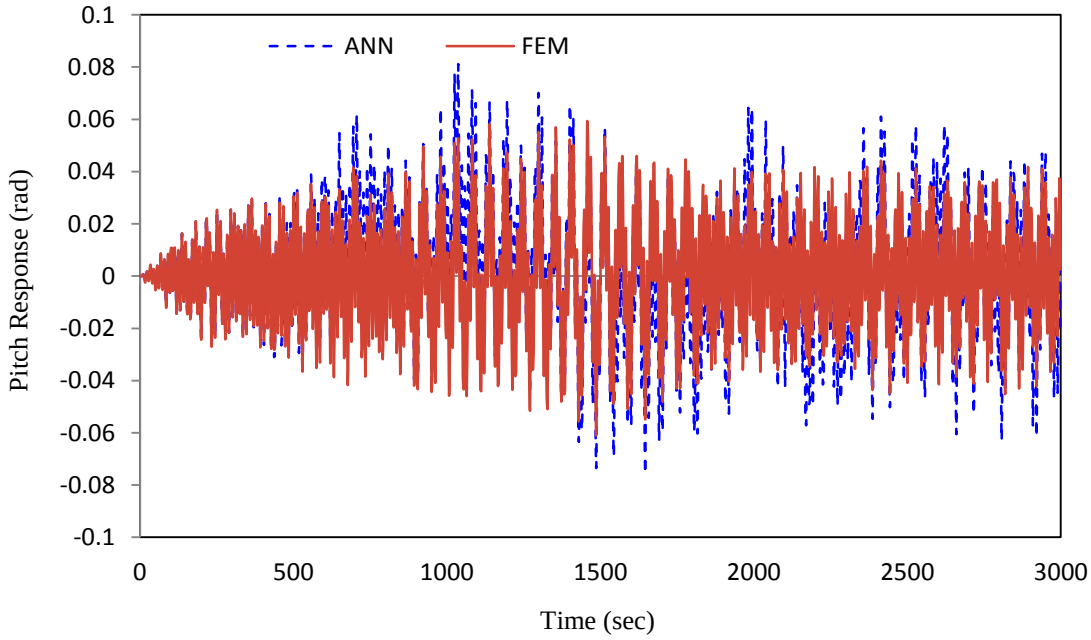

Figure 4.51: Pitch response of predicted time history for 12.65 m wave height and 11.39 sec wave period

4.4.2 Spar Mooring Response

4.4.2.1 Maximum Top Tension

Figure 4.52 shows that top tension predicted response and obtained FEM results are converged. The top tension response prediction of spar hull for validating the network 12.65 m wave height and 11.39 sec wave period is considered in this study. As can be observed, the results predicted by Resp-Pred approach converge very well with those obtained from FEM results. A comparison between the FEM and ANN predicted top tension response is shown in Figure 4.53. In this figure, the FEM and ANN predicted results are plotted for 12.65 m wave height and 11.39 sec wave. The results of Y factors predicted by the Resp-Pred approach versus FEM results and the corresponding trend line are shown in figure 4.53.

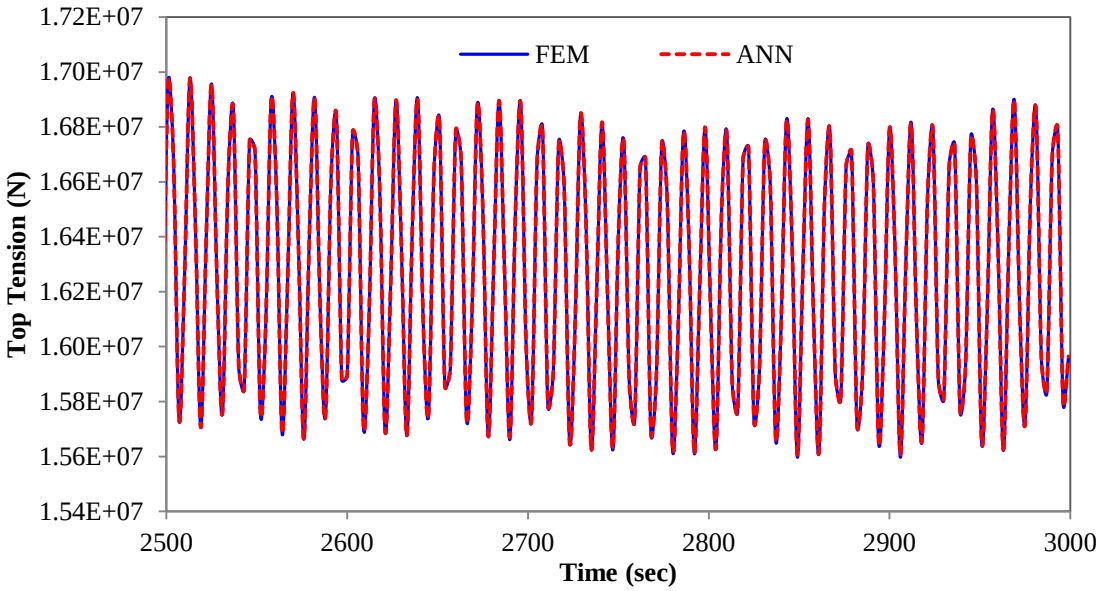

Figure 4.52: Mooring line top tension response of predicted and FEM time history for 12.65 m wave height and 11.39 sec wave period

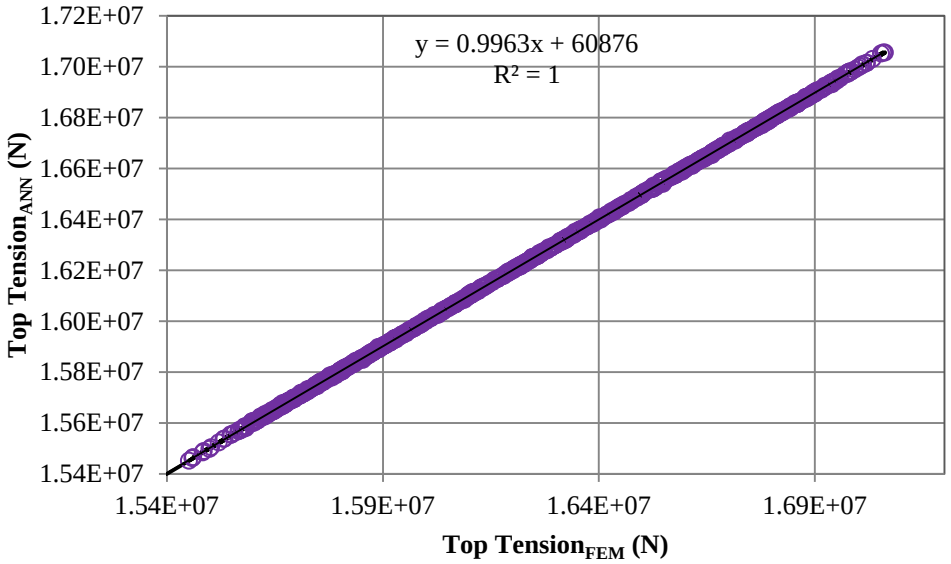

Figure 4.53: Comparison between top tension response of predicted and FEM for 12.65 m wave height and 11.39 sec wave period

Table 4.9 shows the statistical top tension response of ANN and FEM results for 12.65 m wave height and 11.39 sec wave period. The Resp-Pred approach results are better for predicting top tension response as revealed in the higher value of the correlation coefficient of 0.997. The Resp-Pred approach can predict top tension response from newly selected environmental force and mechanical parameter, which is shown in Figure 4.54. The top tension response 3000 sec time history is predicted for 11.30 m wave height and 14.15 sec wave period.

Table 4.9: Statistical mooring line top tension response of ANN and FEM for 12.65 m wave height and 11.39 sec wave period

Mooring line Tension (N)	Max	Min	Mean	Standard deviation
FEM	17062834.5	11182200	16266318	463666.5
Resp-Pred	17085820.59	11182323.9	16263011	463165.8
Difference (%)	0.13	0.001	0.020	0.108

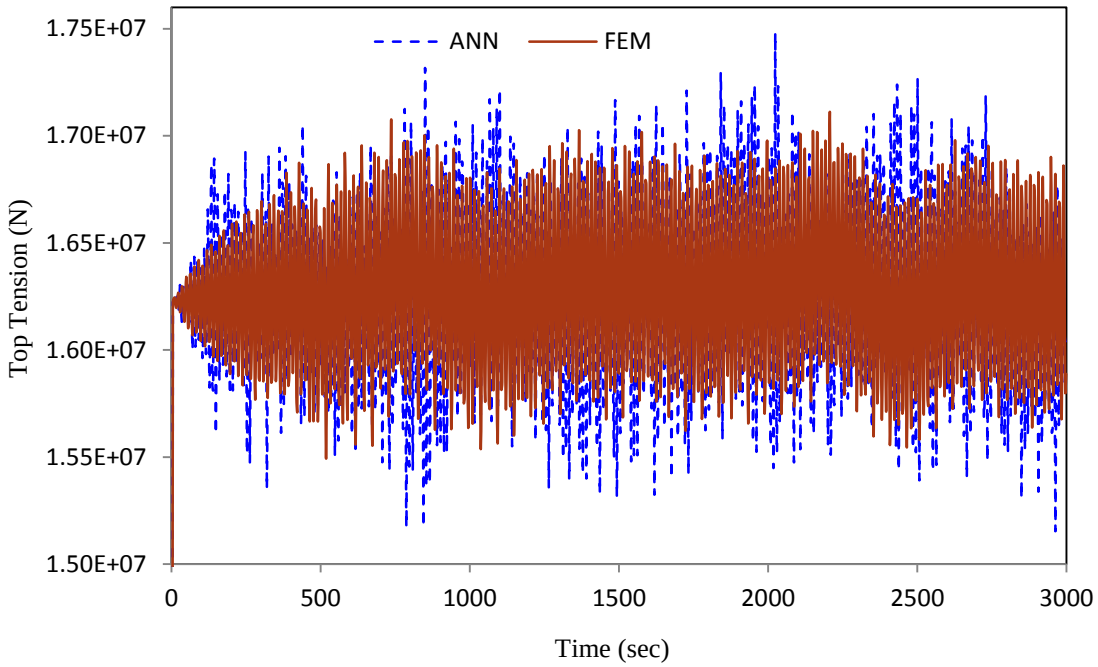

Figure 4.54: Top tension response of predicted time history for 11.30 m wave height and 14.15 sec wave period

4.5 Hybrid FEM-ANN Approach for Response Prediction

In finite element analysis, 6m wave height and 14 sec wave period have been considered as sea-state. These results have been used to train the network. An MLP network having 3-5-1 neurons i.e. 3 neurons in the input layer, 5 neurons in the hidden layer, and 1 neuron in the output layer. Non-linear time histories of 3000 sec for surge, heave, and pitch are used as input in ANN for training the network. Top tension time histories are used in ANN as target for training. After training the network response of mooring line top tension can predict long time history. The ability for more accurate prediction of platform motions by hybrid FEM-ANN approach consequently contribute to a smaller and less expensive spar-mooring system.

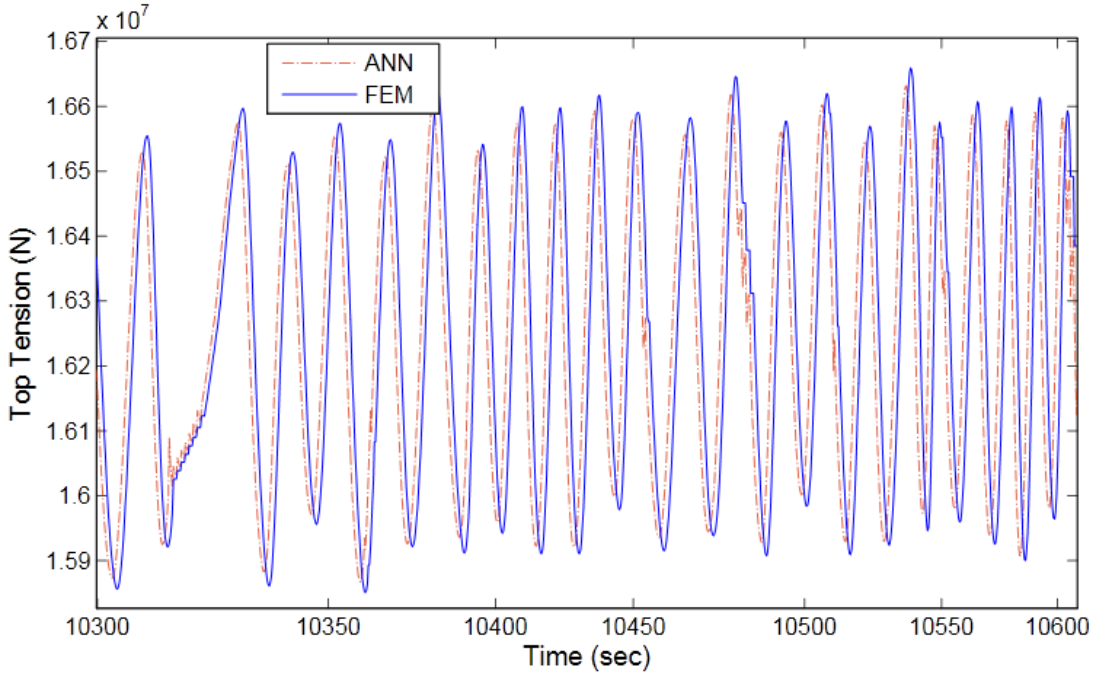

Figure 4.55: Maximum Tension time history of mooring line, FEM vs ANN

3000 sec time history is used to train the neural network in the hidden layer. Three kinds of time steps have been randomly divided up to 3000 sec time series data. Time series 2100 sec (70%) is used for training, 450 sec (15%) for validation, and 450 sec for testing (15%). Training set of data is used to adjust the network according to means square error. The validation set is used to minimize the data over fitting and testing set is used for measuring the network performance during and after the training. Consequently response/output of mooring line top tension is predicted after completing the training from 3001 sec to 14000 sec, which is more than 3 hours. Maximum top tension predict by ANN is 1.544E7 N, whereas FEM predicted value is 1.625E7 N. Figure 4.55 shows the comparison between predicted ANN results and the time consuming FEM results for 10300 to 10600 sec. The results of ANN converge well with the FEM outputs. The error in prediction of response histories for floating spar platform is presented in Figure 4.56.

Table 4.10: Statistical mooring line top tension response of ANN and FEM

Numerical Approach	Mean Value	Standard Deviation	Maximum	Minimum
FEM	1.625E+07	2.406E+05	1.684E+07	1.567E+07
Hybrid FEM-ANN	1.626E+07	2.845E+05	1.710E+07	1.544E+07
Difference (%)	0.071	15.45	1.52	-1.44

The back propagation neural network minimizes the error by trial and error process. It is observed that the combination between 4 sec delay for surge, heave, and pitch motions and 10-5 neurons in the hidden layer quickly minimize the mean square error. From the analysis it is clear that the error is insignificant for the structural solution of floating spar platform.

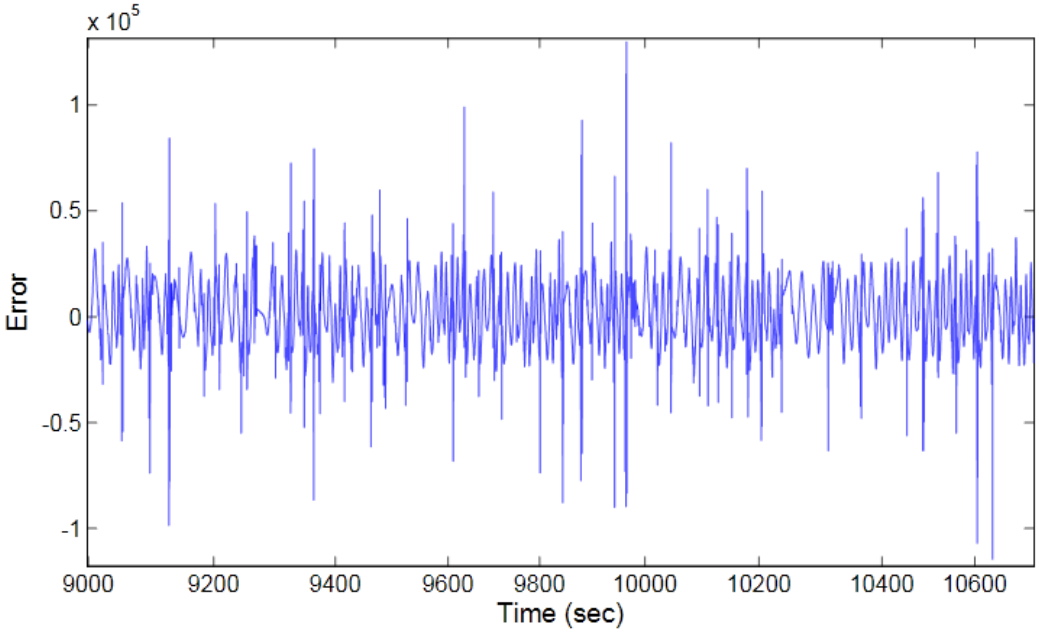

Figure 4.56: Error of ANN results and FEM

Response calculation of spar mooring line for 3000 sec using FEM requires minimum time of 15 hours on Dell Workstation Precision T7500. The computational efforts needed to predict spar platform response using ANN is very small compared to a complete finite element-based simulation. It takes just 20 min on Pentium (R) 4 CPU 3.0 GHz computer.

CHAPTER 5.0 CONCLUSIONS AND RECOMMENDATIONS

5.1 Introduction

This chapter concludes the prediction of waves and response of spar platform using neural networks. It also includes conclusions from coupled finite element analysis of spar platform under waves, current forces, considering various nonlinearities. The integrated coupled analysis considered the mooring lines and hull as a single system. Future research is also suggested for through behaviour understanding of floating spar platform.

5.2 Conclusions

The following outcomes are concluded from this study:

1) The neural network approach is applied to predict maximum wave height and wave period from randomly selected wind forces of Malaysian sea. There are two different models considered for predicting waves, namely nonlinear auto regressive network model (NARX) and feed-forward back-propagation neural network model (NEWFF). The comparison between observed and predicted wave height and wave period are investigated incorporating NARX and NEWFF models. Different levels of accuracy in terms of the root mean square error, correlation coefficient and scatter index are achieved.

    a) The NARX network model's performance is significantly better than those of the NEWFF network model, when wave prediction is made within the range of training data. The NARX network results are better compared to the NEWFF

network in predicting wave height and wave period as revealed in the higher value of the correlation coefficient 0.996 and 0.989, respectively. For NEWFF network the correlation coefficient of wave height and wave period is 0.741 and 0.731, respectively.

b) For predicting waves outside the range of training data, NEWFF network performance is better than NARX network model.

c) The overall network performance is found to be good for predicting waves, which is also used for predicting response of spar platform by FEM and ANN.

2) The effects of coupling on spar hull with mooring lines are precisely investigated using time domain coupled dynamic analysis program.

a) The integrated coupled model clearly shows its significance in terms of hydrodynamic damping on mooring lines.

b) There is a major difference in responses obtained with and without current forces on mooring lines.

c) The mooring tensions decreases after certain wave duration mainly due to the damping of mooring lines in the integrated coupled spar mooring system.

d) In deep sea condition, the spar shows the dominant response of surge near frequency of pitch. It is because surge response at deck level is strongly influenced by pitching motion.

3) Resp-Pred approach by ANN is used for response prediction of spar platform from newly selected environmental forces like wave height and wave period. This approach predicts surge, heave, and pitch response of spar hull and top tension of mooring lines from environmental and structural parameters.

a) The Resp-Pred approach is found to be efficient and it significantly reduces the time for predicting response time-histories of spar hull and mooring lines.
b) The responses of spar platform predicted by Resp-Pred approach are in good agreement with FEM results.
c) The time required to predict response of spar platform using Resp-Pred approach on i3-2100 CPU @ 3.10 GHz and RAM 4.0 GB (normal desktop pc) is 10 sec, whereas finite element analysis requires 23 hours on Dell Workstation Precision T7500 (Intel Xeon E5620 @ 2.40 GHz with 4 processor and RAM 8 GB high computational server).
d) Unlike FEM, ANN approach doesn't require technically skill persons and high performance computing setup to predict the platform response.
e) Therefore the developed method can be used onsite to make quick decisions, whether to continue or stop the production of oil and gas in case of a forecasted storm.

4) The responses (3000 sec time history) of surge, heave, and pitch obtained from FEM are used in hybrid FEM-ANN approach for predicting 14000 sec time history of mooring line top tension.
   a) The time needed to train an ANN is very small compared to a complete finite element analysis of spar platform. The ANN approach fairly matches with the time consuming FEM solution and give a long duration prediction in simple manner.
   b) The hybrid FEM-ANN approach can deal with more data and requires less computing time for training.

c) The trained architecture will help in designing more efficient and economical configuration of mooring systems during preliminary design stages.

The study reveals that an ANN can provide highly accurate prediction of spar platform responses using NEWFF and NARX network. The research findings have potential significance for oil and gas industry.

5.3 Recommendations for Future Work

Spar platform is an innovative and stable offshore platform for oil and gas exploration in deep sea. The study indicates that spar platform has a huge potential in the future, and is expected to greatly promote operations on the deep sea exploration. In particular, the response prediction of spar platforms using ANN is needed to be explored exhaustively. The following recommendations are made:

1. Malaysian sedimentary basin holds great promise for future oil and gas exploration. ANN can help in selecting a suitable platform on the basis of various conditions.
2. The wave induced vortex shedding causes large oscillations of spar platforms that can be controlled by ANN. ANN controlling tools can be used for controlling the response of offshore structures subjected to random ocean waves.
3. ANN can be used for monitoring spar platform responses which may overcome unprecedented severe storms, accidental collisions with supply vessels etc.
4. ANN-based reliability study of spar platform can be used for safety analysis and design.
5. A close form equation can be developed based on Resp-pred approach. This will help practicing engineers to conveniently predict the response of spar platform.

REFERENCE

Agarwal, A., and Jain, A. (2003). Nonlinear coupled dynamic response of offshore Spar platforms under regular sea waves. *Ocean Engineering, 30*(4), 517-551.

Anam, I., Roesset, J. M., and Niedzwecki, J. M. (2003, May 25-30). *Time domain and frequency domain analysis of spar platforms.* Paper presented at the The Thirteenth (2003) International Offshore and Polar Engineering Conference, Honolulu, Hawaii, USA.

Banerji, P., and Datta, T. K. (1997, May 25-30). *Integrity Monitoring of Offshore Platforms Using Artificial Neural Nets.* Paper presented at the Proceedings of the Seventh International Offshore and Polar Engineering Conference, Honolulu, USA.

Beale, M. H., Hagan, M. T., and Demuth, H. B. (2010). Neural Network Toolbox™ 7 User's Guide.

Tension Leg Platform (TLP).GlobalSecurity.org [Cited 20 October 2011]. Available from Internet: <http://www.globalsecurity.org/military/systems/ship/platform-tension-leg.htm>

Blushoes. (2010). 3d model semi submersible oil rig *Turbosquid [Cited 11 May, 2012] Available at <http://www.turbosquid.com/3d-models/3d-model-semi-submersible-oil/513428>*.

Boom, W. d., Chatjigeorgiou, I., Halkyard, J., Leira, B., Ma, N., Du, S., . . . Younsang, W. (2009, 16-21 Auguest). *Floating Production Systems.* Paper presented at the 17th International Ship and Offshore Structures Congress, Seoul, Korea.

Cardozo, S. D., Gomes, H. M., and Awruch, A. M. (2011). Optimization of laminated composite plates and shells using genetic algorithms, neural networks and finite elements. *Latin American Journal of Solid and Structures, 8*, 413-427.

Cepowski, T. (2010). The modeling of seakeeping qualities of Floating Production, Storage and Offloading (FPSO) sea-going ships in preliminary design stage. *Polish Maritime Research, 17*(4), 3-12.

Chai, T. C. (2005). *A Numerical Analysis of Fixed Offshore Structure Subjected to Environmental Loading in Malaysian Water.* Master of Engineering, Universiti Teknologi Malaysia.

Chakraborty, R. C. (2010). Fundamental of Neural Networks:Soft Computing Course Lecture 7-14, notes, slides, Available from Internet:< http://www.myreaders.info/html/soft_computing.html>.

Chang, S., Kim, D., Chang, C., and Cho, S. G. (2009). Active response control of an offshore structure under wave loads using a modified probabilistic neural network *Journal of Marine Science and Technology, 14*(2), 240-247.

Chen, X., Zhang, J., and Ma, W. (2001). On dynamic coupling effects between a spar and its mooring lines. *Ocean Engineering, 28*(7), 863-887.

Chen, X. H., Zhang, J., and Ma, W. (1999). *Coupled time-domain analysis of the response of a spar and its mooring system* (Vol. a.1999). Cupertino, CA, ETATS-UNIS: International Society of Offshore and Polar Engineers.

Cocodia, E. O. (2008, July 6-11). *Creating Better Cost Estimates for Floating Offshore Structures by Assessing Cost Correlation and Understanding Risk.* Paper presented at the The Eighteenth (2008) International Offshore and Polar Engineering Conference, Vancouver, BC, Canada.

Cui, H. Y., and Zhao, D. Y. (2007). Active control of offshore platforms using rough neural networks. *Harbin Gongcheng Daxue Xuebao/Journal of Harbin Engineering University, 28,* 16-21.

D'Souza, R., Dove, P., and Kelly, P. (1993). *Taut Leg Spread Moorings: A Cost-Effective Stationkeeping Alternative For Deepwater Platforms.* Paper presented at the Offshore Technology Conference.

Deka, P. C., and Prahlada, R. (2012). Discrete wavelet neural network approach in significant wave height forecasting for multistep lead time. *Ocean Engineering, 43*(0), 32-42.

Deo, M. C., Jha, A., Chaphekar, A., and Ravikant, K. (2001). Neural networks for wave forecasting. *Ocean Engineering, 28*(7), 889-898.

Diao, Y.-S., Li, H.-J., Shi, X., and Wang, S.-Q. (2005, 18-21 Aug. 2005). *Damage localization for offshore platform by neural networks.* Paper presented at the Machine Learning and Cybernetics, 2005. Proceedings of 2005 International Conference.

Diao, Y., and Li, H. (2006). Study on damage diagnosis of offshore platform by artificial neural networks. *Zhendong yu Chongji/Journal of Vibration and Shock, 25*(4), 98-103.

Dikmen, S. U., and Sonmez, M. (2011). An Artificial Neural Networks Model for the Estimation of Formwork Labour. *Journal of Civil Engineering and Management, 17*(3), 340-347.

DNV. (1996). Guideline for Offshore Structural Reliability: Application to Jacket Platform *Joint Industry Project*. (pp. 80). Norway: Det Norske Veritas

EIA. (2011). Country Analysis Briefs, Malaysia. U.S. Energy Information Administration, [Cited 04 May, 2012] Available at <http://www.eia.gov/countries/cab.cfm?fips=MY>.

Elshafey, A. A., Haddara, M. R., and Marzouk, H. (2009). Dynamic response of offshore jacket structures under random loads. *Marine Structures, 22*(3), 504-521.

Elshafey, A. A., Haddara, M. R., and Marzouk, H. (2010). Damage detection in offshore structures using neural networks. *Marine Structures, 23*(1), 131-145.

Elshafey, A. A., Haddara, M. R., and Marzouk, H. (2011). Estimation of excitation and reaction forces for offshore structures by neural networks. *Ocean Systems Engineering, 1*(1), 1-15.

Fathi, A., and Aghakouchak, A. (2007). Prediction of fatigue crack growth rate in welded tubular joints using neural network. *International Journal of Fatigue, 29*(2), 261-275.

Fedi, G., Manetti, S., Pelosi, G., and Selleri, S. (2002). FEM-trained artificial neural networks for the analysis and design of cylindrical posts in a rectangular waveguide. *Electromagnetics, 22*(4), 323-330.

Glanville, R., Paulling, J., Halkyard, J., and Lehtinen, T. (1991). *Analysis of the spar floating drilling production and storage structure.* Paper presented at the Offshore Technology Conference, Houston, Texas.

GOM, G. o. M. (2000). *Deepwater Development: A reference document for the Deepwater Environmental Assessment Gulf of Mexico OCS*. New Orleans, LA: Gulf of Mexico OCS Regional Office.

Guarize, R., Matos, N. A. F., Sagrilo, L. V. S., and Lima, E. C. P. (2007). Neural networks in the dynamic response analysis of slender marine structures. *Applied Ocean Research, 29*(4), 191-198.

Günther, H., Rosenthal, W., Stawarz, M., Carretero, J., Gomez, M., Lozano, L., . . . Reistad, M. (1997). The wave climate of the Northeast Atlantic over the period 1955-1994: the WASA wave hindcast. *GKSS FORSCHUNGSZENTRUM GEESTHACHT GMBH-PUBLICATIONS-E*.

Haddara, M. R., and Xu, J. (1999). On the identification of ship coupled heave-pitch motions using neural networks. *Ocean Engineering, 26*(5), 381-400.

Hagan, M. T., Demuth, H. B., and Beale, M. H. (1996). Neural Network Design. Boston: MA: PWS Publishing.

Hagan, M. T., and Menhaj, M. (1994). Training Feed-forward Networks With the Marquardt Algorithm. *IEEE Transactions on Neural Networks, 5*(6), 989–993.

Hong-nan, L., and Lin-sheng, H. (2003). Semi-Active TLCD Control of Fixed Offshore Platforms Using Artifical Neural Networks. *China Ocean Engineering, 17*(2).

Hong-yu, C., and De-you, Z. (2010). A new grey neural network and its application to vibration control of offshore platform. *Journal of Dalian University of Technology*.

Hong-yu, C., De-you, Z., and Ping, Z. (2009). Adaptive Predictive Inverse Control of Offshore Jacket Platform Based on Rough Neural Network. *China Ocean Engineering, 2*, 185~198.

Horton, E., and Halkyard, J. (1992). A Spar Platform for Developing Deep Water Oil Fields. *MTS'92*, 998-1005.

Idichandy, V. G., and Mangal, L. (2001). *Studies on structural monitoring of offshore jacket platforms.* Paper presented at the Second International Conference on Experimental Mechanics, Singapore.

Islam, M. M., Khondoker, M. R. H., and Rahman, C. M. (2001). Application of artificial intelligence techniques in automatic hull form generation. *Ocean Engineering, 28*(12), 1531-1544.

Jameel, M. (2008). *Non-linear dynamic analysis and reliability assessment of deepwater floating structure.* PhD thesis, Indian Institute of Technology, Delhi.

Jameel, M., and Ahmad, S. (2011). *Fatigue Reliability Assessment of Coupled Spar-Mooring System*. Paper presented at the the ASME 2011 30th International Conference on Ocean, Offshore and Arctic Engineering (OMAE), Rotterdam, The Netherlands.

Jameel, M., Ahmad, S., Islam, A., and Jumaat, M. Z. (2011, 19-24 June). *Nonlinear Analysis of Fully Coupled Integrated Spar-Mooring Line System.* Paper

presented at the International Offshore and Polar Engineering Conference (ISOPE), Maui, Hawaii, USA.

Jameel, M., Islam, A., Salman, F. A., Khaleel, M., and Jumaat, M. (2012). Wave data for shallow and deep water sedimentary basins of Malaysia. *Advanced Science Letters*, *14*(1), 360-364.

Javadi, A., Tan, T., and Zhang, M. (2003). Neural network for constitutive modelling in finite element analysis. *Computer Assisted Mechanics and Engineering Sciences*, *10*(4), 523-530.

Ji, L., and Zhou, T. (2011). Predicting Product Precision in Fused Deposition Modeling Based on Artificial Neural Network. *Advanced Science Letters*, *4*(6-7), 2193-2197.

Kadi, H. E. (2006). Modeling the mechanical behavior of fiber-reinforced polymeric composite materials using artificial neural networks--A review. *Composite structures*, *73*(1), 1-23.

Kalra, R., Deo, M. C., Kumar, R., and Agarwal, V. K. (2005). Artificial neural network to translate offshore satellite wave data to coastal locations. *Ocean Engineering*, *32*, 1917–1932.

Kim, C. H. (2008). *Nonlinear Waves and Offshore Structures* (Vol. 27). Texas A&M University, USA: World Scientific Publishing Company.

Kim, D. H., Kim, D., and Chang, S. (2009). Application of lattice probabilistic neural network for active response control of offshore structures. *Structural Engineering and Mechanics*, *31*(2), 153-162.

King, K. K. (Producer). (2012, May 25, 2012). Offshore & Ocean Engineering. Retrieved from http://www.fkm.utm.my/~koh/smk4122/Introduction%20to%20Offshore%20Engineering.pdf

Koo, B. J., Kim, M. H., and Randall, R. E. (2004). Mathieu instability of a spar platform with mooring and risers. *Ocean Engineering, 31*(17–18), 2175-2208.

Krogstad, H. E., and F. Barstow, S. (1999). Satellite wave measurements for coastal engineering applications. *Coastal Engineering, 37*(3–4), 283-307.

Lefik, M., and Schrefler, B. (2003). Artificial neural network as an incremental non-linear constitutive model for a finite element code. *Computer methods in applied mechanics and engineering, 192*(28-30), 3265-3283.

Lin, J. (2010). *Vibration Load Identification Based on the Neural Network Model*. Paper presented at the 3rd International Congress on Image and Signal Processing (CISP2010).

Liu, J., Zhong, W., and Zhang, Y. (2011, June 19-24). *Prediction of Floating Platform Mooring Responses in South China Sea.* Paper presented at the The Twenty-first (2011) International Offshore and Polar Engineering Conference, Maui, Hawaii, USA.

Londhe, S., and Panchang, V. (2006). One-day wave forecasts based on artificial neural networks. *Journal of Atmospheric and Oceanic Technology, 23*(11), 1593-1603.

Lopes, T. A. P., and Ebecken, N. F. F. (1997). In-time fatigue monitoring using neural networks. *Marine Structures, 10*(5), 363-387.

Low, Y. (2008). Prediction of extreme responses of floating structures using a hybrid time/frequency domain coupled analysis approach. *Ocean Engineering, 35*(14-15), 1416-1428.

Low, Y., and Langley, R. (2008). A hybrid time/frequency domain approach for efficient coupled analysis of vessel/mooring/riser dynamics. *Ocean Engineering, 35*(5-6), 433-446.

Ma, H., Tang, G.-Y., and Zhao, Y.-D. (2006). Feedforward and feedback optimal control for offshore structures subjected to irregular wave forces. *Ocean Engineering, 33*, 1105–1117.

Ma, H., Tang, G. Y., and Hu, W. (2009). Feedforward and feedback optimal control with memory for offshore platforms under irregular wave forces. *Journal of Sound and Vibration, 328*(4-5), 369-381.

Ma, R., Li, G., and Lin, J. (2009a). Vibration Load Identification of Offshore Platforms Based on Neural Network. *ASME Conference Proceedings, 2009*(43420), 101-104.

Ma, R., Li, G., and Lin, J. (2009b). *Vibration measurement and load identification of offshore platforms.* Paper presented at the International Conference on Mechanical and Electrical Technology, ICMET'09, Beijing.

Ma, W., Lee, M. Y., Zou, J., and Huang, E. (2000). *Deepwater nonlinear coupled analysis tool.* Paper presented at the Offshore Technology Conference, Houston, Texas.

MacGregor, J., Black, F., Wright, D., and Gregg, J. (2000). Design and Construction of the FPSO Vessel for the Schiehallion Field. *Trans RINA. London*.

Mahfouz, A. B. (2007). Predicting the capability-polar-plots for dynamic positioning systems for offshore platforms using artificial neural networks. *Ocean Engineering, 34*(8-9), 1151-1163.

Makarynskyy, O., Makarynska, D., Kuhn, M., and Featherstone, W. E. (2004). Predicting sea level variations with artificial neural networks at Hillarys Boat Harbour, Western Australia. *Estuarine, Coastal and Shelf Science, 61*(2), 351-360.

Makarynskyy, O., Pires-Silva, A. A., Makarynska, D., and Ventura-Soares, C. (2005). Artificial neural networks in wave predictions at the west coast of Portugal. *Computers & geosciences, 31*(4), 415-424.

Mandal, S., hegde, G., and Gupta, K. G. (2004). *Evaluation of Stress Resultant of Offshore Jacket Platform using Neural Network.* Paper presented at the

Proceeding of National Seminar on Construction Management: Latest Trends and Developments Pune, India.

Mandal, S., and Prabaharan, N. (2006). Ocean wave forecasting using recurrent neural networks. *Ocean Engineering, 33*(10), 1401-1410.

Mandal, S., Rao, S., Manjunath, Y., and Kim, D. (2007, December 12-14). *Stability analysis of rubblemound breakwater using ANN.* Paper presented at the Fourth Indian National Conference on Harbour and Ocean Engineering (INCHOE-2007), Surathkal, India.

Mangal, L., Idichandy, V. G., and Ganapathy, C. (1996). ART-based multiple neural networks for monitoring offshore platforms. *Applied Ocean Research, 18*(2-3), 137-143.

Mangal, L., Idichandy, V. G., and Ganapathy, C. (2001). Structural monitoring of offshore platforms using impulse and relaxation response. *Ocean Engineering 28*, 689–705.

Manik, A., Gopalakrishnan, K., Singh, A., and Yan, S. (2008). Neural networks surrogate models for simulating payment risk in pavement construction. *Journal of Civil Engineering and Management, 14*(4), 235-240.

Marshall, P. W. (2005). Interdisciplinary aspects of offshore structures. *Marine Technology Society Journal, 39*(3), 99-115.

Mazaheri, S. (2006). The usage of artificial neural networks in hydrodynamic analysis of floating offshore platforms. *Journal of Marine Engineering, 3*(4), 48-60.

Mazaheri, S., and Downie, M. J. (2005). Response-based method for determining the extreme behaviour of floating offshore platforms. *Ocean Engineering, 32*(3-4), 363 -393.

Mazaheri, S., Mesbahi, E., Downie, M., and Incecik, A. (2003). *Seakeeping Analysis of a Turret-Moored FPSO by Using Artificial Neural Networks.* Paper presented at

the 22nd International Conference on Offshore Mechanics and Arctic Engineering (OMAE2003) Cancun, Mexico.

Mingui, S., Xiaopu, Y., and Sclabassi, R. J. (2003, 14-17 Dec. 2003). *Solving partial differential equations in real-time using artificial neural network signal processing as an alternative to finite-element analysis.* Paper presented at the Neural Networks and Signal Processing, 2003. Proceedings of the 2003 International Conference on.

Miri, R., Sampaio, J., Afshar, M., and Lourenco, A. (2007). *Development of Artificial Neural Networks to Predict Differential Pipe Sticking in Iranian Offshore Oil Fields*. Paper presented at the International Oil Conference and Exhibition, Mexico.

MOG (2010). Oil and Gas Malaysia, Part II: Types of Offshore Platforms Blogger, [Cited 04 May, 2012] Available at <http://minyakdangasmalaysia.blogspot.com/2010/10/part-ii-types-of-offshore-platforms.html>.

Moghim, M., Shafei, F. A. R. M., and Bahreyninezhad, A. (2007). Prediction of Wave and Current Forces on Slender Structures using Artificial Neural Networks. *Journal of Hydraulics, 37*, 4.

Montasir, O. A. A., Kurian, V. J., Narayanan, S. P., and Mubarak, M. A. W. (2008). *Dynamic Response of Spar Platforms Subjected to Waves and Current*. Paper presented at the International Conference on Construction and Building Technology.

Muzathik, A. M., Nik, W. B. W., Samo, K. B., and Ibrahim, M. Z. (2011). Ocean Wave Measurement and Wave Climate Prediction of Peninsular Malaysia. *Journal of Physical Science*, *22*(1), 77–92.

Nakamura, M., Ohmachi, T., and Shima, T. (2003). *Model Experiments on Dynamic Positioning System using Neural Network Controller*. Paper presented at the

Proceedings of The Thirteenth International Offshore and Polar Engineering Conference, Honolulu, Hawaii, USA.

Nallayarasu, D. S. (2009). *Offshore Structures*. PhD, Indian Institute of Technology Madras, Chennai - 600036, India, Scribd [Cited 12 May, 2012] available at,<http://www.scribd.com/doc/38316942/Offshore-Structures-Dr-S-Nallayarasu>.

Ng, C., Kurian, V., and Montasir, O. A. A. (2010). *Experimental and Analytical Investigation of Classic Spar Responses*. Paper presented at the International Conference on Sustainable Building and Infrastructure, Kuala Lumpur.

Paplińska-Swerpel, B., and Paszke, Ł. (2006). Application of Neural Networks to the Prediction of Significant Wave Height at Selected Locations on the Baltic Sea. *Archives of Hydro-Engineering and Environmental Mechanics, 53*(3), 183-201.

Pina, A. A. d., Pina, A. C. d., Albrecht, C. H., Lima, B. S. L. P. d., and Jacob, B. P. (2010). *Applying Computational Intelligence in the Design of Moored Floating Systems for Offshore Oil Production*. Paper presented at the 2nd International Conference on Engineering Optimization, Lisbon, Portugal.

Prislin, I., Steen, A., and Halkyard, J. (2001, June 17-22). *Upending of a Spar Offshore Platform: Prediction of Motions and Loading*. Paper presented at the The Eleventh (2001) International Offshore and Polar Enghleering Conference, Stavanger, Norway.

QLEE. (2011). SPAR Platform - UT *Turbosquid [Cited 11 May, 2012] Available at <http://www.turbosquid.com/3d-models/3d-max-spar-platform--/589373>*.

Rai, R., and Mathur, B. (2008). Event-based Sediment Yield Modeling using Artificial Neural Network. *Water Resources Management, 22*(4), 423-441.

Ran, Z., Kim, M. H., Niedzwecki, J. M., and Johnson, R. P. (1996). *Response of a Spar platform in Random Waves and Currents (Experiment vs. Theory)*. Paper presented at the International Journal of Offshore and Polar Engineering, ISOPE.

Ran, Z., Kim, M. H., and Zheng, W. (1999). Coupled Dynamic Analysis of a Moored Spar in Random Waves and Currents (Time-Domain Versus Frequency-Domain Analysis). *Journal of Offshore Mechanics and Arctic Engineering, 121*, 194-200.

Razalli, R. M. (2005). The Malaysian Oil and Gas Industry : An Overview *JURUTERA.* (pp. 8-12): The Monthly Bulletin of the Institution of Engineers, Malaysia.

Ruck, D. W., Rogers, S. K., and Kabrisky, M. (1990). Feature selection using a multilayer perceptron. *Journal of Neural Network Computing, 2*(2), 40-48.

Sadeghi, K. (2007). An Overview of Design, Analysis, Construction and Installation of Offshore Petroleum Platforms Suitable for Cyprus Oil/Gas Fields. *K. Sadeghi, GAU J. Soc. & Appl. Sci., 2*(4), 1-16.

Sarkar, I., and Roesset, J. M. (2004). *Variability of Results of Dynamic Analysis of Spars.* Paper presented at the The Fourteenth (2004) International Offshore and Polar Engineering Conference, Toulon, France.

Shafiefar, M., Ardeshir, B., and Moghim, M. N. (2011). Prediction of wave and current forces on slender structures using artificial neuralnetworks. *Transactions Hong Kong Institution of Engineers, 18*(1), 30-35.

Shafiefar, M., and Moghim, M. N. (2005). Prediction of Wave and Current Forces on Slender Structures in the Form of Time Series Using Artificial Neural Networks. *International Journal of Maritime Technology, 2*(1), 13-24.

Shahin, M. A., Jaksa, M. B., and Maier, H. R. (2008). State of the art of artificial neural networks in geotechnical engineering. *Electronic Journal of Geotechnical Engineering, 8*, 1-26.

Simoes, G., Tiquilloca, L. M., and Morishita, M. (2002). Neural-network-based prediction of mooring forces in floating production storage and offloading systems. *Industry Applications, IEEE Transactions on, 38*(2), 457-466.

Steen, A., Kim, M. H., and Irani, M. (2004). *Prediction of Spar Response: Model Tests vs Analysis*. Paper presented at the Offshore Technology Conference, Houston, Texas, U.S.A.

Tahar, A., and Kim, M. (2008). Coupled-dynamic analysis of floating structures with polyester mooring lines. *Ocean Engineering, 35*(17-18), 1676-1685.

Tolman, H. L., Alves, J. H. G. M., and Chao, Y. Y. (2005). Operational Forecasting of Wind-Generated Waves by Hurricane Isabel at NCEP*. *Weather and forecasting, 20*(4), 544-557.

Tolman, H. L., Balasubramaniyan, B., Burroughs, L. D., Chalikov, D. V., Chao, Y. Y., Chen, H. S., and Gerald, V. M. (2002). Development and Implementation of Wind-Generated Ocean Surface Wave Modelsat NCEP*. *Weather and forecasting, 17*(2), 311-333.

Tsai, C. P., Lin, C., and Shen, J. N. (2002). Neural network for wave forecasting among multi-stations. *Ocean Engineering, 29*(13), 1683-1695.

Tuhaijan, S. N. A., Kurian, V. J., and Liew, M. S. (2011). *Wave-Current Interaction on Offshore Spar Platforms*. Paper presented at the Paper presented at the National Postgraduate Conference 2011 (NPC 2011), Universiti Teknologi PETRONAS, Tronoh, Perak, MALAYSIA.

Twomey, B. G. (2010). Study assesses Asia-Pacific offshore decommissioning costs, *Oil and Gas Journal* pp. 51-55.

Umbrello, D., Ambrogio, G., Filice, L., and Shivpuri, R. (2008). A hybrid finite element method–artificial neural network approach for predicting residual stresses and the optimal cutting conditions during hard turning of AISI 52100 bearing steel. *Materials & Design, 29*(4), 873-883.

Wang, Y., Duan, M., Wang, D., Liu, J., and Dong, Y. (2011). *A Model for Deepwater Floating Platforms Selection Based on BP Artificial Neural Networks.* Paper

presented at the International Offshore and Polar Engineering Conference, Maui, Hawaii, USA.

Weggel, D. C. (1997). *Nonlinear Dynamic Responses of Large-Diameter Offshore Structures.* PhD, The University of Texas, Austin

Wei, W., and Gong-you, T. (2004). Feedback and Feedforward Optimal Control for Offshore Jacket Platforms. *Oceanologia Et Limnologia Sinica, 18*(4), 515-526.

Wu, X., Ghaboussi, J., and Garrett, J. H. (1992). Use of neural networks in detection of structural damage. *Computers & Structures, 42*(4), 649-659.

Xu, J., and Haddara, M. R. (2001). Estimation of wave-induced ship hull bending moment from ship motion measurements. *Marine Structures, 14*(6), 593-610.

Ya-jun, Z., and De-you, Z. (2003). Neural Network-Based Active Control for Offshore Platforms. *China Ocean Engineering, 17*(3), 461-468.

Ya-jun, Z., De-you, Z., and Jun, M. (2003). Active control of offshore platforms using neural networks. *Chuan Bo Li Xue/Journal of Ship Mechanics, 7*(5), 65-69.

Yamamoto, I., Masam Ihara, Hirayama, H., Okamoto, N., Matsuura, M., and Kobayashi, E. (2002). *Improvement of Position Keeping Performance and Its Effect on the Operation Rate in FPSO Tandem Offloading.* Paper presented at the Proceedings of The Twelfth (2002) International Offshore and Polar Engineering Conference, Kitakyushu, Japan.

Yan-Jun, L., Gong-You, T., and Cheng-Ming, Z. (2010, 26-28 May 2010). *Feedforward and feedback control for nonlinear systems of offshore platforms.* Paper presented at the Control and Decision Conference (CCDC), 2010 Chinese.

Yasseri, S., Bahai, H., Bazargan, H., and Aminzadeh, A. (2010). Prediction of safe sea-state using finite element method and artificial neural networks. *Ocean Engineering, 37*(2-3), 200-207.

Yun, C. B., and Bahng, E. Y. (1997). Substructural identification of offshore structures using neural networks. *ISOPE, GOLDEN, CO(USA), 1997, 4*, 210-215.

Zeng, Z., Yan, H., and Fu, A. M. N. (2001). Time-series prediction based on pattern classification. *Artificial Intelligence in Engineering, 15*(1), 61-69.

Zhang, F., Yang, J.-m., Li, R.-p., and Chen, G. (2008). Coupling effects for cell-truss spar platform: comparison of frequency- and time-domain analyses with model tests. *Journal of Hydrodynamics, Ser. B, 20*(4), 424-432.

Zhang, G., and Eddy Patuwo, B. (1998). Forecasting with artificial neural networks: The state of the art. *International journal of forecasting, 14*(1), 35-62.

Zhen, W., and Zhigao, Z. (2010). *Damage detection of offshore platform structures using time domain response data.* Paper presented at the International Conference on Intelligent Computation Technology and Automation, Changsha, Hunan, China

Zhou, X., and Luan, S. (2009). *Study on wave impact force prediction of different shore connecting structure based on improved BP neural network.* Paper presented at the 5th International Conference on Wireless Communications, Networking and Mobile Computing, WiCom '09. , Beijing, China.

Zubaydi, A., Haddara, M. R., and Swamidas, A. S. J. (2002). Damage identification in a ship's structure using neural networks. *Ocean Engineering, 29*, 1187–1200.

APPENDIX

The code used for predicting response of spar platform and wave forces with Artificial Neural Network

```
********************************************************************************


Nonlinear Response Prediction of Spar Platform using Artificial Neural
Network. Structural and Environmental data is used as input and Finite
Element Method (FEM) results used as target.
Copyright (c) 2011-12, Department of Civil Engineering, Faculty of
Engineering, University of Malaya, 50603 Kuala Lumpur, Malaysia.

%% 1. Clean Up
clc; clear all; close all;

%% 2. Import input data from Excel file
x=zeros(12);
for i=1:12
    x =  xlsread('D:\My Work\ANN\Spar_Platform\FEMInput.xls',i);
    [inputn,inputns] = mapminmax(x);
    input{i}=inputn(:);
end

%% 3. Import target data from Excel file
 y=zeros(12);
for i=1:12
    y =  xlsread('D:\My Work\ANN\Spar_Platform\FEMOutput.xls',i);
    [targetn,targetns] = mapminmax(y);
    target{i}=targetn(:,2);
end

%% 4. Create the response prediction network
 hiddenlayer = 20;

 net = newff(input,target,hiddenlayer,{'tansig','purelin'},'trainlm');

% Network setup

 net.trainParam.lr=0.3;%(learning rate)

 net.trainParam.mc=0.6;%(momentum)

 net.performFcn = 'mse';

 net.trainParam.goal = 1e-4;

 net.trainParam.min_grad = 1e-20;

 net.trainParam.epochs = 5000; %(number of epochs)

%% 5. Setup Division of Data for Training, Validation, Testing
 net.divideParam.trainRatio = 70/100;
 net.divideParam.valRatio = 15/100;
 net.divideParam.testRatio = 15/100;
```

```
%% 6. Train the Network
 surge_net = train(net,input,target);

% View the Network
 view(surge_net)

%% 7. Simulation the network
expected_output = sim(surge_net,input);

Error = expected_output- target;

%% 8. Import data from Excel file for prediction

x_Test =  xlsread('D:\My Work\ANN\Spar_Platform\FEMInput.xls',13);

%% 9. Normalize new values

predict_inputn = mapminmax('apply', x_Test, inputns);

%% 9. Convert data to standard neural network cell array form for
prediction

predict_inputc = con2seq (predict_inputn);

%% 10. Simulation the network for new environmental data

ANN_result = sim(surge_net,predict_inputc);

%% 11. Reverse data to cell array to standard neural network
ANN_result_stm = cell2mat(ANN_result);

%% Reverse the normalize process
ANN_surge = mapminmax('reverse',ANN_result_stm,targetns);

%% 12. Export output data to Excel sheet
xlswrite('ANN_Predt_sur', ANN_surge, 1, 'C2');

%% 13. Performance of the network
error = y13-ANN_surge;
perf = mse(error);
```

****


```
%% 1. Clean up
clc; clear all; close all;

%% 2. Import data from Excel file for Training

import = xlsread('C:\Users\user\Documents\MATLAB\Final work\Wave\Wave
data.xls');
data = import';
```

```
%% 3. Input/Target format data
input = data(5,:);

target = data(6:7,:);

%% 4. Process matrices by mapping row minimum and maximum values to [-
1 1]
X = con2seq(input);
T = con2seq(target);

%% 5. Create a Nonlinear Autoregressive Neural Network Architecture
Time delay
delay = 2;

% Neuron in hidden layer
neuronsHiddenLayer = 5;

% Network Creation
net = narxnet(1:delay,1:delay,neuronsHiddenLayer);

%% 6. Prepare the data for Training and Simulation

The function PREPARETS prepares time series data for a particular
network, shifting time by the minimum amount to fill input states and
layer states. Using PREPARETS allows you to keep your original time
series data unchanged, while easily customizing it for networks with
differing numbers of delays, with open loop or closed loop feedback
modes.

[p,Pi,Ai,t] = preparets(net,X,{},T);

%% 7. Setup division of data for Training, Validation, Testing
net.divideParam.trainRatio = 70/100;
net.divideParam.valRatio = 15/100;
net.divideParam.testRatio = 15/100;

%% 8. Train the network
[net,tr] = train(net,p,t,Pi,Ai);

% View the Network
view(net)

%% 9. Plot performance
plotperform(tr);

%% 10. Simulation the network
wave_Tr = sim(net,p,Pi,Ai);

%% 11. Reverse the processing element of training data
ANN_wave_Pre = cell2mat(wave_Tr);

exp_output = target(:,1:end-delay);

%% Performance check the network
error = gsubtract(ANN_wave_Pre,exp_output);

wave_ht_error = error(1,:)';

wave_period_error = error(2,:)';

perf_avg = mse(error);

perf_ht = mse(wave_ht_error);
```

```
perf_t = mse(wave_period_error);
wave_ht_exp = exp_output(1,:)';

wave_ht_pred = ANN_wave_Pre(1,:)';

wave_period_exp = exp_output(2,:)';

wave_period_pred = ANN_wave_Pre(2,:)';

ny = length(wave_period_error);

RMSE = sqrt(perf_t);

BIAS = sum(wave_period_error)/ny;

R = corrcoef(wave_period_exp,wave_period_pred);


*******************************************************************************


%% Finite Element Method (FEM) data is used to train for response
prediction of Spar Platform 3000 sec motion data such as surge, heave
and pitch uses as input and 3000 sec top tension uses as target.
Training the network and predict top tension for 14000 sec.
% Copyright (c) 2011, Department of Civil Engineering, University of
Malaya, Kuala Lumpur, Malaysia.

%% 1. Clean Up
clc; clear all; close all;

%% 2. Importing data from Excel file

S = xlsread('E:\My Work\Mooring Tension\train_data_mooring1.xls');
S=S';

%% 3. Input/Target format data
X = con2seq(S(1:4,:));
T = con2seq(S(5,:));

% Input and target series are divided in two groups of data:
% 1st group: used to train the network
% 2nd group: this is the new data used for simulation R will be used
for predicting new targets S will be used for network validation after
prediction

%% 4. Input/Output for training
N = 3000; % Multi-step ahead prediction

P = X(1:end-N);
Q = T(1:end-N);
G = Q;
%% 5. Input/Output for Prediction
R  = X(end-N+1:end);
Z = T(end-N+1:end);
W = Z;
%% 6. Process matrices by mapping row minimum and maximum values to [-
1 1]

%Input/Output for training
[P,Ps] = mapminmax(P);
[Q,Qs] = mapminmax(Q);
```

```
 %Input/Output for prediction
[R,Rs] = mapminmax(R);
[Z,Zs] = mapminmax(Z);

%% 7. Neural Network Architecture
% Time delay
delay = 5;

% Neuron in hidden layer
neuronsHiddenLayer = 15;

% Network Creation
net = narxnet(1:delay,1:delay,neuronsHiddenLayer);

%% 8. Training the network

[Xs,Xi,Ai,Ts] = preparets(net,P,{},Q);

% Train the network
net = train(net,Xs,Ts,Xi,Ai);

% View the Network
view(net)

%% 9. Prediction of training output
% Performance for the series-parallel implementation, only
% Multi-step-ahead prediction
Y = net(Xs,Xi,Ai);

perf = perform(net,Ts,Y);

%% 10. Data preperation for N-step ahead prediction

inputSeriesPred = [P(end-delay+1:end),R];

targetSeriesPred = [Q(end-delay+1:end), con2seq(nan(1,N))];

%% 11. Convert neural network open-loop feedback to closed loop

netc = closeloop(net);

view(netc)

[Xs,Xi,Ai,Ts] = preparets(netc,inputSeriesPred,{},targetSeriesPred);

yPred = netc(Xs,Xi,Ai);

perf = perform(net,yPred,Z);

%% 12. Reverse the processing element

Output = mapminmax('reverse',yPred,Zs);

errors = cell2mat(Output)-cell2mat(Z);
```

LIST OF AUTHOR PUBLICATIONS

1. **Md. Alhaz Uddin,** Mohammed Jameel, Hashim Abdul Razak, A. B. M. Saiful Islam (2012). Response Prediction of Offshore Floating Structure using Artificial Neural Network. *Advanced Science Letters*, Vol. 14, pp. 186-189. DOI: http://dx.doi.org/10.1166/asl.2012.4049.

2. Mohammed Jameel, **Md. Alhaz Uddin**, Hashim Abdul Razak, Syed Danish Hasan (2012). Calculation of Offshore Structural Response using Artificial Neural Network-Review. *Ships and Offshore Structures.* (Under review).

3. **Md. Alhaz Uddin,** Mohammed Jameel, Hashim Abdul Razak (2012). The Application of Artificial Neural Network in Fixed Offshore Structures. *Indian Journal of Marine Sciences*, (Under review).

4. **Md. Alhaz Uddin,** Mohammed Jameel, Hashim Abdul Razak (2012). *Nonlinear Response Prediction of Deep Water Floating Structures using Artificial Neural Network*. In: The 6th Asia-Pacific Workshop on Marine Hydrodynamics, 3rd - 4th September 2012, Universiti Teknologi Malaysia, Johor, Malaysia pp. 52-55.

5. **Md. Alhaz Uddin,** Mohammed Jameel, Hashim Abdul Razak (2012). The application of artificial neural network for predicting response of spar platform. *Applied Ocean Research*, (Under review).

6. Mohammed Jameel, **Md. Alhaz Uddin,** Hashim Abdul Razak, A. B. M. Saiful Islam (2012). *Prediction of Mooring Line Top Tension of Coupled Spar Platform using Artificial Neural Network*. 32nd International Conference on

Ocean, Offshore and Arctic Engineering (OMAE2013) in Nantes, France , June 9-14, 2013. (Accepted).

7. **Md. Alhaz Uddin,** Mohammed Jameel, Ahmad , Suhail, Hashim Abdul Razak, A. B. M. Saiful Islam (2012). *Prediction of Spar Platform Mooring Tension using Artificial Neural Network.* The 23rd International Ocean and Polar Engineering Conference (ISOPE) in Alaska, USA. June 30 - July 5, 2013. (Accepted).